FIELD SCALE TRIALS OF A

GEOSYNTHETIC CAPILLARY BREAK

A Thesis Submitted to the College of

Graduate Studies and Research

In Partial Fulfillment of the Requirements

For the Degree of Master of Science

In the Department of Civil and Geological Engineering

University of Saskatchewan

Saskatoon

By

Adam D. A. Meier

February 2011

Permission to Use

In presenting this thesis in partial fulfilment of the requirements for a Postgraduate degree from the University of Saskatchewan, I agree that the Libraries of this University may make it freely available for inspection. I further agree that permission for copying of this thesis in any manner, in whole or in part, for scholarly purposes may be granted by the professor or professors who supervised my thesis work or, in their absence, by the Head of the Department or the Dean of the College in which my thesis work was done. It is understood that any copying or publication or use of this thesis or parts thereof for financial gain shall not be allowed without my written permission. It is also understood that due recognition shall be given to me and to the University of Saskatchewan in any scholarly use which may be made of any material in my thesis.

Requests for permission to copy or to make other use of material in this thesis in whole or part should be addressed to:

Head of the Department of Civil and Geological Engineering

University of Saskatchewan

Saskatoon, Saskatchewan

S7N 5A9

Permission to Use

In presenting this thesis in partial fulfilment of the requirements for a Postgraduate degree from the University of Saskatchewan, I agree that the Libraries of this University may make it freely available for inspection. I further agree that permission for copying of this thesis in any manner, in whole or in part, for scholarly purposes may be granted by the professor or professors who supervised my thesis work or, in their absence, by the Head of the Department or the Dean of the College in which my thesis work was done. It is understood that any copying or publication or use of this thesis or parts thereof for financial gain shall not be allowed without my written permission. It is also understood that due recognition shall be given to me and to the University of Saskatchewan in any scholarly use which may be made of any material in my thesis.

Requests for permission to copy or to make other use of material in this thesis in whole or part should be addressed to:

Head of the Department of Civil and Geological Engineering

University of Saskatchewan

Saskatoon, Saskatchewan

S7N 5A9

ABSTRACT

This thesis discusses the field testing of a newly-developed product, a geosynthetic capillary break (GCB). The GCB was developed for use in engineered soil covers when a cover incorporating a capillary break effect would be desirable, but the coarse-grained material (gravel or sand) is unavailable or uneconomical. Engineered soil covers aim to reduce the amount of acid generated from sulphide bearing waste by limiting the ingress of water and/or oxygen. The GCB is a geosynthetic system that is composed of a finely ground rock flour sandwiched between two nonwoven geotextiles and manufactured as a composite layer by needle punching in a process similar to the used for GCL (geosynthetic clay liner). The goal of the GCB is to recreate the capillary break that is achieved with soil layers using a geosynthetic product that is only a few centimetres thick and that can be rolled up and for transportation,

The GCB concept has been demonstrated in a previous study (Park, 2005) based on laboratory column studies and computer modelling. The goal of this project was to determine the effectiveness of the GCB when applied at field scale. Four 25 square test plots were constructed at the tailings management area (TMA) of the HudBay Minerals Inc.(HudBay) mine site located near Flin Flon, MB. One plot contained 1 m of cover soil over top of the GCB (Plot A), one contained only 1 m of cover soil (Plot B), one contained 0.3 m of cover soil over top the GCB (Plot C), and one consisted of a conventional capillary break system with 1 m of cover soil over lying 0.2 m of sand. All of the plots, along with a control plot with no cover, were instrumented with water

content sensors and gas sampling ports to monitor the movement of water and oxygen through the various covers. Matric suction sensors were also installed in Plots A and B to measure the water suction within the covers. A meteorological station was installed to gather climatic data which was used to develop a water balance for each of the plots. The plots were constructed and instrumented in the fall of 2005. Data was collected and analyzed until spring of 2007.

Data from the water content sensors show that the GCB was effective in increasing the water content in the soil portion of the cover system. The suction sensors show that the suction across the GCB drops significantly (40 kPa versus less than 1 kPa) as compared to plots which contain no GCB. Data from the gas concentration sensors show that the plots containing capillary breaks reduce the oxygen flux into the tailings. The plots containing the GCB (Plots A and C) resulted in the lowest flux rates, followed by the sand capillary break (Plot D)and no capillary break (Plot B), respectively. This reduction in oxygen flux will reduce the amount of acid generated from waste, as oxygen is required for the creation of acid mine drainage. Overall the study demonstrated that at field scale that the GCB is effective in limiting the ingress of water and oxygen into the tailings under the observed conditions and the manufactured GCB is comparable to the performance of the previous hand constructed column tests.

ACKNOWLEDGEMENTS

I would like to acknowledge my supervisors, Ian Fleming and Lee Barbour. Your patience and guidance throughout this process has been invaluable. I would also like to thank the staff at O'Kane Consultants Inc. The support provided by Brian, Dave, Ivan, and especially my sister, Denise, has made the completion of this project possible. I would also like to acknowledge my fellow graduate students, Randi, Dana, Heather, and Chad. Your help and also sharing in similar experiences has helped me throughout this process. Thank you to the staff at HudBay. The support provided by Riley, Erin, and Stephen in the construction of the plots, as well as the collection of the data was greatly appreciated.

Most importantly I would like to thank my wife Susan. You have been there to support me throughout this process and in every aspect of my life. Know that I could not have completed this without your support.

TABLE OF CONTENTS

LIST OF TABLES

LIST OF FIGURES

LIST OF APPENDICES

CHAPTER 1 INTRODUCTION

1.1 Background

Acid rock drainage (ARD) is an environmental challenge faced by the mining industry worldwide. Over 500 Mt of solid waste is produced every year by Canadian mining companies (O'Kane, 1998). Sulphide-bearing waste covers more than 10,000 ha within Canada (Melis, 1983). Acid rock drainage is caused when sulphide-bearing tailings or waste react with oxygen and water to produce sulphuric acid. This production of acid is often detrimental to the quality of water in both the surface and subsurface systems (Nicholson *et al.*, 1989).

A common way to isolate the sulphide-bearing waste from the environment is through the use of a barrier, such as a soil cover or an engineered liner (Bussière, 2003). Engineered soil covers, commonly referred to as dry covers, are one method of mitigating the amount of oxygen and water that enters into potentially acid generating waste.

One of the types of soil covers used to mitigate the influx of water and oxygen is a cover incorporating a capillary barrier (CB) effect. The design of capillary break reclamation soil covers requires a textural contrast in adjacent soil layers in order to create a zone of high saturation. A conventional soil cover system of this type is constructed by placing a layer of finer textured soil on top of a coarser textured soil. At many mine sites the required volumes of these coarse and more valuable soils are unavailable or uneconomical. In addition, the placement of these relatively thin soil

layers requires a level of construction control which limits the use of existing mining equipment.

A geosynthetic composite, referred to as a geosynthetic capillary break (GCB), has been recently developed to provide a 'capillary break' similar to that produced by soil layers. The GCB is manufactured as a geocomposite system in which a thin layer of finely ground rock flour overlies a coarse nonwoven geotextile. The goal of this system is to create a capillary break simply by rolling out the manufactured GCB over top of the tailings. The GCB layer would be protected by an overlying layer of cover soil which also serves as a rooting layer for vegetation. Initial laboratory and column studies which demonstrated the performance of the GCB have already been completed at laboratory scale (Park, 2005). This study will focus on evaluating the performance of the GCB system in full-scale field trials. For this field study the GCB product was manufactured in a limited production run of 2,500 m^2 at a geosynthetics manufacturing facility in eastern Canada.

1.2 Site Description

The field trials of the geosynthetic capillary break were carried out at the tailings management facility (TMA) of HudBay Minerals Inc. (HudBay) at their mining operation (54^o 46' N latitude and 101^o 54' W longitude) near Flin Flon, Manitoba, Canada. The mining community of Flin Flon is located on the border of Saskatchewan and Manitoba, approximately 450 km north east of Saskatoon, Saskatchewan, Canada, (Figure 1-1). The average precipitation in Flin Flon is approximately 460 mm (Environment Canada National Climate Archive, years 1971 – 2005). Rainfall accounts for 342 mm of the annual precipitation while the snowfall accounts for the remaining 25% (118 mm).

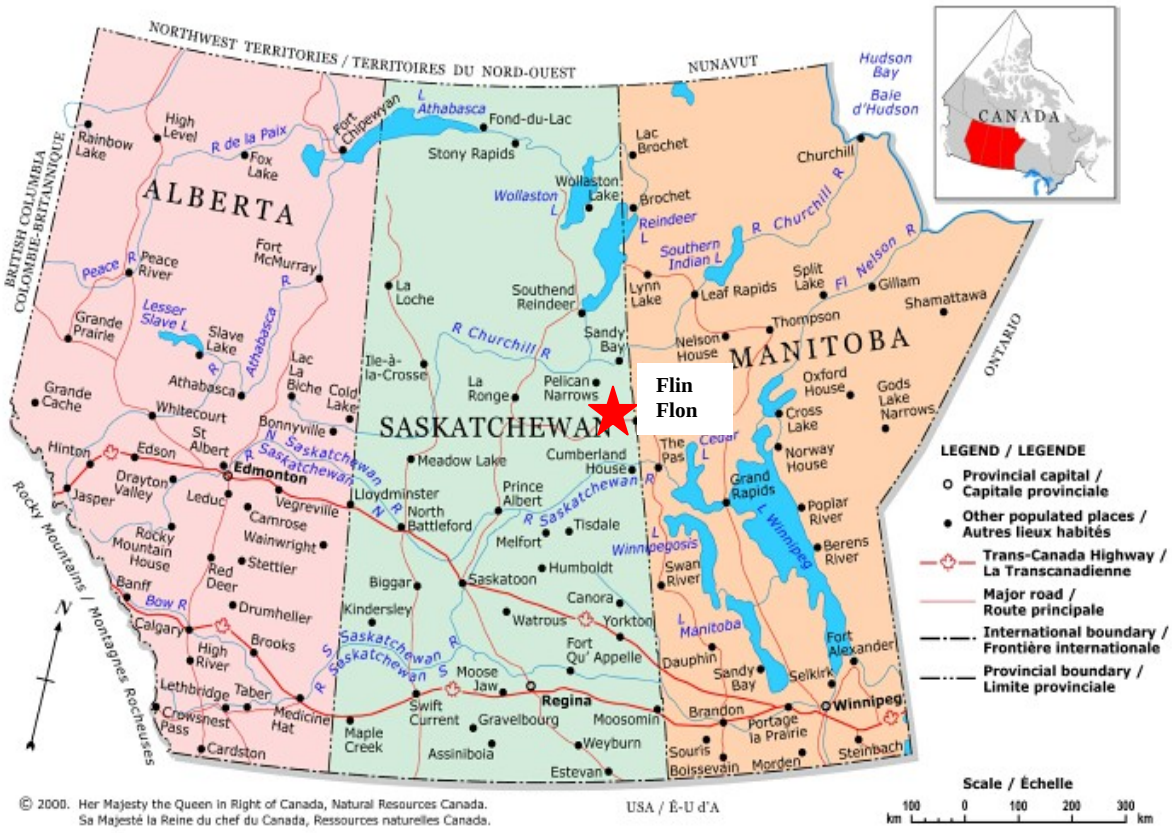

Figure 1-1 Location of Flin Flon, MB (National Resources Canada Atlas of Canada, 2007)

The HudBay tailings facility in Flin Flon Manitoba presents an ideal location for testing of the new GCB. HudBay has a large tailings facility; however, there is a limited supply of high quality cover soil material in the immediate surrounding area.

The HudBay mining operation has been in operation since the 1930's. The tailings are hydraulically placed by pumping tailings slurry into the TMA. The area on which the test plots are constructed has been inactive since 2003. Figure 1-2 shows an air photo of the TMA, with the southern portion highlighted with the red rectangle. The test plots are located within the blue circle.

1.3 Research Objectives

The general objective of this project is to evaluate the performance of a field scale prototype GCB as a moisture and oxygen limiting barrier in a soil cover system. In order to achieve this objective, the research was divided into three parts:

- Construct and instrument a series of test plots on the TMA using GCB and conventional soil capillary break (CB) covers.
- Collect and interpret the monitoring data.
- Evaluate the ability of the test covers to store water, maximize saturation, and limit oxygen ingress to the tailings as compared to a conventional CB cover.

1.4 Scope

The scope of this thesis is limited to the evaluation of the GCB at field scale. The evaluation of the GCB included monitoring field scale tests plots that are constructed with or without a GCB. The plots were not vegetated. The GCB was evaluated based on its ability to store water and limit oxygen diffusion into the underlying waste.

1.5 Overview of Thesis

This thesis is divided into five chapters. Chapter two discusses previous studies on engineered soil covers, instrumentation and monitoring of soil covers, as well as the laboratory development and testing of the GCB. An overview of the design and construction of the test plots is described in Chapter three. Chapter three also describes the instrumentation used to monitor the performance of each of the test covers and the laboratory and *in-situ* testing that was completed. Chapter four presents the collected

Figure 1-2 Location of test plots within TMA (Google Earth, 2007)

data and interprets the results. Finally Chapter five contains the conclusions and recommendations for future work.

CHAPTER 2 LITERATURE REVIEW

2.1 Introduction

This chapter provides a review of literature relevant to the evaluation of the geosynthetic capillary barrier. The subject areas reviewed thus include: past field studies of engineered cover systems; the use of geosynthetics to control moisture movement; as well as review the previous laboratory studies of the GCB.

2.2 Engineered Soil Covers

Acid rock drainage is caused when sulphide-bearing tailings or waste rock reacts with oxygen and water to produce sulphuric acid. Over 500 Mt of solid waste is produced every year by Canadian mining companies (O'Kane *et al.*, 1998) and sulphide-bearing waste covers more than 10,000 ha within Canada (Melis, 1983). The generation of low pH effluent causes the mobilization of metals which upon release will be detrimental to the quality of water in both the surface and subsurface systems (Nicholson *et al.*, 1989).

Sulphide occurs in many forms, but it is most commonly found in the minerals pyrite and pyrrhotite (O'Kane *et al.,* 1998). Acid rock drainage (ARD) is "the result of the combined chemical and biological oxidation of sulphide minerals and the contaminant release of associated metals, such as iron, aluminum, manganese, and other toxic heavy metals" (O'Kane *et al.,* 1998). The oxidation process of sulphide minerals requires the presence of oxygen and water.

Bussière (2003) reported that a common way to isolate these types of waste from water and oxygen is to employ barriers such as liners or surface covers. O'Kane *et al.* (1998) stated that the purpose of a cover system is to minimize the entry of water and oxygen, which in turn reduces both the rate of the acid production and the volume of the resulting effluent. Engineered soil covers are used as an acceptable method for mitigating the amount of oxygen and water that enters into potentially acid generating waste. Many different types of cover systems have been used with the type of cover system selected dependant on the environment, type of waste, and materials available for construction.

2.2.1 Oxygen Limiting Covers

It has been shown that the availability of oxygen greatly affects the rate at which sulphuric acid is formed in sulphide-bearing tailings (Nicholson *et al.,* 1989). In addition, the work of Nicholson *et al.* (1989, 1990) and others have investigated the use of cover systems to mitigate the movement of oxygen through cover systems (Akindunni *et al.* 1991; Lundgren, 2000; Bussière *et al.* 2003.)

According to Nicholson *et al.* (1989) and O'Kane *et al.* (1998) the primary control on sulphide oxidation is the presence of oxygen, regardless of the origin and concentration of the sulphide mineral. This emphasizes the importance of understanding and preventing the migration of oxygen through cover systems. The most effective way to decrease the movement of oxygen is to place the tailings or waste under water; however, this method is impractical for many long-term waste management applications. In the majority of situations, the most effective procedure to mitigate the amount of oxygen entering the waste is to keep the cover material close to saturation. Nicholson *et*

al. (1989) stated that oxygen diffuses more easily through geological materials that have large gas-filled pores compared to water filled pores and that the diffusion coefficient of oxygen through a porous medium can decrease by up to four orders of magnitude from dry conditions to saturation.

2.2.2 Oxygen Diffusion in Unsaturated Soil

As previously stated, the degree of saturation of a geological material overlying a sulphide bearing material can greatly affect the diffusion of oxygen into the waste. Studies have been conducted (Mbonimpa *et al.,* 200;, Aachib *et al.,* 2002) to estimate the relationship between the gas phase oxygen diffusion coefficient and the degree of saturation for porous media.

The one-dimensional diffusive flux of gas can be expressed by Fick's first law (Crank, 1975; Hillel ,1980) which states:

$$J = -D_e \frac{\partial C}{\partial Z} \qquad [2.1]$$

where:

J = diffusive mass flux of a gas ($ML^{-2}T^{-1}$);

D_e = the oxygen effective diffusion coefficient (L^2T^{-1});

C = the O_2 concentration (ML^{-3}); and,

Z = the depth or distance (L).

The work of Aachib *et al.* (2002) describes laboratory procedures to measure the oxygen diffusion coefficient in unsaturated soils. The expression they proposed to estimate the diffusion coefficient (D_e) related to the degree of saturation is as follows:

$$D_e = \frac{1}{n^2}\left[D_a^o \theta_a{}^p + HD_w^o \theta_w{}^p\right] \qquad [2.2]$$

where:

n = porosity;

D_a^o = free (undisturbed) diffusion coefficient in air (1.8×10^{-5} m^2/s @ 22^oC);

θ_a = volumetric air content [$n(1-S_r)$], (S_r = degree of saturation);

H = dimensionless form of Henry's equilibrium constant (H=0.03 @ 20^oC);

D_w^o = free diffusion coefficient in water (2.2×10^{-9} m^2/s @ 22^oC);

θ_w = volumetric water content (nS_r); and,

p = material constant (shown in most cases a good estimation to be 3.5).

2.2.3 Capillary Barrier Effect

Capillary barriers have been studied by Nicholson *et al.* (1989), Rooney *et al.* (1997), Stormont and Morris (1998), O'Kane *et al.* (1998), Khire *et al.*(2000), Henry and Holtz (2001), and Bussière *et al.* (2003). This type of cover system is constructed by placing a layer of finer grained soil directly over a layer of coarser grained soil. A capillary barrier works because of the textural contrast between these two layers. Under low net percolation rates, the maximum suction that can develop within the coarser layer is limited to a value of suction value near the residual water content of the coarser soilas illustrated in Figure 2-1. If the air-entry value of the finer soil layer is greater than these low levels of suction then the finer grained soil remains close to saturation. The high degrees of saturation within the finer soil is related to a significantly lower oxygen diffusion in that layer. If the capillary barrier is formed on a slope, water can travel downward, just above the interface between the coarser and finer materials. This is

commonly referred to as interflow (Henry and Holtz, 2001). The tailings area utilized for the GCB field trials are flat, and the study is assumed to be one dimensional.

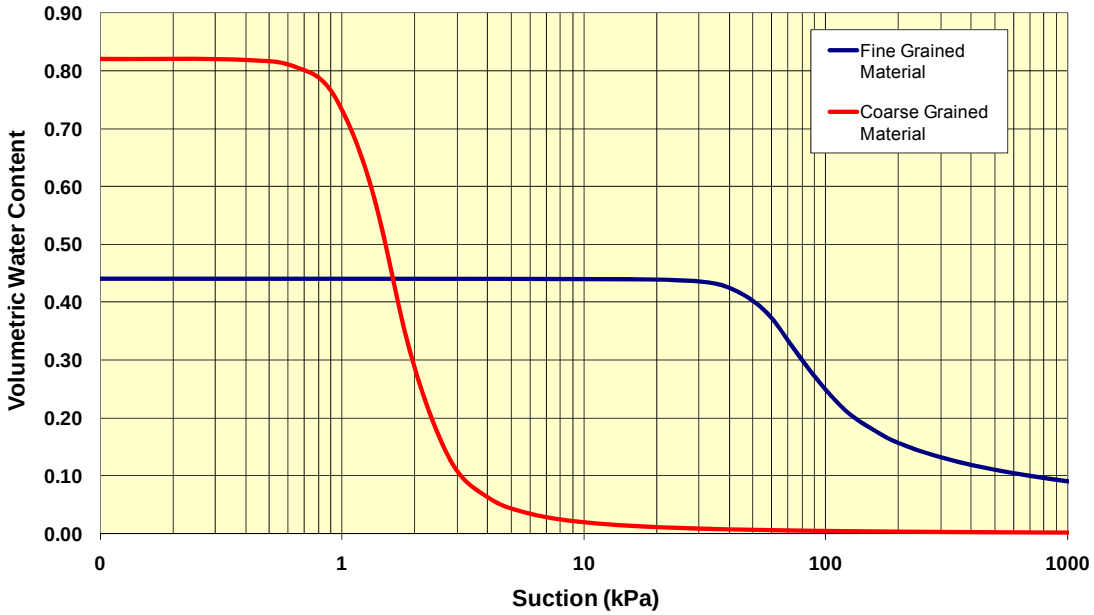

Figure 2-1 Water retention functions of coarse and fine grained material

The presence of a capillary break also enhances the ability of the finer layer to store moisture. The work of Stormont and Morris (1998) highlighted that soil moisture storage within the finer grained soil is much greater in a capillary barrier system than would be at field capacity. The reason for this is that the value of 'field capacity' is based on the idea that the finer grained soil is part of a deep uniform soil profile that will drain until a suction value is reached which is similar to the value that occurs at the residual water content of the soil. However, in the case of the capillary break, it is the residual suction of the coarser layer which controls this equilibrium suction condition and the residual suction is much lower than that of the finer grained soil layer (and consequently θ (water content) is much higher). The work of Stormont and Morris

(1998) suggested a method of estimating the additional storage capacity of capillary barrier systems based on an estimate of the soil suction profile through both cover layers under limiting conditions of drainage and wilting point drying.

The work of Akindunni *et al.* (1991) used numerical simulations to show how a capillary barrier cover can effectively remain close to saturation, thus reducing the diffusion of oxygen. The results from their simulations illustrate how the moisture-retaining ability of a finer cover material is dependent on its air entry value (AEV) relative to the suction at residual water content of the underlying coarser layer. This suction level, along with the AEV of the finer layered soil controls the thickness of the finer cover layer that will remain at full saturation.

2.2.4 Field Evaluation of Cover Systems

Studies by O'Kane (1996), O'Kane *et al.* (1998), Ayres (1998), Yanful *et al.* (1997 and 1999), Boese (2003), and Adu-Wusu and Yanful. (2006) used field trials to monitor and evaluate the performance of engineered soil covers. Their work employed various types of instrumentation to quantify climatic conditions for water balances, soil conditions (water content, temperature and suction), and net fluxes (net percolation, runoff, interflow). All of these measurements are used to evaluate the effectiveness of a specific engineered soil cover in the climate in which it is tested.

O'Kane (1996) and O'Kane *et al.* (1998) describe the instrumentation and monitoring of a test cover constructed at the Equity Silver Mine in British Columbia, Canada. The engineered soil cover (not a CB cover) consisted of a 0.3 m layer of non-compacted till placed over 0.5 m of a compacted till material. These papers described in detail the laboratory program and field instrumentation used to evaluate the performance

of the cover system. Components of the instrumentation program included equipment to measure gaseous oxygen and carbon dioxide, meteorological monitoring, net percolation, soil temperature, matric suction and water content. The field data showed that the lower compacted till layer directly on top of the waste rock maintained a high degree of saturation (90% or higher), which was a positive result as it was designed as a oxygen limiting layer. The net percolation that passed through the cover system into the mine waste was about 5% of the annual precipitation.

Ayres (1998) described the monitoring of two field sites to establish input data for a numerical model. The field sites consisted of one cover system placed on tailings and another on a natural soil surface, both located at a uranium tailings facility at Cluff Lake, Saskatchewan, Canada. It was estimated that the net infiltration through the cover system on the tailings was 9% of the precipitation.

Yanful *et al.*, (1999) explored the testing of different cover soil configurations. Their experiments consisted of a test plot containing a compacted clay layer placed above and below a layer of coarse gravel. One half of the test plot was covered with a coarse stone cap and the other half was covered by a topsoil cap. It was found that the layers of coarse stone used as part of the cover system allowed the compacted till to remain at relatively high degrees of saturation.

Boese (2003) describes the instrumentation and monitoring of test plots constructed in Fort McMurray, Alberta, Canada. The plots consist of 0.35 m, 0.5 m, and 1 m thick cover systems. The cover systems contained a thin layer of peat over varying thicknesses of secondary soil. It was found that only the 1 m thick cover was able to

store sufficient moisture from precipitation to satisfy transpiration requirements for all of the growing seasons.

Adu-Wusu and Yanful. (2006) described the development and monitoring of three different test plots at the Whistle mine near Capreol, Ontario, Canada. Each of the plots consisted of a 0.90 m non-compacted pit-run gravelly sand. The gravelly sand was covered with different materials for each of the test plots: a sand bentonite mixture (0.46 m thick), a sandy silt layer (0.60 m thick) and an 8 mm thick geosynthetic clay liner (GCL). Results from the first three years of monitoring show that the net percolation through the GCL was around 7%. This is compared to 20 % and 59.6% through the sand-bentonite and sandy silt respectively.

A detailed list of instrumentation available for use in the evaluation of soil covers can be found in the works of O'Kane (1996, 1998), Ayres (1998), and Boese (2003). The selection of the types of instrumentation used in this study was based on these works. A comprehensive description of the specific equipment used in this study can be found in Chapter 3.

2.2.5 Water Balance

A water balance analysis is a useful tool in comparing the performance of engineered cover systems. In the context of monitoring moisture movement in cover systems, the water balance may be written as follows (as per Boese, 2003)

$$\Delta S = PPT - R - DP - I - AET \qquad \text{(mm)} \qquad [2.3]$$

where:

ΔS = increase in soil moisture storage;
PPT = precipitation;

R = runoff;

DP = deep percolation;

I = interflow; and,

AET = actual evapotranspiration.

The use of the water balance analysis allows for the change in moisture storage to be calculated. The change in moisture storage can also be measured, and net (deep) percolation can be estimated by comparing the calculated and measured change in storage by varying net percolation in the water balance equation. The amount of percolation can be used as part of the evaluation of the performance of each of the cover systems.

2.3 Geosynthetics

There are many types of geosynthetics that are used to limit moisture movements. This discussion will focus on past work involving geotextiles to limit the movement of water through a CB effect and will not discuss the use of geomembranes or geosynthetic clay barriers. The use of geosynthetics to limit the movement of water has been described by Henry (1990), Henry and Holtz (1995), Stormont and Morris (2000), Park (2005) and Park and Fleming (2005, 2006). The works of Henry (1990) and Henry and Holtz, (1995) focused on the effect of nonwoven geotextiles to limit upward (wicking) movement of water into roadways, helping to limit the affects of frost heave. Stormont and Morris (2000) characterized the hydraulic properties of unsaturated geotextiles and described their use in capillary barrier systems. Park (2005) and Park and Fleming (2005, 2006) described the development of the geosynthetic capillary break (GCB) and verified

its performance in soil cover applications through the use of large column tests and numerical simulations of performance.

2.3.1 Geotextiles as Moisture Limiting Layers

Work by Henry (1990) and Henry and Holtz (2001) showed that the inclusion of a geotextile can be utilized in a capillary barrier system. The laboratory work of Henry (1990) showed that including a geotextile in roadway construction can be beneficial in reducing the upward flow of moisture. The geotextile used in her experiments was a nonwoven, needle-punched polypropylene fabric with a mass per unit area of 500 g/m^2, a nominal thickness of 2.8 mm, an equivalent opening size of 0.15 mm and cross-plane hydraulic conductivity of 0.3 cm/s.

Stormont and Morris (2000) described the results of tests used to characterize the hydraulic properties of nonwoven geotextiles under unsaturated conditions. Two nonwoven geotextiles were tested: one made of polyester (1.8 mm thick, 0.04 mm apparent opening size (AOS), 266 g/m^2) and the other made of polypropylene (5.9 mm thick, 0.18 mm AOS, 340 g/m^2). Their work showed that these nonwoven geotextiles exhibited water retention properties similar to those of coarse uniform sand such that the geotextile has a low hydraulic conductivity under unsaturated conditions.

Column tests performed by Stormont and Morris (2000) evaluated the ability of nonwoven polypropylene geotextiles to limit the downward movement of water. The tests were performed in 100 mm diameter columns 250 mm high. Three columns were prepared for comparison. One column consisted of 50 mm of packed silty sand overlain by geotextile and then overlain by 200 mm of the same silty sand. The lower silty sand in the second column was replaced with coarse sand but still contained the geotextile

between the silty sand and coarse sand layers. The third column consisted of 50 mm of coarse sand overlain by the silty sand with no geotextile. Tensiometers were placed above and below the geotextile, or above and below the interface of the two sand layers in the column that did not contain the geotextile. Initial suction heads were in the 2 to 3 m range.

Water was added to the top of the columns at a constant rate of $2x10^{-4}$ mm/sec while the suction heads were being monitored. All of the columns responded in a similar manner when the advancing wetting front reached the interface. The suction heads above the interface decreased to well below 1 m, while the suction heads below the interface did not change substantially. This shows that downward flow was hindered in each of the columns by the presence of the textural break provided by the geotextile. Eventually "breakthrough" occurred when water moved across the interface. The suction head in the soil just above the interface when breakthrough occurred is taken as the breakthrough pressure head. The observed breakthrough heads showed that breakthrough occurs at lower suction heads in the columns containing the geotextiles (150 and 160 mm) as compared to the column with no geotextile (300 mm). This suggests that the geotextile may provide a better capillary barrier material than the coarse sand. The breakthrough heads in the two columns are very close suggesting that the breakthrough is independent of the underlying material when a geotextile is used. Their work suggests that as long as there is a significant hydraulic contrast between materials to form a capillary break, it does not matter what types of materials are used (coarse grained materials or non-woven geotextiles).

2.3.2 Laboratory Development of a Geosynthetic Capillary Break

Previous work on the development of the GCB has been carried out by Park (2005), Park and Fleming (2005 and 2006), including characterization of the materials utilized in the GCB, and evaluation of the GCB through the use of column tests. The results from their work showed that the inclusion of the GCB in a cover system is beneficial in preventing the mitigation of moisture and oxygen.

2.3.2.1 Materials used in the Geosynthetic Capillary Break

As discussed early, a common capillary barrier cover system consists of coarser grained material, such as sand or gravel, placed below a finer grained material, such as silt. The purpose of the GCB is to create the capillary barrier effect in a prefabricated geosynthetic system. Park (2005) determined that a suitable GCB would contain a finely ground rock flour between a thick geotextile on the bottom with a thin geotextile on top. It was determined that a non-woven, needle punched, continuous-fibre polypropylene geotextile would be suitable for the purpose of the GCB. A product sold by Terrafix Geosynthetics Inc. known as Terrafix 1200R satisfied all the necessary criteria. The finely ground rock flour chosen for use in the GCB is distributed as "Industrial Grade #75" by L.V. Lomas Chemicals in Ontario, Canada. The rock flour is finely ground nepheline syenite rock flour. The grain size distribution for this material is presented in Park (2005) along with other relevant material properties.

2.3.2.2 Hydraulic Properties of Materials

The water retention functions of the two GCB materials and the soils used as tailings and cover soil used in the column experiment were measured using a single specimen pressure plate cell (Fredlund, 2000). The results of the pressure plate tests can be seen in Figure 2-2.

The water retention functions were fitted with the Fredlund and Xing (1994) closed-form equation for a given material, expressed as:

$$\theta_i = \theta_s \left[1 - \frac{\ln(1 + (\psi / h_r))}{\ln(1 + (10^6 / h_r))} \right] \frac{1}{\left[\left\{ \ln[e + (\psi / \alpha_f)^{n_f}] \right\}^{m_f} \right]} \qquad [2.4]$$

where θ_s is the saturated volumetric water content, ψ (kPa) the suction, α_f (kPa) the fitting parameter corresponding to the inflection point, n_f the fitting parameter related to the rate of desaturation of the soil in the transition phase, m_f the fitting parameter related to the curvature of the function in the high suction range and h_r the constant used to represent the soil suction at the residual water content (usually estimated to be 10^6 kPa).

Park (2005) then used the method proposed by Fredlund *et al.* (1994) to predict the unsaturated hydraulic conductivity functions for the materials based on the measured water retention functions and the values of saturated hydraulic conductivity determined in the laboratory (Figure 2-3).

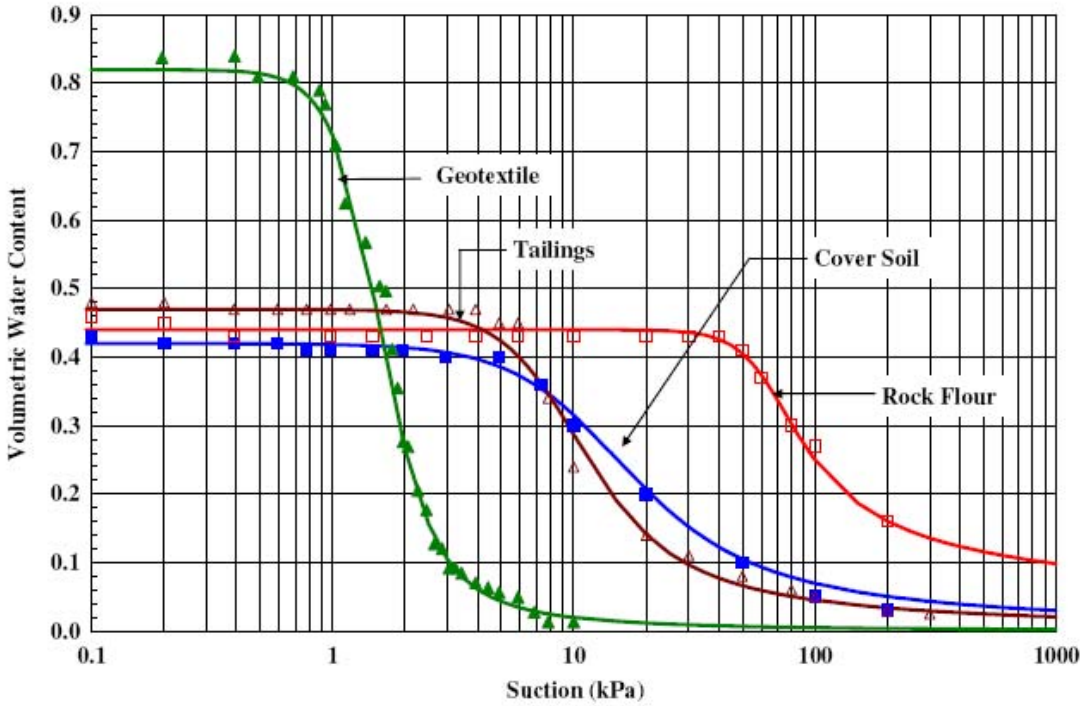

Figure 2-2 Water retention functions of tested materials (Park and Fleming, 2006)

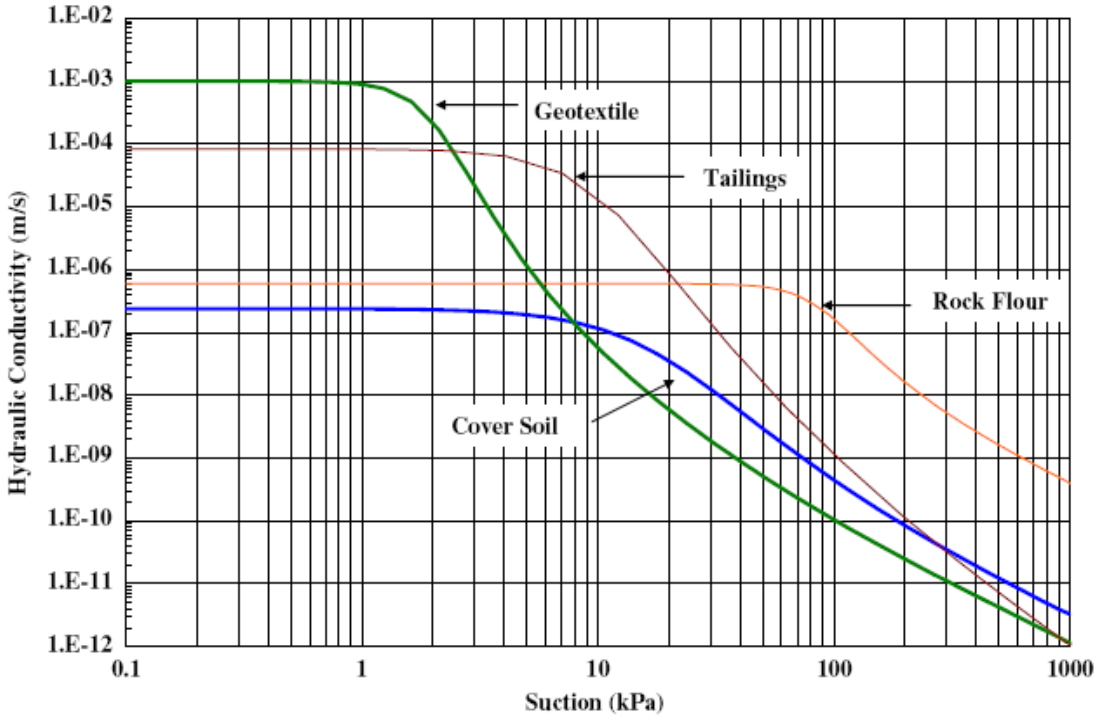

Figure 2-3 Hydraulic conductivity functions of tested materials (Park and Fleming, 2006)

2.3.2.3 Column Tests

One dimensional column tests were performed by Park (2005) to evaluate the performance of the GCB. Columns were set up with and without the GCB under cover soil thicknesses of 0.3 and 0.6 m. The experiments were run under infiltration or evaporation conditions for a period of 10 days. The experiments showed that the movement of moisture was lower in the columns in which the GCB was included.

2.3.2.4 Numerical Simulations

Numerical simulations were undertaken by Park and Fleming (2006). The geometry was based on previously modeled studies by Nicholson *et al.* (1989), Barbour (1990) and Akinidunni *et al.* (1991). A 2.5 m thick layer of tailings was overlain by 1 m of cover soil. The finite element model SEEP/W (Geo-slope International 2004) was used to simulate steady state infiltration rates under unsaturated conditions. The model was run at three different infiltration rates (1×10^{-6} m/s, 1×10^{-7} m/s, and 1×10^{-8} m/s), with and without the GCB between the layer of tailings and cover soil. Figure 2-4 shows the results of the numerical simulation.

It was noted that the inclusion of the GCB reduced the suction just above the tailings cover soil interface. This reduction becomes more pronounced as the infiltration rate decreases from 1×10^{-6} m/s to 1×10^{-8} m/s.

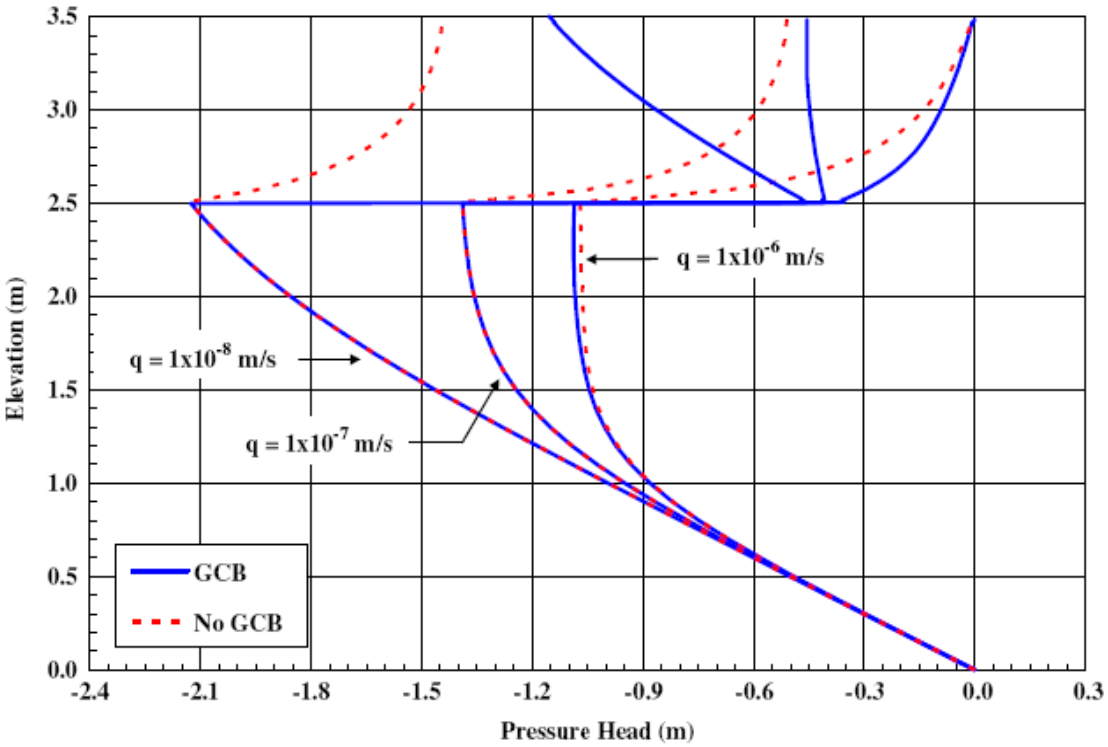

Figure 2-4 Computed pressure profiles (Park and Fleming, 2006)

2.4 Chapter Summary

This chapter described literature relevant to the field evaluation of a geosynthetic capillary break. Section 2.2 illustrated how engineered soil covers can be used to mitigate oxygen and moisture movement into waste and reviewed specific studies that demonstrated the field performance of engineered soil covers. These studies provided a description of instrumentation methods that will be also utilized in this study. Section 2.3 presented a summary of studies in which geotextiles were used to limit water movement under unsaturated conditions. The work of Stormont and Morris (2000) illustrated how the inclusion of a nonwoven polypropylene geotextile can be effectively used as a capillary barrier.

Park (2005) and Park and Fleming (2005, 2006) showed the early development of the GCB. Their work characterized the hydraulic properties of the materials used in the GCB and demonstrated through the use of column tests and numerical simulations how including a GCB in a cover system can be beneficial in mitigating water and oxygen movement into mine waste.

CHAPTER 3 FIELD AND LABORATORY PROGRAM

3.1 Introduction

This chapter describes the design and construction of the test plots used to evaluate the geosynthetic capillary break (GCB). The test sites are located in the tailings management area (TMA) of HudBay in Flin Flon, Manitoba. The details of instrumentation installed at the site; including measurement of water content, matric suction, and meteorological data, is also described. The *in-situ* and laboratory testing program will also be discussed in this chapter.

3.2 Test Plot Design

The purpose of this research is to evaluate the effectiveness of a newly-developed GCB cover system in mitigating the influx of water and oxygen into mine tailings at field scale and to evaluate the affect, if any, of the manufacturing process. The experimental design is based on a side by side comparison of a homogeneous soil cover and a conventional soil cover capillary break system with cover systems that utilize the GCB.

The dimensions of the five test plots (25 m by 25 m) were chosen so that the same construction procedures could be used as those used for full-scale construction. Two of the test plots contain the GCB placed directly on the tailings surface and were covered with 0.3 and 1 m thicknesses of cover soil, respectively. Another test plot consists of 1 m of cover material placed directly on the tailings. The fourth test plot was built as a conventional soil capillary break cover system constructed with 0.2 m of sand placed on

the tailings and covered by 1 m of cover soil. The last plot is a control plot and contains only a thin layer of sand placed directly on top of the tailings to provide dust control. The cover soil used in all of the plots is a locally available material. The properties of this soil are discussed in Chapter 4. A summary of the five test plot cover designs is shown in Table 3-1.

Table 3-1 Test plot description

Test Plot	Cover System Description
A	GCB covered by 1m cover soil
B	1 m cover soil
C	GCB covered by 0.3 m cover soil
D	Conventional sand capillary break 0.2 m thick covered with 1 m cover soil
E	Bare Tailings (Control Plot)

3.3 Test Plot Construction

The test plots were constructed in early October of 2005. At the time of construction, the tailings in the area of the test plots was covered by a 2.5 mm thick layer of sand that acts to prevent dusting of the tailings when they freeze and/or dry. The tailings are fine and thus are susceptible to blowing when dry and exposed to high winds. The sand was scraped away from the tailings over the area in which the test plots were to be constructed. The cover materials were then placed and leveled by the bucket of an excavator to the desired thicknesses.

3.3.1 Construction of a GCB Plot

The GCB was constructed on site by layering a composite GCB over a thick non-woven geotextile. The GCB was assembled on site from the two materials as it was

found to be easier for construction and more cost effective for shipping and manufacturing. The lower layer consisted of an existing product, a non-woven polypropylene geotextile known as 1200R manufactured by Terrafix Geosynthetics Inc. (properties shown in Table 3-2, AOS is the apparent opening size). This geotextile makes up the bottom layer and was placed directly on top of the bare tailings. The top layer is a prototype geosynthetic product also produced by Terrafix Geosynthetics Inc. and was placed directly on top of the 1200R. It consists of a layer of rock flour needle-punched in between a layer of Terrafix 1200R on the bottom and a thin layer of a woven geotextile on top. The purpose of the top geotextile is to hold the rock flour in place.

Table 3-2: Properties of Terrafix 1200R (Park, 2006)

Mass per unit area (g/m^2)	AOS (mm)	Thickness (mm)	Porosity	K_s (m/s)
550	0.05 -0.15	4	0.82	1.5×10^{-3}

All geosynthetic products were placed on the tests plots and rolled out into place. Figure 3-1 illustrates the transport of the GCB composite using an excavator. It was then guided into place by two people while being lowered as shown in Figure 3-2. Figure 3-3 shows the GCB composite (shown in white) being placed over top the nonwoven 1200R, (black). The cover soil was then placed over the resulting GCB geocomposite.

3.3.2 Summary of Construction of Soil Test Plots

The remaining two test plots (Plots B and D) were constructed by placing the cover soil material, and sand in the case of Plot D, with an excavator. The material was hauled to test plots and end dumped beside the test plots. An excavator was then used to place and level the materials to the proper grades.

Figure 3-1 Transportation of GCB roll with excavator

Figure 3-2 Placement of GCB over geotextile

Figure 3-3 GCB placed on top of lower geotextile

3.4 Field Instrumentation Program

The field instrumentation program was designed to monitor the performance of each of the test plots in mitigating water and oxygen from entering the tailings. The instrumentation program was designed in consultation with O'Kane Consultants personnel and was based on previous soil cover monitoring studies, such as O'Kane *et al.* (1998), Ayres (1998), and Boese (2003). Specific parameters that were monitored at the test site include volumetric water content, soil suction, soil temperature, oxygen and carbon dioxide gas concentration, as well as detailed meteorological parameters.

Access tubes were installed in all five of the plots to accommodate manual measurements of water content using the Diviner 2000® portable soil moisture capacitance probe, manufactured by Sentek Sensor Technologies (Sentek, 2004).

Automated water content sensors, manufactured by Sentek Sensor Technologies (Sentek, 2003), and soil suction/temperature sensors, manufactured by Campbell Scientific Inc. (Campbell Scientific Inc, 1993) were installed in the plots containing the GCB overlain by 1 m of cover soil as well as the plot consisting of 1 m of cover soil. These sensors provide real-time, near continuous, readings of water content and suction. A weather station was installed to measure precipitation, temperature, relative humidity, net radiation, and wind speed. Gas sampling ports were installed in each plot to allow oxygen and carbon dioxide concentrations to be measured at various depths within the cover system. Figure 3-4 is a plan view of the layout of the test plots and the instrumentation that was installed. Figure 3-5 shows cross sections of test plots A, B, C, and D.

3.4.1 Volumetric Water Content Measurements

The monitoring of the volumetric water content profiles in each of the plots is very important in evaluating how each of the covers responds to precipitation events. Water content measurements were taken using both manual and automated water content sensors. These measurements allow for the calculation of the moisture storage at various times in each of the plots. This data is then used in water balance calculations.

a) Diviner 2000®

The Diviner 2000® portable soil moisture probe is manufactured by Sentek Sensor Technologies. The system uses Frequency Domain Reflectometry (FDR) to

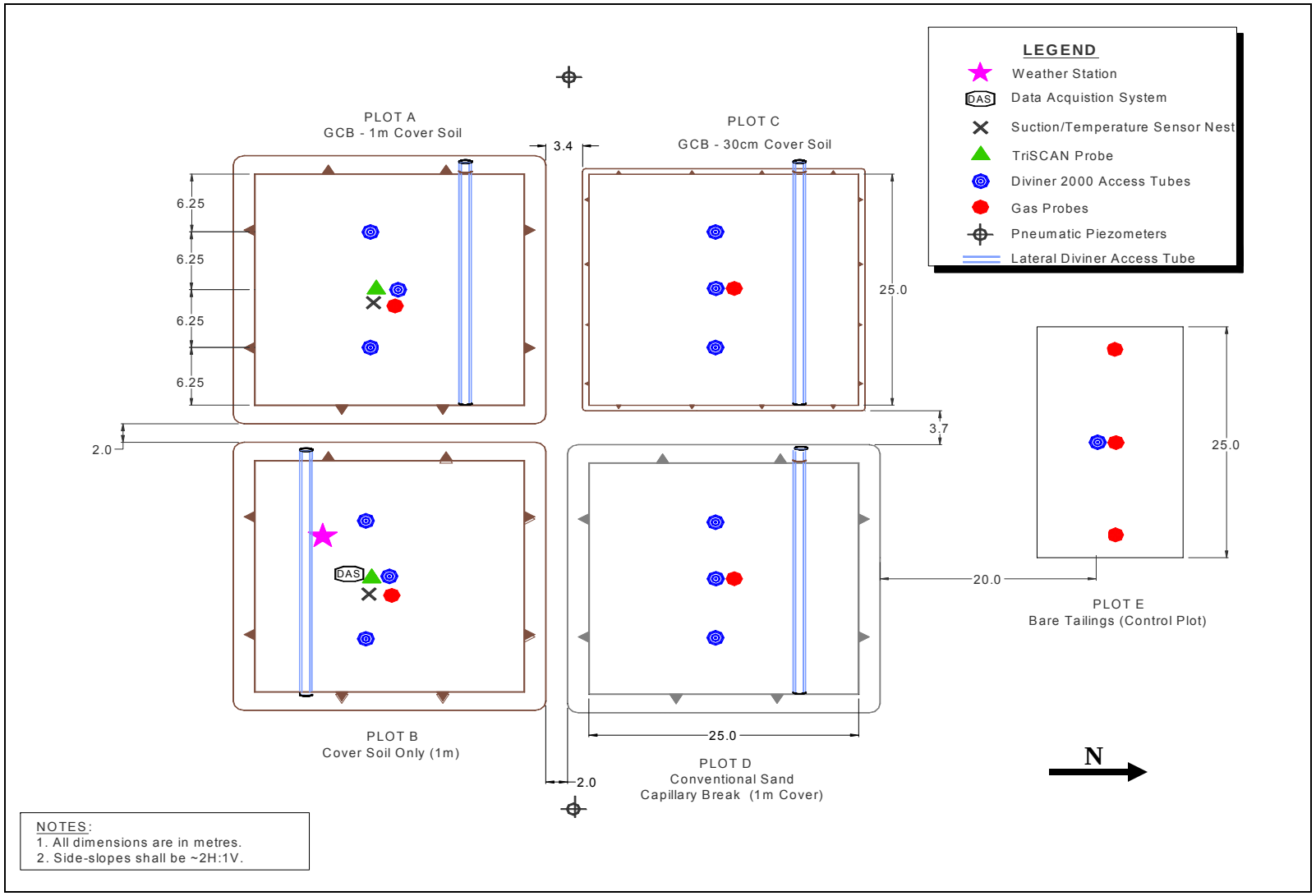

Figure 3-4 Plan view of test plots and instrumentation

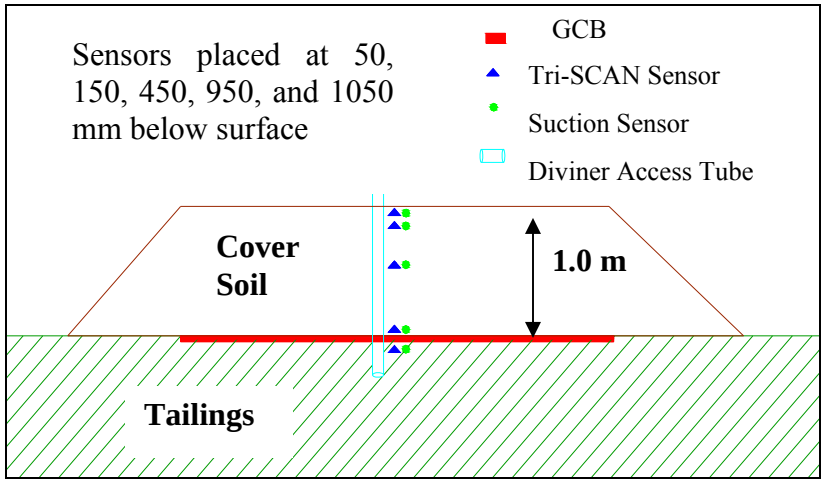

(a) Cross section of Plot A (1 m cover soil over GCB)

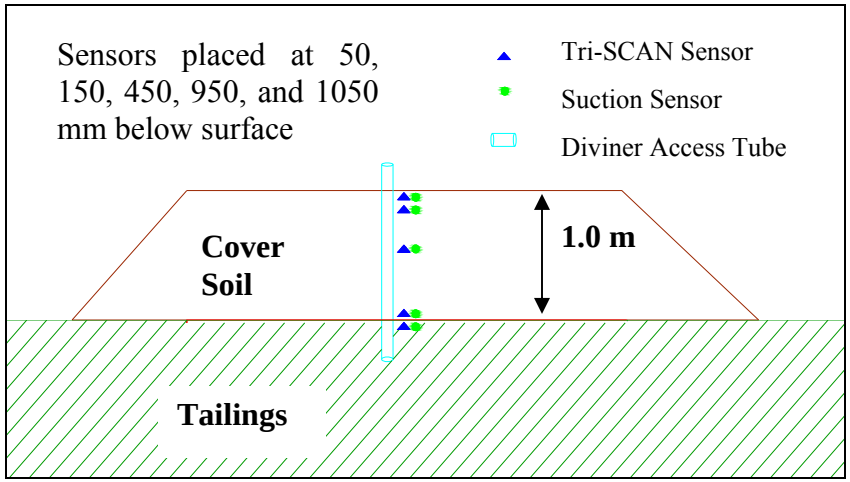

(b) Cross section of Plot B (1m cover only)

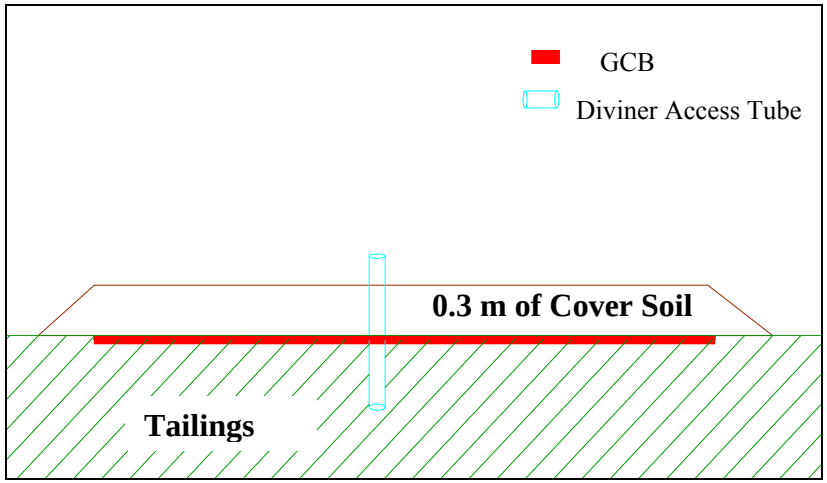

(c) Cross section of Plot C (0.3 m cover soil over GCB)

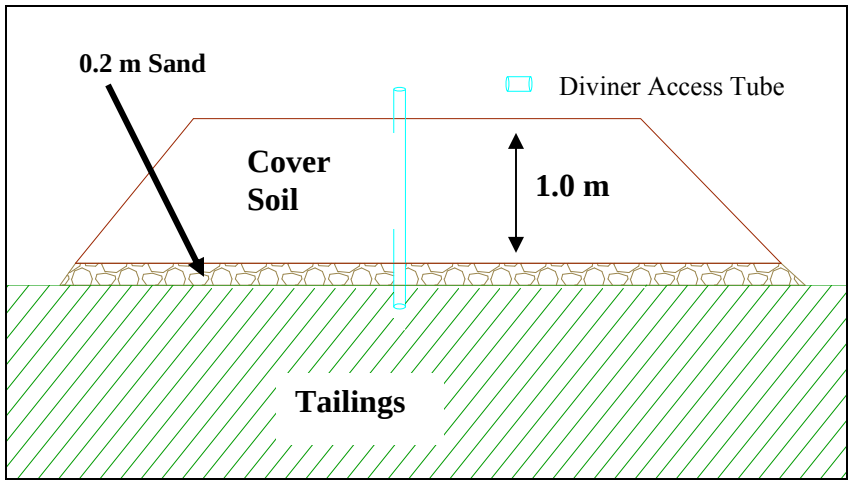

(d) Cross section of Plot D (1m cover soil over 0.2 m sand)

Figure 3-5 Cross sections of test plots A, B, C, and D

obtain near continuous moisture readings throughout the soil profile at discrete times (Sentek, 2004). The probe is connected to a portable display unit which records moisture profiles from the probe and can be downloaded to the laptop computer. The probe takes moisture readings at 0.1 m intervals up to a depth of 1.6 m. When taking a reading, the probe is run down a specially designed PVC access tube installed in the soil.

Three access tubes were installed in each of the five plots. One access tube was installed in the center of the plot, with one 6.25 m east and one 6.25 m west of the center access tube running along an east-west line. The initial design of the instrumentation had specified that two additional tubes be placed on the same side of the center tube in order to define any lateral moisture variations due to edge effects. It was found during construction, however, that the close proximity of the tubes would cause problems for soil placement. It was then determined to evenly space the tubes 6.25 m apart and 6.25 m away from the edge of the plots, as shown in Figure 3-4.

The tubes were installed by a method that is a variation of the procedure outlined by Sentek. The Sentek procedure installs the tubes after the soil has been placed. This is done so that the measurements are representative of the soil in the plots. It was determined that this procedure would not be effective in the plots containing the GCB system, as this would require puncturing and augering through the GCB.

It was determined that for each of the plots, the tubes would be installed into the tailings by the method outlined by Sentek but that the cover soil would be placed around the access tubes. A metal cutting ring was placed on the bottom of the access tube and the tube was driven into the tailings using a sledge hammer and a spacer placed on top of the tube to avoid damage to the tube. Once the tube has been driven a few inches, a

special auger supplied with the Diviner® installation kit was used to remove tailings through the center of the tube. This procedure was repeated until the desire depth was achieved. The soil in the tube was then removed and the tube cleaned using tools in the installation kit. A rubber bung was then placed in the bottom of the tube to ensure a water proof seal. Figure 3-6 shows the installation of a Diviner® access tube. This procedure was done on the bare tailings for Plot B and after the sand was placed on Plot D. In the case of Plots A and C, the tubes were installed along the overlapped seam after the GCB was placed. The lateral Diviner® tubes were installed for future potential profiling of the water content across the test plots, but were not used as part of this investigation due to timing.

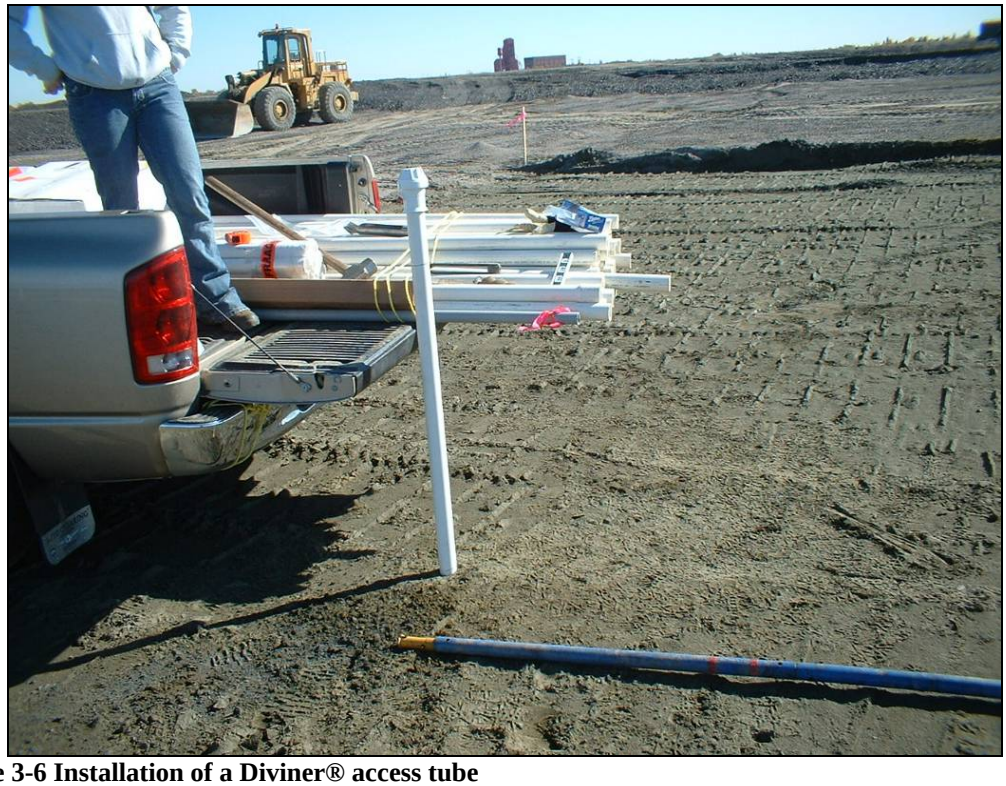

Figure 3-6 Installation of a Diviner® access tube

Figure 3-7 illustrates Plot B after the installation of the access tubes, but before the placement of the cover soil. The cover soil was then placed around the tubes with the bucket of the excavator. The tubes were installed in all of the plots before the cover soil was placed to ensure that a difference in readings between the plots was not caused by a difference in installation techniques. Figure 3-8 shows Plot B after the placement of the cover soil.

Each of the tubes was cut 90 mm above the surface after the cover soil was placed. This allowed for 40 mm of pipe loss (from the installation of the top cap). This results in readings starting at a depth of 50 mm from the surface with subsequent readings taken at 100 mm increments (depths of 50 mm, 150 mm, 250 mm, etc from surface). This allows for readings to be taken directly above and below the cover soil/tailings interface, corresponding to depths of 950 and 1050 mm. The top cap sections were then glued to the top of the access tubes. The top section has a screw off cap that allows for the entry of the probe and provides a waterproof seal when the tube is not in use. Two sets of readings were taken in the fall of 2005, three sets in the spring of 2006, and weekly readings through May to August of 2006. Additional sets of readings were taken in October of 2006 before the ground was frozen, and in May of 2007 after the ground had thawed. It was found after the first few sets of readings that the intervals of 100 mm were too large to capture the thin depth of elevated water contents adjacent to the GCB. A smaller interval of 50 mm was applied to try and capture the water contents in this zone.

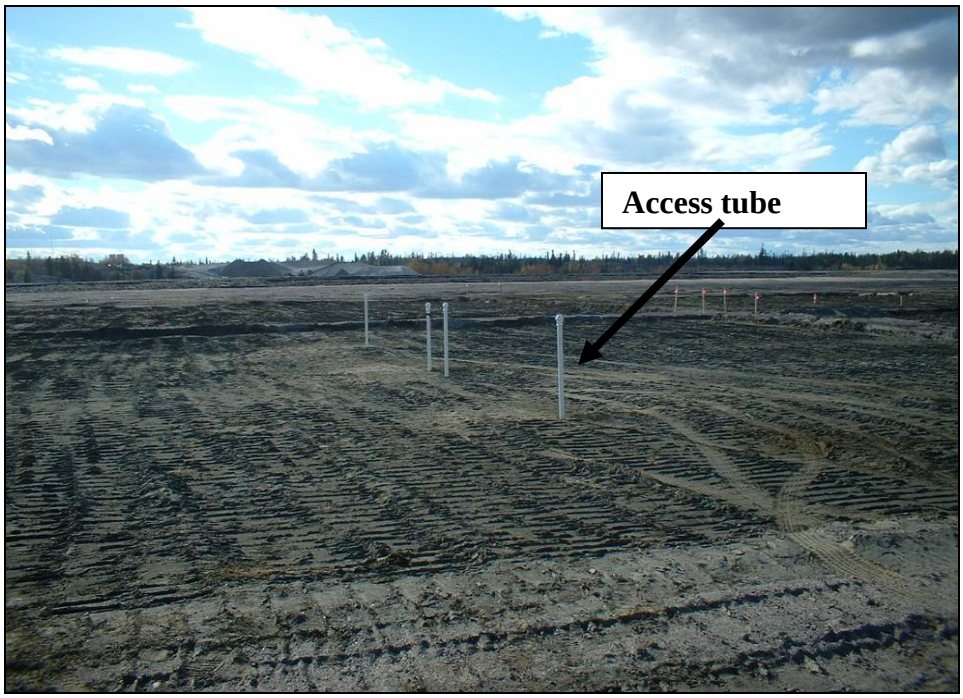

Figure 3-7 Plot B after installation of access tubes before placement of cover soil

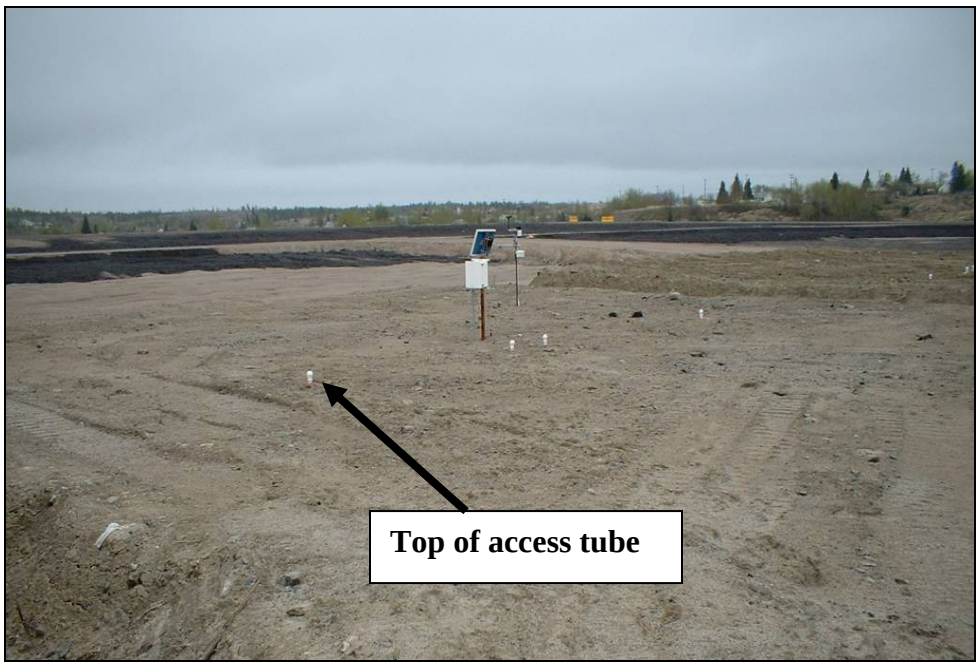

Figure 3-8 Plot B after placement of cover soil

This was accomplished by making a 50 mm spacer out of additional section of PVC tubing and taking two sets of readings for each tube. The first set of readings was done in the original fashion by threading the screw cap of the reading probe into threads on the top of the tube. A second set of readings was then taken by placing the spacer between the probe and the top of the tube. This adjusted all the readings upward by a distance of 50 mm. The two profiles were then combined to form one complete profile with 50 mm increments.

b) Tri-SCAN® Sensors

Sentek Sensor Technologies distributes the Tri-SCAN® sensors. Tri-SCAN® sensors are used for in place continuous monitoring of soil moisture and salinity at discrete depths. The sensors are made to record water content at user specified times. The sensors utilize Frequency Domain Reflectometry (FDR) for both the moisture and salinity measurements (Sentek, 2003). Both the Diviner® and Tri-SCAN® use the same operating principles (FDR) but the Diviner® gives a near continuous water content profile at discrete times while the Tri-SCAN® giving near continuous water contents at discrete depths.

The sensors were attached to a rail placed inside the same access tubes that were used for the Diviner® 2000 system. The rails have attachments for the sensors every 100 mm and allow for up to 15 sensors to be attached. Two access tubes for the Tri-SCAN® sensors were installed; one in the center of Plot A and the other in the center of Plot B as seen in Figure 3-4. The tubes were installed in the same manner as the Diviner® access tubes.

Five sensors were installed in each of the access tubes. The sensors were placed at depths of 50, 150, 450, 950, and 1050 mm from the surface of the cover soil. The depths were chosen to measure the changes in water content at and near the surface, near the middle of the cover soil profile, and also directly above and below the tailings/cover soil interface. A wire from the sensors was connected to the DAS and was buried in a 300 mm trench for protection. The sensors were programmed to read every three hours.

c) Calibration of Water Content Sensors

The Diviner 2000® and the Tri-SCAN® both calculate the volumetric water content using a calibration equation and the measured scaled frequency. The scaled frequency is determined by placing the sensor in a PVC tube and measuring the raw count frequency when the tube is suspended in air and in a water bath. These two readings represent the extreme range of water contents to which the sensors could be exposed. The scaled frequency of a measurement in soil is then calculated by:

$$SF = \frac{(F_A - F_S)}{(F_A - F_W)} \qquad [3.1]$$

where:

F_A = frequency reading in the access tube while suspended in air,
F_S = reading in the access tube in soil,
F_W = reading in the access tube in the water bath.

The scaled frequency readings (ranging from 0 to 1) are then used to calculate the volumetric water content. Both the Diviner 2000® and Tri-SCAN® use the following

formula when calculating the volumetric water content based on the scaled frequency, which is expressed as:

$$VWC = \left[\frac{(SF) - C}{A} \right]^{\frac{1}{B}} \qquad [3.2]$$

where:

VWC = volumetric water content,

SF = scaled frequency,

A,B,C = calibration constants.

The default calibration constants are based on a default material. If a specific calibration for the materials being used at the site is not done, the sensors will only give relative changes in volumetric water content.

A procedure developed by O'Kane Consultants was used to transform the scaled frequency readings from the site to calibrated volumetric water content readings for the site specific materials used in the trials. A 19 L (5 gallon) pail of each material was collected from the site and brought back to O'Kane's office in Saskatoon. The samples were oven dried and allowed to cool to room temperature. The material was then placed in a 19 L pail with a normalization tube placed in the center. The normalization tube is a 609.6 mm (2 feet) section of 50.8 mm (2 inch) PVC tubing with a closed off cone shaped end and is provided with the Diviner 2000® system. The sample is lightly compacted in the five gallon pail. The sensors are placed in the tube and the raw counts are recorded. A small sample is then taken from the pail, weighed, and oven dried to calculate the gravimetric water content. The pail is weighed and the height of sample within the pail is measured. The gravimetric water content, volume and weight of sample are then used to calculate the volumetric water content of the material. Water is then added to the sample

and the procedure is repeated. This procedure is done for approximately 5 or 6 points between oven dry and full saturation. The points are then plotted on a graph as scaled frequency versus volumetric water content. The calibration constants A, B, and C in Equation 3.2 are then adjusted to fit the curve developed from the laboratory calibration. These calibration constants were applied to the scaled frequency readings recorded in the field to obtain calibrated volumetric water content readings from the field. The calibration curves can be found in Appendix A.

3.4.2 Matric Suction and Soil Temperature

CS 229 Soil Moisture Matric Water Potential Sensors were used to measure *in-situ* matric suction and soil temperature. The CS 229 sensors are manufactured and distributed by Campbell Scientific Canada Corp. These sensors use a heat dissipation method for the measurement of matric suction. A 50 mA current is supplied to the sensor's heating element and the thermocouple in the sensor measures the temperature rise. The amount of temperature rise varies with the amount of water in the porous disk, which changes as the surrounding soil wets and dries. A second-order polynomial equation is applied to the temperature rise, which is calibrated in a laboratory for each individual sensor (Campbell Scientific Inc., 1993).

Calibration for all of the CS 229 sensors was completed by O'Kane Consultants. .Five CS 229 sensors were installed along a vertical profile in the center of Plots A and B. At the time the test plots were constructed only four calibrated sensors were available, since the CS 229 sensors require several weeks to calibrate. The four available sensors were installed during the construction of the plots in October of 2005. The deepest two sensors in each of the two plots were installed so that the remaining sensors could be

installed with a minimal amount of disturbance. The two sensors that were installed in each of the plots were placed just below and above the tailings/cover soil interface (Plot B), or just below and above the GCB in the case of Plot A. This corresponds to depths of 950 and 1050 mm from the surface of the finished test plots. These two sensors were connected to the data acquisition system (DAS) in October of 2005.

The remaining 6 sensors were installed in May of 2006 after calibration was complete. The sensors were installed to depths of 450, 150, and 50 mm from the surface of the cover soil in Plots A and B. Each of the five sensor depths in the plots correspond to the depths of the adjacent Tri-SCAN® sensors. A hole was dug with a shovel to a depth of approximately 500 mm in each of the plots. A small hole approximately 300 mm deep was drilled horizontally in the side of holes at the required depths using a cordless drill and a 3/16 inch bit. The CS 229 sensors were then placed in the holes and packed with the cover soil material. The large holes were backfilled and a 300 mm trench was constructed from the location of the sensor nest to the base of the DAS. The wires connected to the DAS were placed in the trench and the trench was backfilled to protect the wires from the elements and wildlife and connected to the DAS.

3.4.3 Meteorological Measurements

Meteorological data is required to develop a water balance. A HOBO micro station manufactured by ONSET Computer Corporation was used to measure air temperature, relative humidity, wind speed, and rainfall. Figure 3-9 shows a picture of these sensors and the data logger. The data logger allows for connection to a laptop though the use of a 9-pin serial connection. The laptop that was used did not have a 9-pin connection, so a 9-pin to USB adapter purchased from Hoskin Scientific was utilized.

The data logger was programmed to take hourly readings with daily maximums, minimums, and averages calculated following downloads.

a) Net Solar Radiation

In order to calculate potential evapotranspiration, net radiation needs to be measured and recorded. The NR-LITE Net Radiometer manufactured by Campbell Scientific Inc. was used to measure net radiation. The NR-LITE consists of a two flat sensors, one pointing up towards the sky and the other facing down towards the surface of the soil. The upward facing sensor measures solar and far infra-red radiation. The downward sensor measures the energy that is reflected from the surface of the soil. The difference in the two readings is calculated and a single output is recorded as net radiation. The NR-LITE is connected to the CR10X control module and downloaded onto the laptop.

3.4.4 Data Acquisition System (DAS)

The data acquisition system (DAS) is an important part of the monitoring system for a site with automated sensors. The automated sensors attached to the DAS allow for the continuous monitoring of parameters with little human interaction once the system is in place. The DAS for this particular project includes a control module, a multiplexer, a current excitation module and a power source, all of which are manufactured by Campbell Scientific Inc. This DAS records measurements from the automated water content sensors, the matric suction/soil temperature sensors, as well as the net radiometer. It allows for connection to a laptop for quick and easy retrieval of recorded measurements. Figure 3-10 shows the DAS with all of its components.

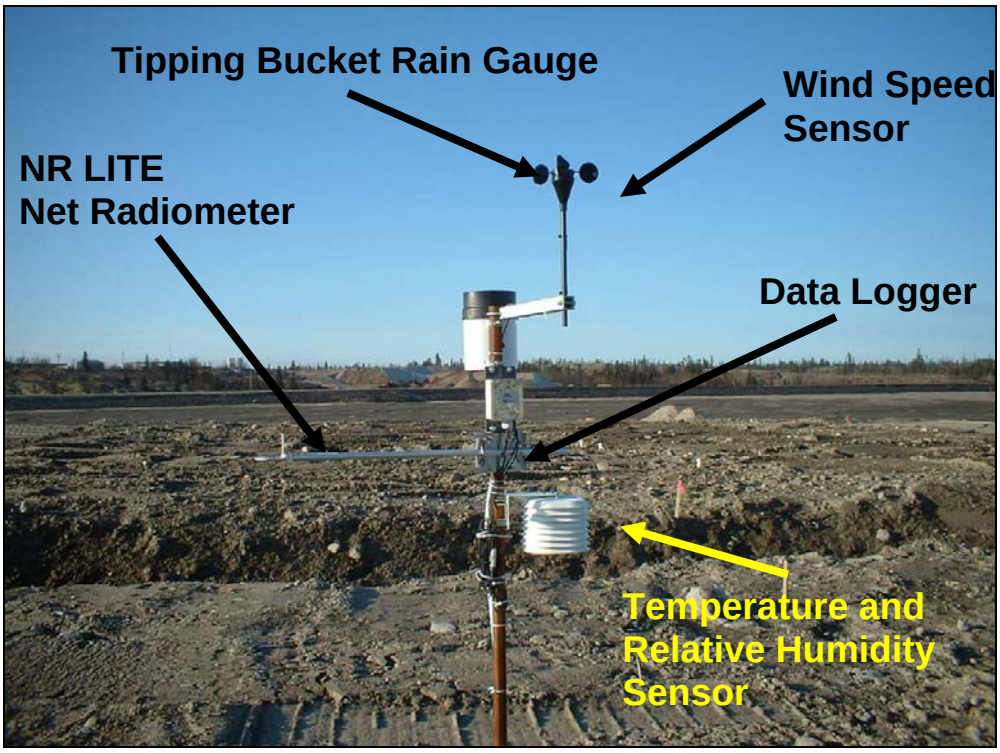

Figure 3-9 Meteorological station

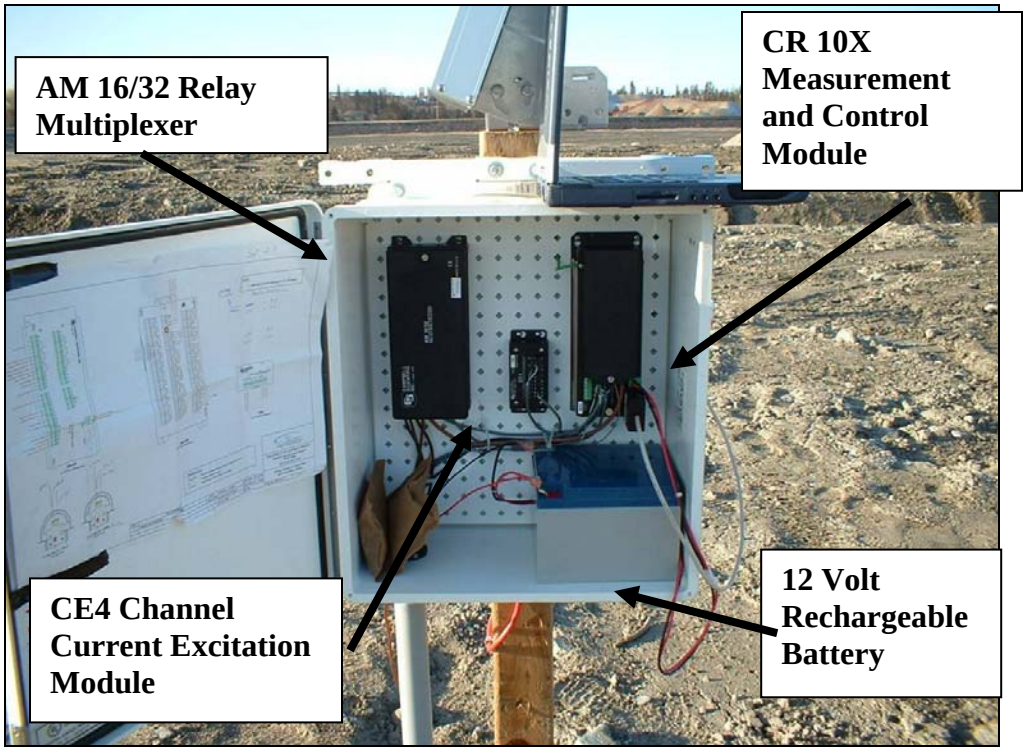

Figure 3-10 Data acquisition system (DAS)

a) Control Module

The CR10X measurement and control module manufactured by Campbell Scientific Corp. was used to collect and store data from the automated sensors. The control module allows for the programming of the data collection program including sensor selection and frequency of readings. The control module has a 9 pin serial port for connection to a laptop computer. This connection is used to transfer control programs and to collect data.

b) Multiplexer

The CR10X only has 6 available connection ports for matric suction/soil temperature sensors. This is exceeded by the number of sensors used in this project (10). Consequently an AM16/32 relay multiplexer was used which allows for up to 16 sensors to be connected to the CR10X while only using one connection port on the CR10X.

c) Current Excitation Module

The CS 299 matric potential/soil temperature sensors require a constant current for the heating element. A CE4 current excitation module was used to supply this current. Continuous power is supplied from the power source to the CE4 through the CR10X.

d) Power Source

The remote location of the sites requires a self sustaining power supply. This is accomplished by the use of a Solarex solar panel and a rechargeable 12 volt battery. Figure 3-11 shows the solar panel which is connected to the 12 volt battery contained within the protective fiberglass enclosure. The battery allows for a continuous power

supply with the solar panel recharging the battery. The daily minimum voltage of the battery is recorded on the CR10X to monitor if the battery and solar panel are working properly. The minimum daily voltage is recorded on the laptop when the control module is downloaded.

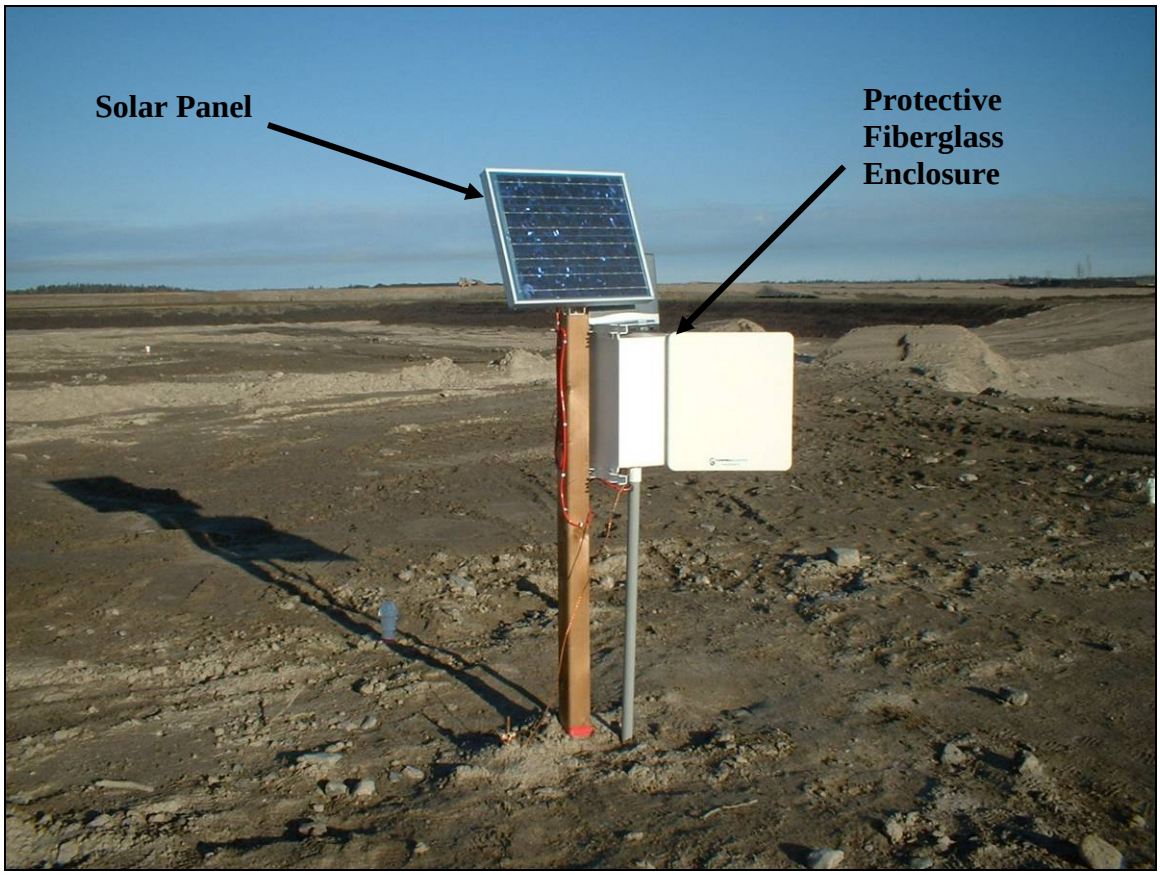

Figure 3-11 Solar panel power source and protective fiberglass enclosure

3.4.5 Piezometers

A slotted screen standpipe piezometer was installed in the same area of the TMA as the test plots in April of 2004. This well is located approximately 200 m northwest of the test plots. The depth to water in the standpipe casing is measured by using an

electronic dip meter. The elevation of the water was calculated from the known elevation of the standpipe casing.

Two P-102-SS Pneumatic Wellpoint Piezometers manufactured by RST Instruments were installed at the beginning of November of 2005. These piezometers are located directly east and west of the test plots, as shown in Figure 3-4. The pneumatic piezometers are read by connecting them to a readout box with a pressurized nitrogen supply. The piezometer tubing is pressurized until a small diaphragm opens when the pore pressure is exceeded. The pore pressure reading at equilibrium is recorded and the hydraulic head at the piezometer tip can be calculated from the known elevation of the piezometer.

Another slotted screen standpipe piezometer was installed directly west (10 m)of the test plots in April of 2006. This standpipe was also read with the electronic dip meter.

3.4.6 Oxygen and Carbon Dioxide Profiles

Gas access ports were installed in the centre of each of the five test plots. The gas ports were constructed using the method used by Strunk (2007) and others. The gas access ports are constructed out of a 1" diameter PVC pipe, porous stone air distributors (as used in fish tank filters), window screen, brake tubing and three way stopcocks. The porous stones are inserted into a section of brake tubing of a desired length and covered by a small section of window screen secured in place by a nylon zip tie. The window screen acts as a filter. The brake line is then attached to the PVC pipe with duct tape. A three-way stop cock is inserted into the top of the brake line and secured with a piece of

wire to ensure an airtight seal. Figure 3-12 (a) shows a PVC pipe with five access ports before installation and Figure 3 12 (b) shows a close up of one of the access ports.

(a) Gas access ports **(b) Close up of access port**

Figure 3-12 Gas access ports

Since it was considered undesirable to auger through the GCB in Plot A (GCB below 1 m of cover soil), it was decided that to measure the oxygen and carbon dioxide concentrations in and below the GCB that a needle attached to the brake line might be effective. The type of needle used to fill sports balls was attached to the one end of the brake line instead of the air distributor stone. The needle was then securely fastened to

the bottom of the PVC pipe. The intent was to puncture the GCB with the needle in order to measure the oxygen and carbon dioxide levels below the GCB.

The gas sampling ports were installed in July of 2006. A hand auger was used to auger a 76.2 mm (3 inch) diameter hole in the center of each of the plots. The PVC pipe containing all of the ports was then inserted into the hole once the desired depth was achieved. Once the PVC pipe was inserted, the hole was then backfilled with alternating layers of sand and bentonite pellets. The sand was placed 70 mm below and above the sampling ports, with bentonite placed between the ports to isolate each zone to be sampled. Approximately 600 mm of the PVC pipe was left exposed for access to the stopcocks and each of the ports was labeled.

A Gastech GT CO_2 portable gas monitor (Thermo Scientific Corp., Lower Thrillsville Ohio, USA) was used to monitor gas concentrations. When measuring gas concentrations the instrument is attached to the stopcocks and the valve opened. The GT CO_2 is equipped with a pump which withdraws air under vacuum from the sampling zone. After the readings stabilize, the concentrations of oxygen and carbon dioxide are recorded and the stopcock is turned to the off position to isolate the port from the atmosphere. A capped 600 mm section of a 76.2 mm (3 inch) diameter PVC pipe was placed over the exposed stopcocks to serve as protection when not in use. Figure 3-13 (a) shows the set of stopcocks exposed after installation, with Figure 3-13 (b) showing the protective cover placed over the exposed tubing. Figure 3-14 illustrates a gas access port while samples are being taken.

(a) Gas access ports after installation **(b) Protective covering over gas ports**

Figure 3-13 Gas access ports and protective covering after installation

Figure 3-14 Gas access ports in use with Gastech GT CO_2 portable gas monitor

3.5 *In-situ* Test Program

In-situ measurements were conducted to quantify the density and hydraulic conductivity of the materials being used. Density was measured using a nuclear density gauge and the field saturated hydraulic conductivity was measured using a Guelph Permeameter. The *in-situ* testing program was completed during the summer of 2006.

3.5.1 *In-Situ* Density

A program to measure the *in-situ* density was completed in August of 2006. A Troxler 3411 nuclear density gauge was used to measure the dry density in the top 609.6 mm (24 inch) of the cover soil profile in each of the plots. The density gauge is the property of HudBay and is used to monitor construction activities around the TMA.

The ASTM Standard Test method D-2922-96, 'Density of Soil and Soil-Aggregate in Place by Nuclear Methods' (ASTM, 1992 b) was followed when using the nuclear density gauge. A steel kick plate is placed on the surface of the cover soil and a steel rod is driven into the soil to the desired depth. The rod is marked in 50.8 mm (2 inch) increments and can be driven into the soil to a maximum depth of 304.8 mm (12 inch) The steel rod is removed and the measuring rod in the density gauge is placed in the newly former hole. The density gauge then measures the wet density and water content. The dry density is calculated using these measurements and is then shown on the display. For measurements below 304.8 mm a hole was dug with a shovel so that a new surface is created in which to place the density gauge. The same procedure of driving the steel rod and placing the density gauge is followed.

The density gauge was calibrated for water content measurements, which are used to calculate the dry density from the wet density readings. Five readings at a depth of

152.4 mm (6 inch) were taken with the density gauge and the water content readings were recorded. Soil samples were then removed from the depth that the water content readings were taken and placed in plastic bags. The samples were taken back to the soil laboratory at the mine and oven dried in order to calculate the gravimetric water content. The difference between the calculated gravimetric water content measured with the density gauge and the samples was used to apply a correction factor that is programmed into the gauge.

There were ten groups of readings completed on each of the plots. Each plot had a cluster of three profiles, with 50.8 mm depth increments, measured at three locations for a total nine profiles on each of the plots in the top 304.8 mm. A 304.8 mm deep hole was dug in Plots A, B, and D in order to record the density from 304.8 mm to 609.6 mm (24 inch). Triplicate readings were taken for each depth. Figure 3-15 illustrates the Troxler Density Gauge in use in a 304.8 mm hole.

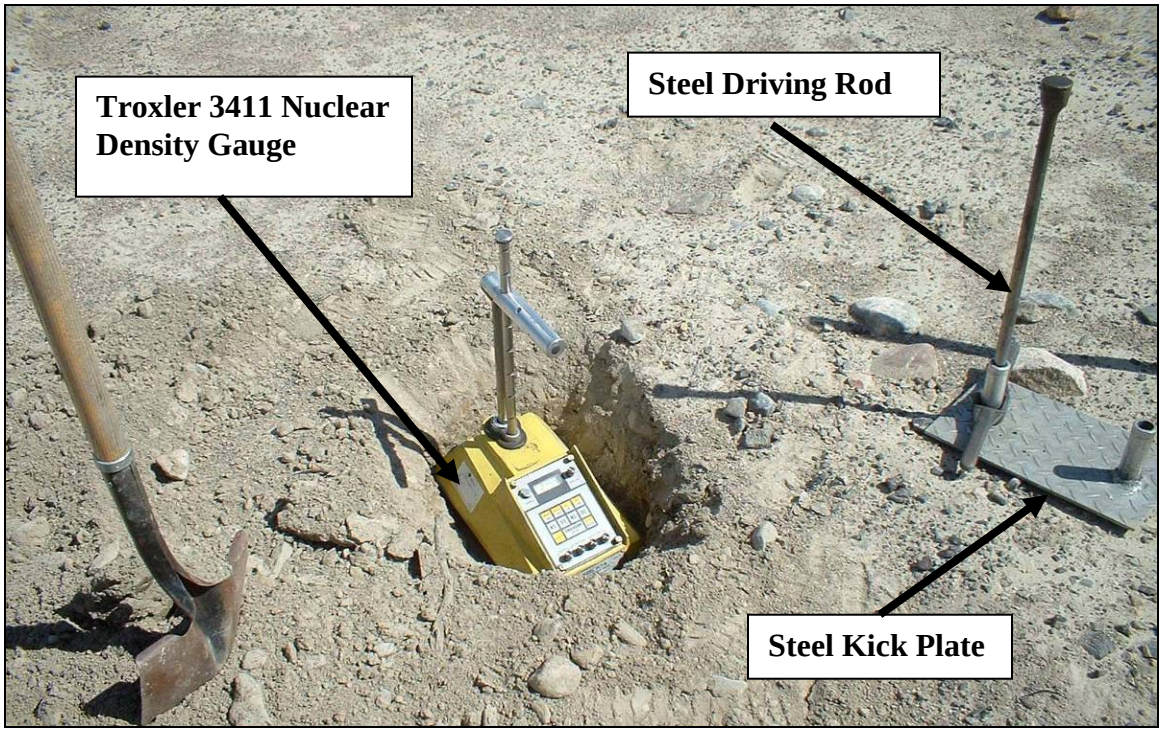

Figure 3-15 Troxler 3411 nuclear density gauge

3.5.2 *In-Situ* Hydraulic Conductivity

A Guelph Permeameter was used to measure the *in-situ* field saturated field hydraulic conductivity. The principle behind the permeameter is to measure the rate of steady infiltration in a hole of known dimensions with water at two different ponding depths. The difference in infiltration rates are used to calculate the field saturated hydraulic conductivity. The Guelph Permeameter has been extensively studied by Reynolds *et al.,* (1983, 1985), Meiers (2002), and has been used by others in estimating the field saturated hydraulic conductivity in cover systems.

The Guelph Permeameter comes with an installation kit that has properly sized tools for making a hole of known dimensions. A coarse auger bit is attached to a handle and is used to auger a hole down to just above the desired depth. A finishing auger is then attached to the handle to make a flat bottom in the hole. In fine grained materials, the auguring process may cause the sides of the hole to become smeared. This can greatly affect the readings, as smearing will slow down the rate in which the water flows and give an unrepresentative value of hydraulic conductivity. For this reason, a scouring tool consisting of a wire brush is attached to the handle and run down the hole. This tool scours the edge of the hole lessening the affects of smearing. Figure 3-16 shows the coarse and finishing auger bits, as well as the scouring tool. For the till used for the cover soil, some smearing could affect the readings, although it would not be as drastic as a material with a higher clay content.

After the hole is properly sized, the Guelph Permeameter is placed in the hole. The Permeameter consists of a water reservoir attached to a tube, a plunger, and a tripod. The reservoir tube is placed in the hole and supplies the water. The plunger at the top of

the assembly is used to set the depth of water in the hole. The entire assembly is supported by a tripod. Figure 3-17 depicts the Guelph Permeameter assembly when in operation.

The plunger is used to set the depth of water in the hole. In accordance with the manual, the first water depth in the hole when taking a reading is set to 50 mm. Water is allowed to flow from the reservoir into the hole to maintain a head of 50 mm. The depth of water remaining in the reservoir is recorded at regular intervals and the difference between intervals is calculated. When the infiltration reaches a steady state, the rate of infiltration is recorded. The plunger is then raised to allow the water depth in the hole to reach 100 mm and the procedure is repeated. The saturated field hydraulic conductivity can be calculated using the formula supplied in the Guelph Permeameter manual or the geometric mean method.

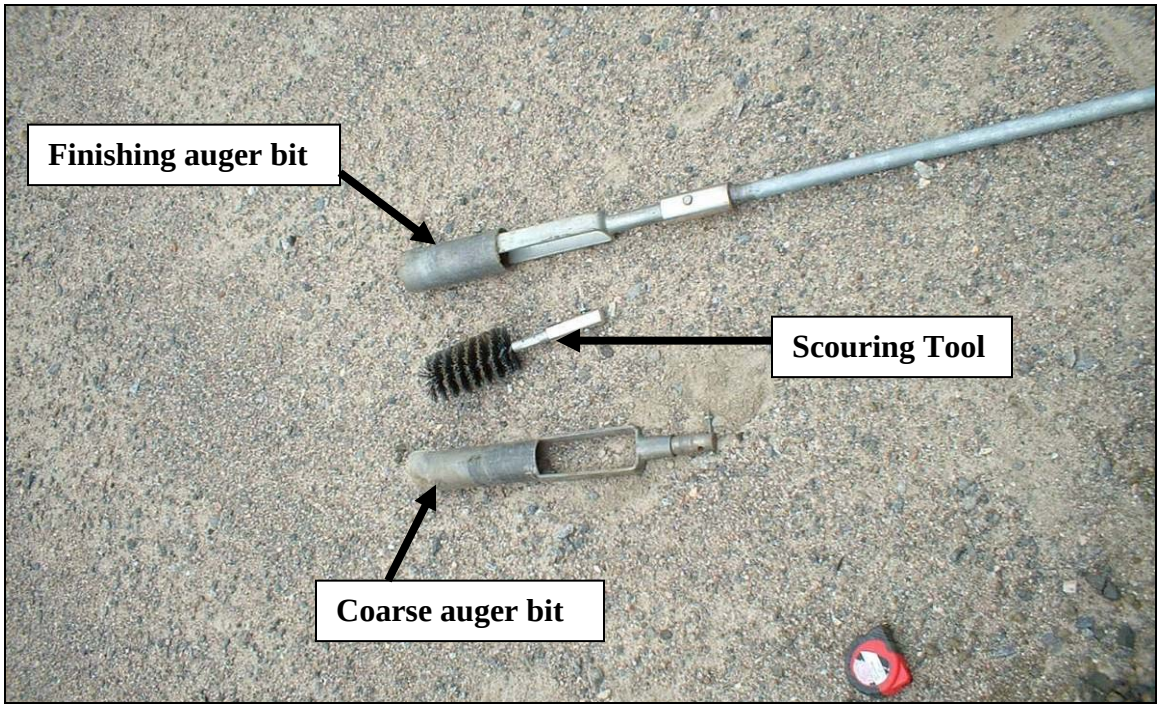

Figure 3-16 Installation tools for Guelph Permeameter

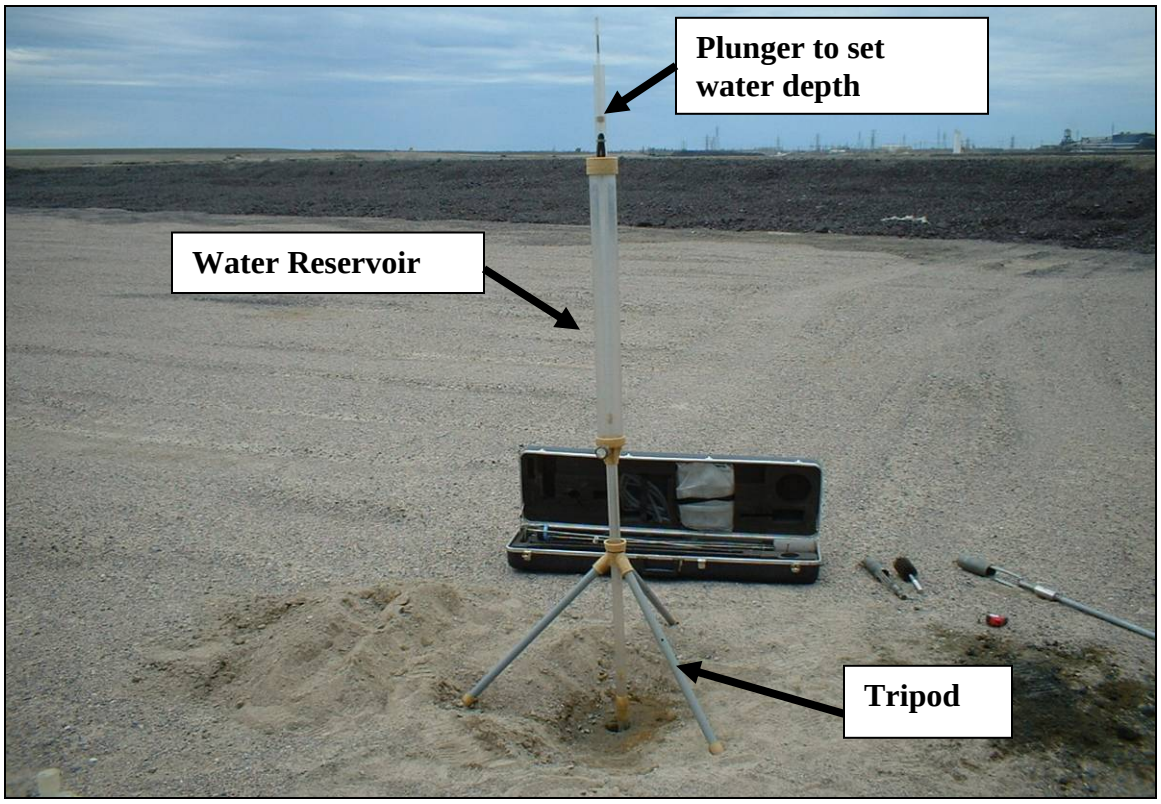

Figure 3-17 Guelph Permeameter

3.6 Laboratory Program

A laboratory program was used to measure properties of the materials being used in the field trials. The laboratory tests include specific gravity, grain size distribution, and standard proctor curves.

3.6.1 Specific Gravity

Samples of the cover soil and tailings were collected and analyzed for specific gravity using the ASTM D854-06 "Standard Test Methods for Specific Gravity of Soil Solids by Water Pycnometer".

3.6.2 Grain Size Distribution

Samples of the cover soil, tailings, and sand were analyzed for grain size distribution. The ASTM standard D422-63 "Standard Test Method for Particle-Size Analysis of Soils" was used for each of the samples.

3.6.3 Laboratory Compaction and Moisture/Density Relationship

In order to use the Troxler 3411, the maximum dry density and optimum water content from a standard proctor curve test needed to be obtained. The ASTM standard D698-00a "Standard Test Methods for Laboratory Compaction Characteristics of Soil Using Standard Effort" was used on a representative sample of the cover soil material.

3.7 Chapter Summary

For the field scale evaluation of the GCB, five plots were designed and built. The plots consisted of four test plots, two of which included the GCB with varying thicknesses of cover soil, one test plot with only cover soil, one plot containing a conventional sand capillary break, as well as a control plot with only a thin layer of sand on top of the tailings to prevent dusting. The test plots were constructed and the majority of the instrumentation was installed in October of 2005. Instrumentation installed included sensors to measure volumetric water content, matric suction, soil temperature, oxygen and carbon dioxide concentrations, as well as a weather station to measure meteorological data. *In-situ* measurements for density and field saturated hydraulic conductivity were completed in the summer of 2006.

CHAPTER 4 DATA PRESENTATION AND DISCUSSION

4.1 Introduction

This chapter presents the findings from the field trials of the GCB. The results from the laboratory, *in-situ* testing, and field monitoring will be presented and discussed. From the collected data, changes in suction, water volumes and water storage are presented and used to compare the performance of each of the test plots. The findings from the gas concentration probes will also be shown and discussed.

4.2 Laboratory Program

The laboratory testing was completed to measure basic geotechnical properties of the materials being used in the field trials. The cover soil and the tailings were tested for grain size and specific gravity. A series of standard proctor tests on the cover soil was also used during material specific calibration of *in-situ* density testing.

4.2.1 Grain Size Analysis

A sample of the cover soil was collected from each of the four test plots, as well as a sample of the tailings from the control plot. A grain size analysis was completed on each of the five samples according to the procedure outlined in Section 3.6.2. Figure 4-1 shows the results from the grain size distribution testing. The results for the four cover soil samples are consistent showing a well graded SM to SC soil. Table 4 1 summarizes the percent gravel, sand, silt, and clay of the five samples. Each of the soil samples

contained 12% gravel, with the percent sand ranging between 54% and 62%. The percent silt ranged from 18% to 26%, and the clay from 4% to 8%.

The tailings are more uniform than the cover soil and are composed primarily of silt sized particles (about 84.5%). The rest of the sample contains 10% fine sand and 5.5% clay sized particles.

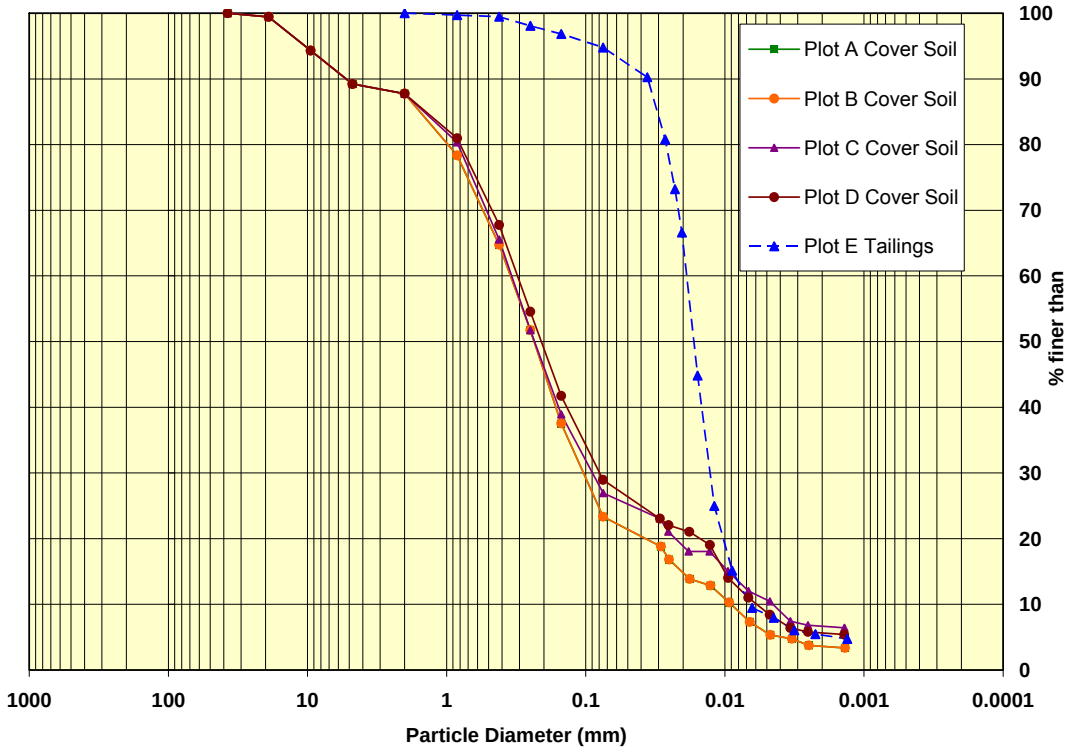

Figure 4-1 Grain size analysis for cover soil and tailings

Table 4-1 Summary of grain size distribution

Plot	Material	% Gravel	% Sand	% Silt	% Clay
A	Cover Soil	12	54	26	8
B	Cover Soil	12	66	18	4
C	Cover Soil	12	62	19	7
D	Cover Soil	12	61	21	6
E	Tailings	0	10	84.5	5.5

4.2.2 Specific Gravity

Four samples of cover soil, one from each of the test plots, and one sample of tailings from the control plot were collected and analyzed for specific gravity (SG) as described in Section 3.6.1. Two tests were completed on each of the five samples. Table 4-2 summarizes the results of the specific gravity testing.

Table 4-2 Summary of specific gravity testing (g/cm^3)

	Run 1	Run 2	Average
Plot A Cover Soil	2.64	2.68	2.66
Plot B Cover Soil	2.70	2.70	2.70
Plot C Cover Soil	2.65	2.61	2.63
Plot D Cover Soil	2.66	2.61	2.64
		Average	**2.65**
Plot E Tailings	**3.02**	**2.81**	**2.92**
		Average	**2.92**

The specific gravity of the four cover soil samples had a maximum value of 2.70 and a minimum value of 2.61, with an average of 2.65 for the eight tests completed. The specific gravity of the tailings had a maximum value of 3.02 and a minimum value of 2.81, with an average of 2.92.

4.2.3 Standard Proctor Curve

A large composite sample of cover soil was collected from the four test plots and a standard Proctor test was completed. Figure 4-2 illustrates the results from the standard Proctor testing. The optimum water content is approximately 7.5%, with a maximum dry density of 2100 kg/m^3.

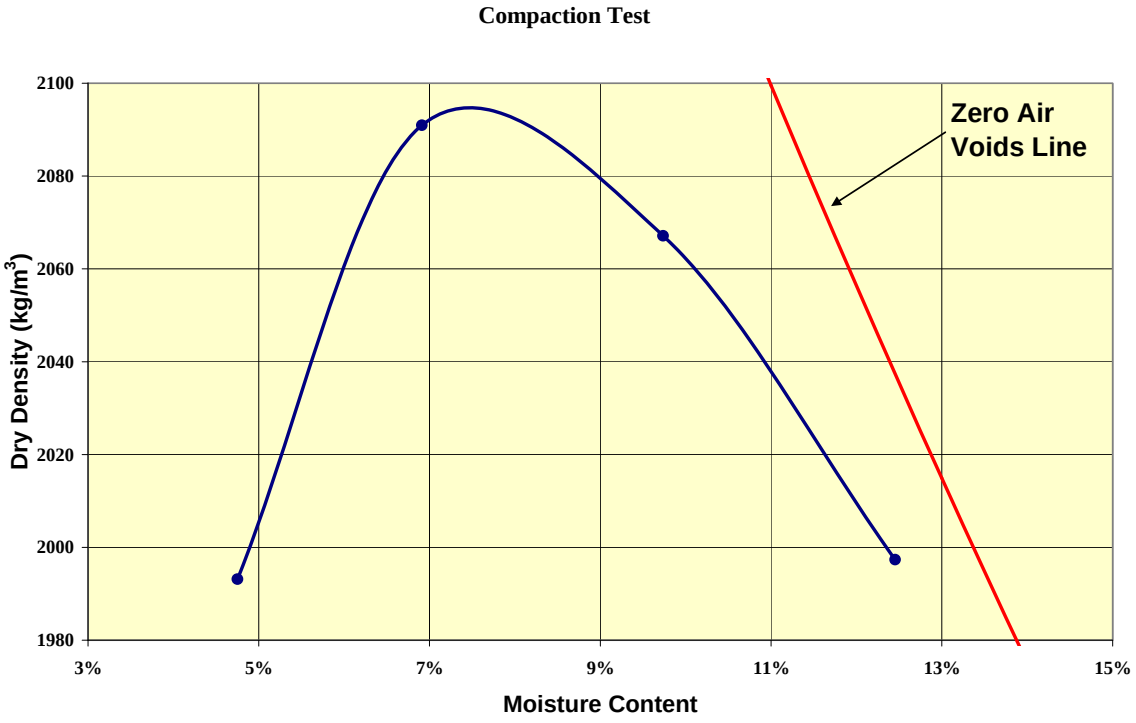

Figure 4-2 Standard Proctor curve for cover soil

4.2.4 Estimation of Hydraulic Properties for Cover Soil

The water retention and hydraulic conductivity functions and for the tailings and the materials used in the GCB (rock flour and geotextile) were completed by Park (2005) and are presented in Section 2.3.2.2. The functions found by Park for these materials were used in this study. The hydraulic properties of the cover were estimated using the grain size distribution and the modified Kovács method (Kovács, 1981) provided in the GeoStudio software (2004). The software can estimate the water retention function of a given material from the grain size distribution and the porosity. Figure 4-3 shows the estimated water retention function. The porosity used is a representative of the results of the density testing (discussed in Section 4.3.1).

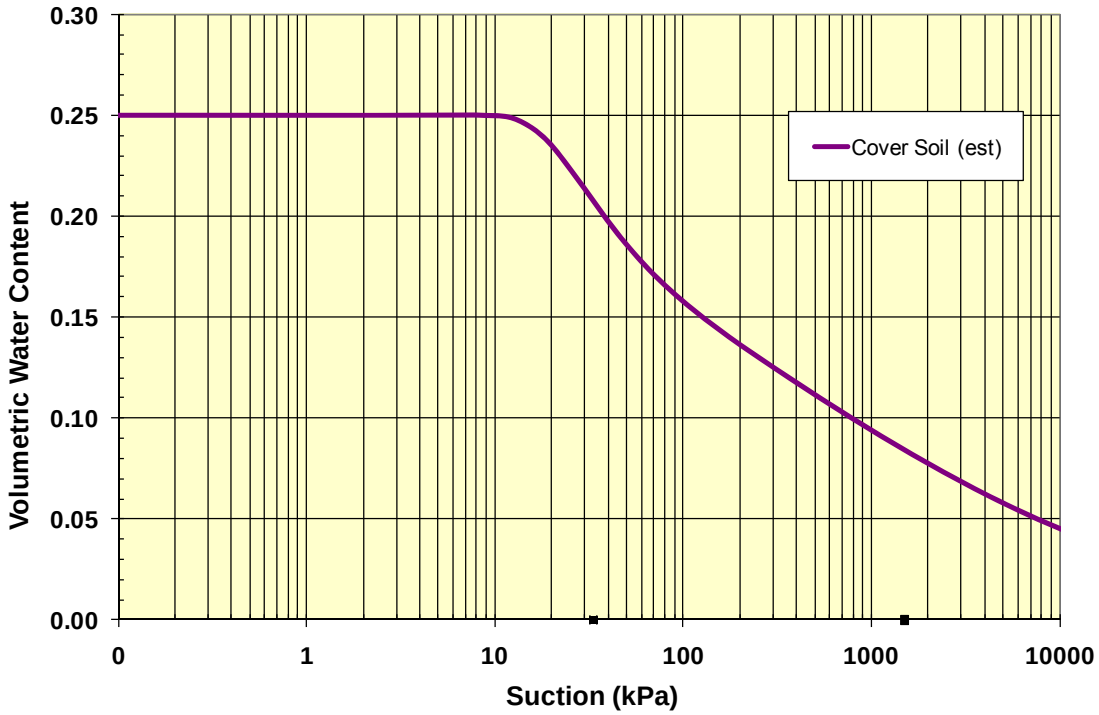

Figure 4-3 Estimated water retention function for cover soil

4.3 *In-situ* Test Program

In-situ testing was completed in order to quantify the dry density and field saturated hydraulic conductivity of the test covers. All of the testing was completed in the summer of 2006, approximately 9 months after the construction of the test covers. Dry density tests were completed on each of the four test covers, and field saturated hydraulic conductivity testing was undertaken on all plots with the use of a Guelph Permeameter.

4.3.1 *In-Situ* Dry Density

The *in-situ* dry density testing was completed on the top 250 mm of all four soil covered test plots, and down to 600 mm for Plots A, B, and D. Figure 4-4 shows the results of the

dry density testing, with the average dry density at each depth and the extent of the maximum/minimum measured. At each depth above 300 mm 27 tests were conducted at each depth interval. For the depths between 300 and 600 mm, 9 tests were completed at each depth. The average dry density ($\rho_{dry)}$ for each plot at a given depth is represented by the symbols, with the maximum and minimums at each depth represented by the error bars. All four plots show a similar trend in the top 300 mm. The dry density increased slightly with depth for each of the four plots. The increase in density with depth could be an artifact of the placement method. The cover soil was placed by an excavator and because of the size of the plots the soil had to be driven on. This would result in the deeper layers being driven on more times than the shallower layers. This may be the cause for the increase in density with depth. The sudden decrease in density at a depth of 360 mm is most likely due to an error caused by the method of testing. This is the depth at which a hole is required to be dug and the density gauge placed in. The decrease in density may be a result of the disturbance of the soil during the hole excavation. Table 4-3 shows a summary of the dry density testing in the top 300 m of testing. The data from below 300 mm was discounter due expected error in the testing method. Even though there is a large variation in the results in the testing, the average dry density for the four plots is similar. Plot A had the lowest average dry density (1895 kg/m^3) and Plot D had the highest average dry density (2040 kg/m^3). The porosity (n) was calculated using the specific gravity found in Section 4.2.2, the dry density testing results, and the equation $n = 1-(\rho_{dry}/SG)$.

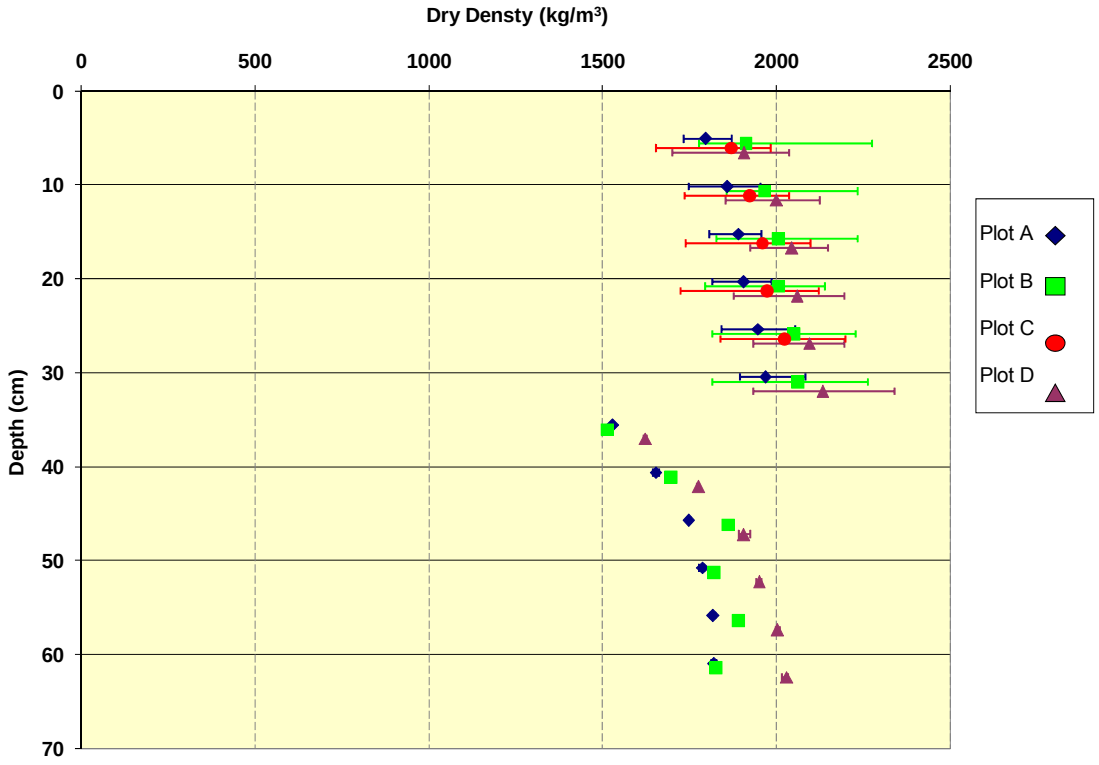

Figure 4-4 Dry density testing results

Table 4-3 Summary of *in-situ* dry density testing above 300 mm

Plot	# of Tests	Maximum Dry Denisty (kg/m^3)	Minimum Dry Denisty (kg/m^3)	Average Dry Denisty (kg/m^3)	Standard Deviation Dry Density	Maximum Porosity (n)	Mimimum Porosity (n)	Average Porosity (n)
A	162	2083	1733	1895	75	0.35	0.22	0.29
B	162	2276	1778	2001	122	0.34	0.16	0.26
C	135	2199	1655	1951	120	0.37	0.16	0.26
D	162	2340	1702	2040	118	0.35	0.11	0.23

4.3.2 *In-Situ* Hydraulic Conductivity

A Guelph Permeameter, as described in Section 3.5.2, was used to measure field saturated hydraulic conductivity (K_{fs}). Five tests were carried out on the cover soil, including one shallow test in each of the four plots and one deep test on Plot B. Deeper tests were tried on Plots A and D but the gravel and cobble content of the cover soil made it very difficult to auger a proper hole as required for the Guelph permeameter. The

tailings on the control plot were very easy to auger. Four tests were carried out on the control plot, two shallow and two deep. The results from the Guelph testing can be found in Table 4-4. The average K_{fs} for each of the materials can be found in Table 4-5. The geometric mean method described by Meiers (2002) was used to calculate the K_{fs} from the results of the Guelph tests.

Table 4-4 Summary of *in-situ* hydraulic conductivity testing

Plot	Material	Depth (mm)	K_{fs} (m/s)
A	Cover Soil	170	6.5E-07
B	Cover Soil	200	2.7E-07
B	Cover Soil	800	1.4E-06
C	Cover Soil	200	6.9E-07
D	Cover Soil	220	3.6E-07
E	Tailings	250	9.9E-06
E	Tailings	750	1.0E-05
E	Tailings	300	2.1E-05
E	Tailings	900	2.7E-05

Table 4-5 Average field saturated hydraulic conductivity

	Average K_{fs} (m/s)
Cover Soil	6.6E-07
Tailings	1.7E-05

4.4 Meteorological Measurements

Meteorological measurements have been taken since the end of October of 2005 with the weather station that was described in Section 3.4.2. The sensors were programmed to take hourly readings. Daily max, min, and averages were calculated from the hourly data after they were downloaded from the logger and can be seen in Appendix B.

4.4.1 Precipitation

Precipitation in the form of rainfall was recorded by the use of a tipping bucket rain gauge. The rain gauge was in operation starting at the end of November of 2005. Figure 4-5 shows the daily and cumulative rainfall recorded by the data logger. There were two fairly major precipitation events recorded during the summer and fall of 2006. On August 5 and September 18 the daily rainfall exceeded 40 mm. For the 2006 calendar year, the total recorded rainfall was 411 mm. This exceeds the yearly average rainfall of 343 mm (Environment Canada National Climate Archive, years 1971 – 2005).

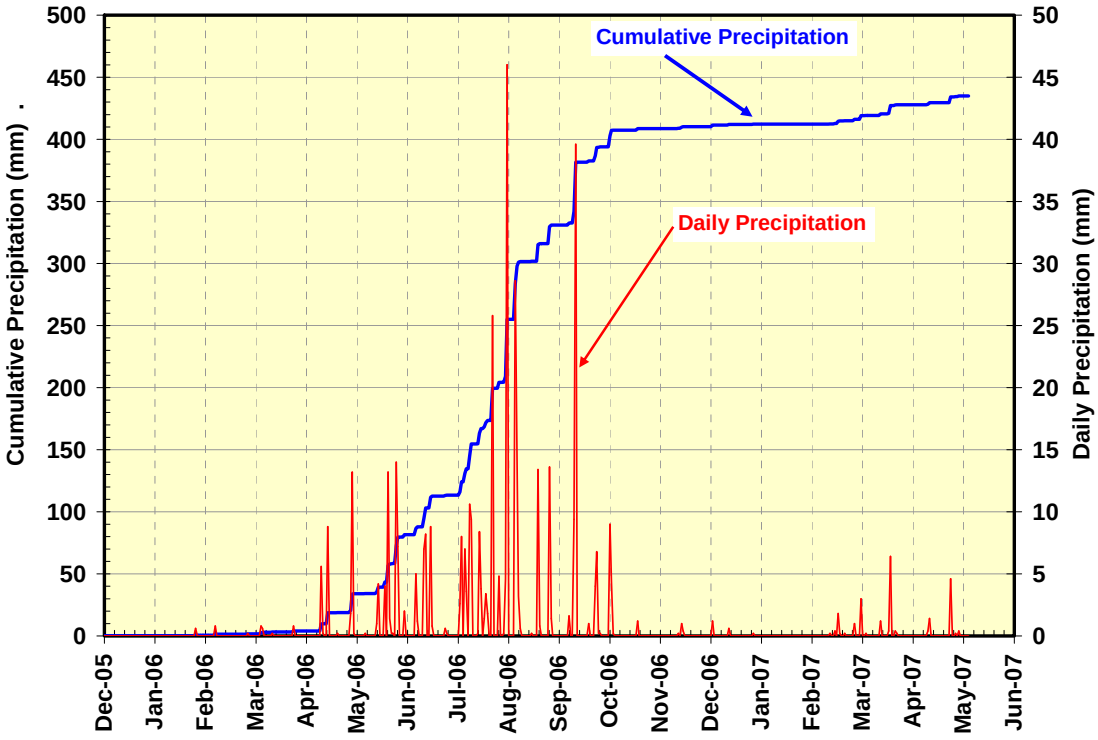

Figure 4-5 Daily and cumulative precipitation from rainfall

4.4.2 Air Temperature

Figure 4-6 shows the daily maximum, minimum, and average air temperature that was calculated from the recorded hourly readings collected from the weather station. The temperature was above freezing for the 2006 calendar year at the beginning of April. The maximum temperature recorded in the summer of 2006 was 33°C recorded on July 6. The air temperature fell below 0°C in the fall of 2006 near the end of October.

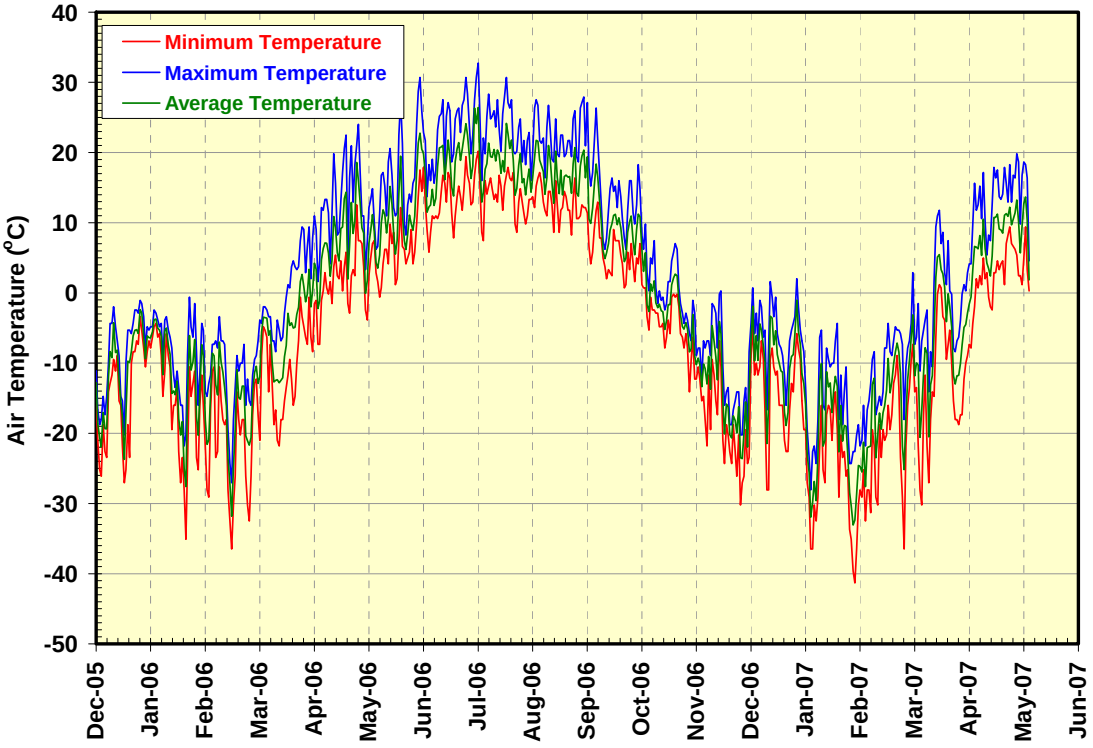

Figure 4-6 Recorded air temperature data

4.4.3 Net Radiation

Figure 4-7 shows the daily and cumulative net radiation that was measured with the NR LITE Net Radiometer. For the summer months of 2006, the cumulative net radiation was slightly over 1200 MJ/m^2. The peak daily net radiation in 2006 was 14 MJ/m^2 recorded on July 9.

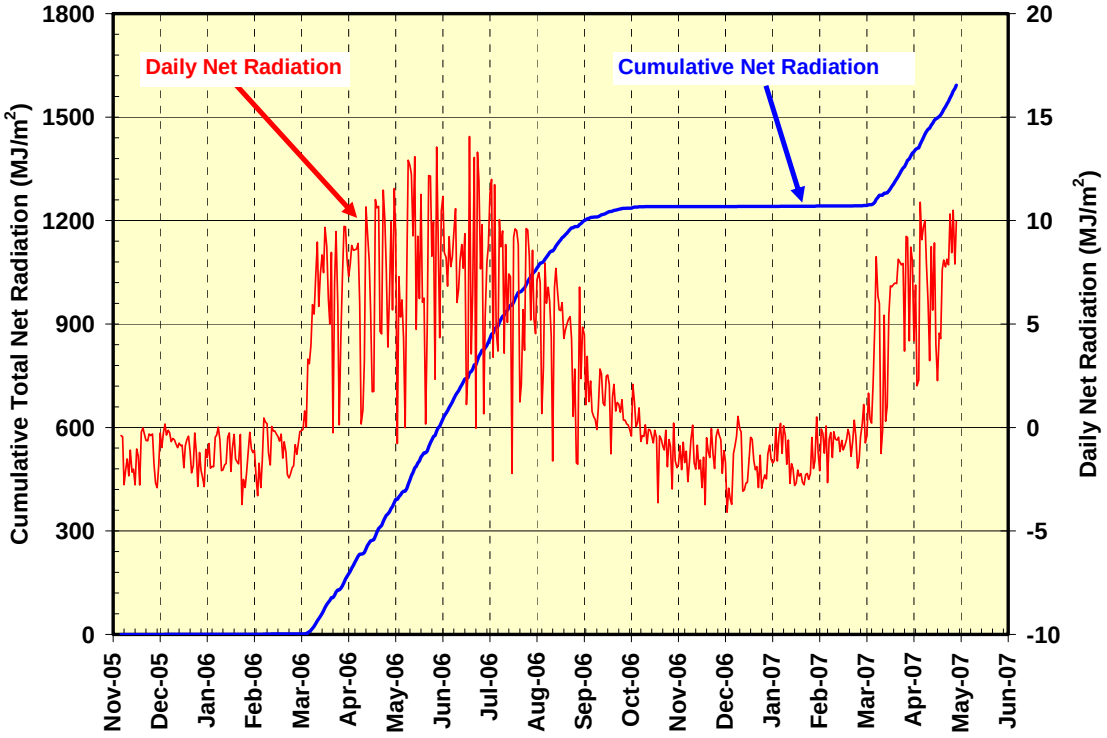

Figure 4-7 Recorded net radiation data

4.4.4 Relative Humidity

Figure 4-8 shows the daily average, maximum, and minimum relative humidity that was recorded with the meteorological station. This data along with air temperature, net radiation and wind speed was used to calculate potential evapotranspiration.

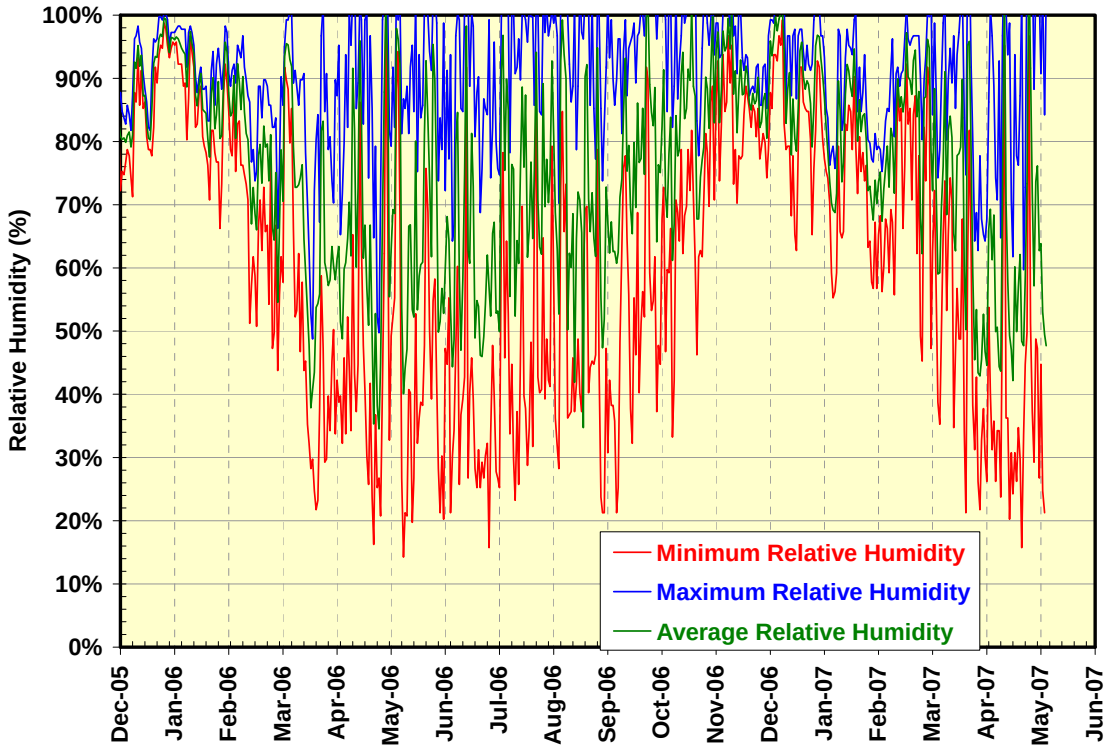

Figure 4-8 Recorded relative humidity data

4.4.5 Potential Evapotranspiration

The Penman Method (Penman, 1948) is a method to calculate potential evaporation (PE) rates from recorded meteorological measurements of air temperature, windspeed, relative humidity, and net radiation data. Figure 4-9 illustrates the daily and cumulative potential evapotranspiration calculated with the use of the Penman Method. Negative PE values are regarded as a net of 0, as can be seen in the winter months. In 2006, the cumulative PE from March to October was 560 mm.

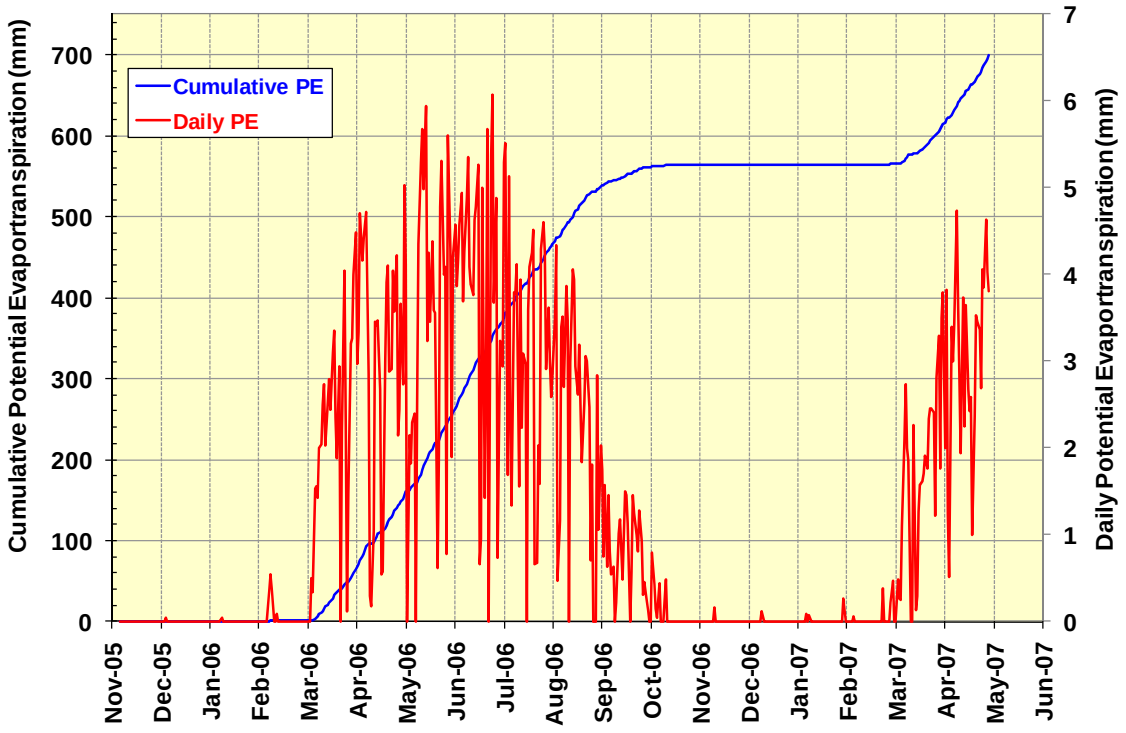

Figure 4-9 Potential evapotranspiration

4.5 Piezometers

Two pneumatic piezometers and one slotted screen standpipe piezometer were installed directly next to the test plots to augment data collected from the existing slotted screen standpipe located approximately 200 m away. The pneumatic piezometer installed to the west of the test plots was destroyed by birds. A splice kit was used to repair the broken tubing, but that too was destroyed by birds. Figure 4-10 shows the depth to the phreatic surface based on readings from the remaining three piezometers referenced to the surface of the tailings. The results show that the water table is fairly constant between 4 an 4.5 m below the tailings surface.

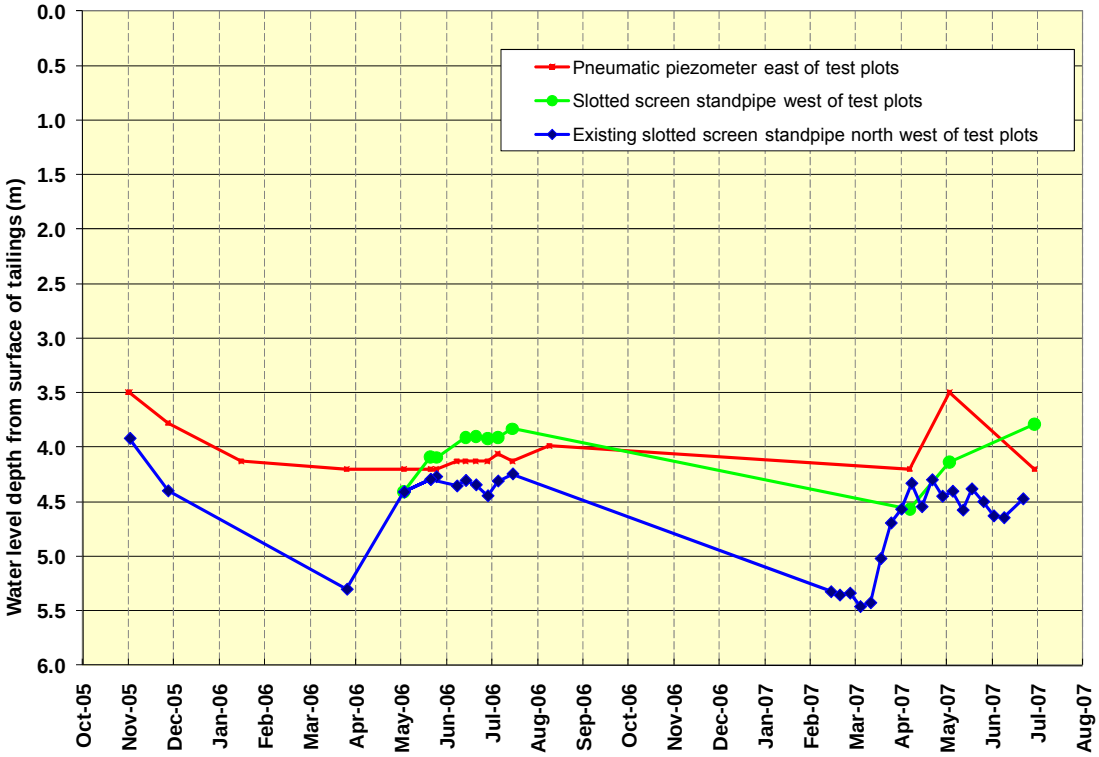

Figure 4-10 Piezometer readings

4.6 *In-Situ* Soil Temperature

Figures 4-11 and 4-12 show the recorded soil temperatures for Plots A and B respectively. Soil temperature/matric suction sensors were installed at depths of 950 and 1050 mm below the surface in Plots A and B in the fall of 2005. Three more sensors were installed in the early summer of 2006 at depths of 50, 150, and 450 mm from the surface in those same two plots. The sensor on Plot A at 1050 mm depth was damaged in the fall of 2006.

The two sensors at depths of 950 and 1050 mm recorded that the ground at that depth was above freezing in late April of 2006. The maximum temperature in the summer of 2006 for the top sensor (50 mm depth) for both plots was slightly above 30^{o}C.

The deepest two sensors in both plots reached maximums of slightly above 15°C. Freezing of the soil in fall of 2006 began on October 20 for the top two sensors (50 and 150 mm), November 12 for the middle sensor (450 mm) and December 5 for the bottom two sensors (950 and 1050 mm). The data from the soil temperature sensors was used to determine at what times each soil layer was frozen. This is important because all of the water content and matric suction sensors only give proper readings when the ground is not frozen. The soil temperature data allows for the removal of erroneous data caused by taking readings when the ground is frozen.

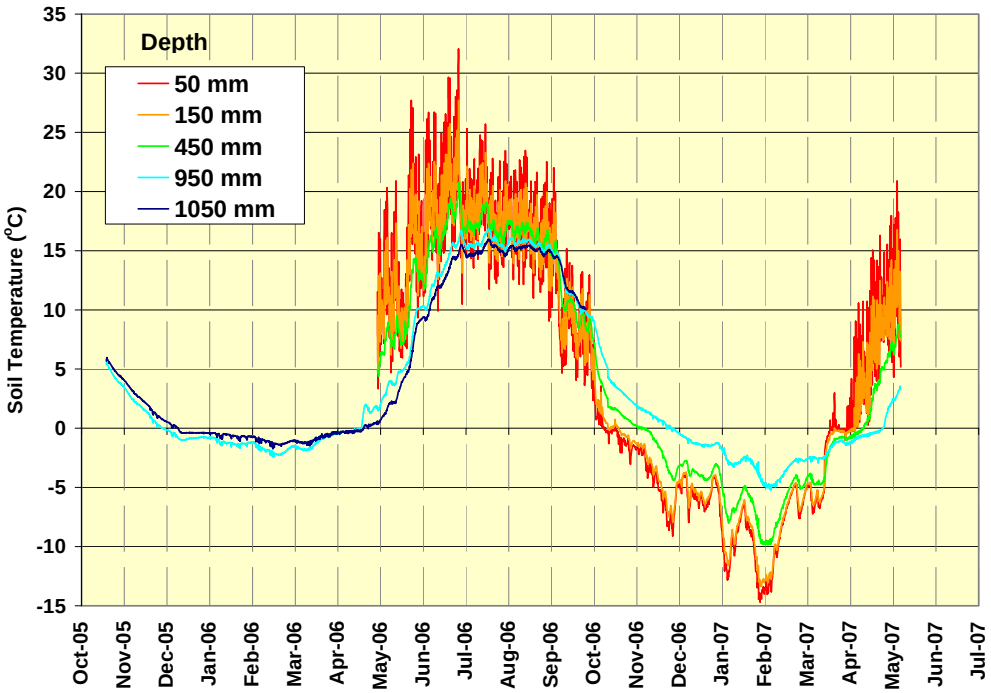

Figure 4-11 Soil temperature data for Plot A

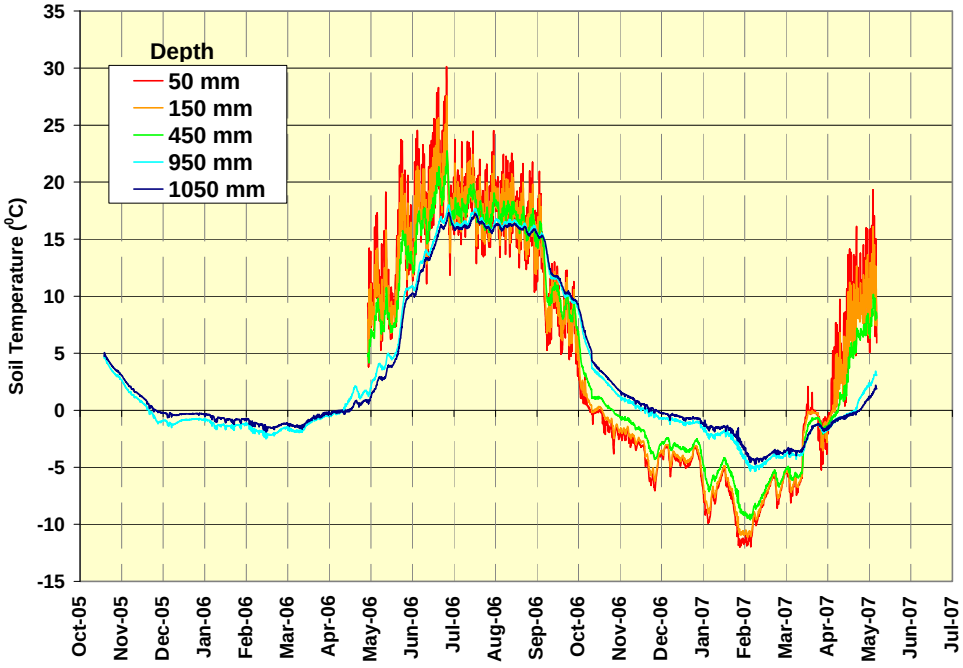

Figure 4-12 Soil Temperature data for Plot B

4.7 Matric Suction

Figures 4-13 and 4-14 show the matric suction and daily precipitation readings from Plots A and B respectively. The graphs show the months of May through October when the ground is not frozen. The normal range over which the sensors are considered accurate is between approximately 1 kPa and 4000 kPa. The sensors will read below 1 kPa but are not considered reliable, conservatively the measured data below 1 kPa has been removed from the graphs.

The results show a clear reduction in suction across the GCB in Plot A (Figure 4-13). The suction sensors installed in the tailings (1050 mm) are similar in the two plots at around 40 kPa, which is consistent with the measured depth to the water table of approximately 4 m. The sensor at the 950 mm depth in Plot B shows suction around 40 kPa, similar to that of the sensor in the tailings while the sensor at the same

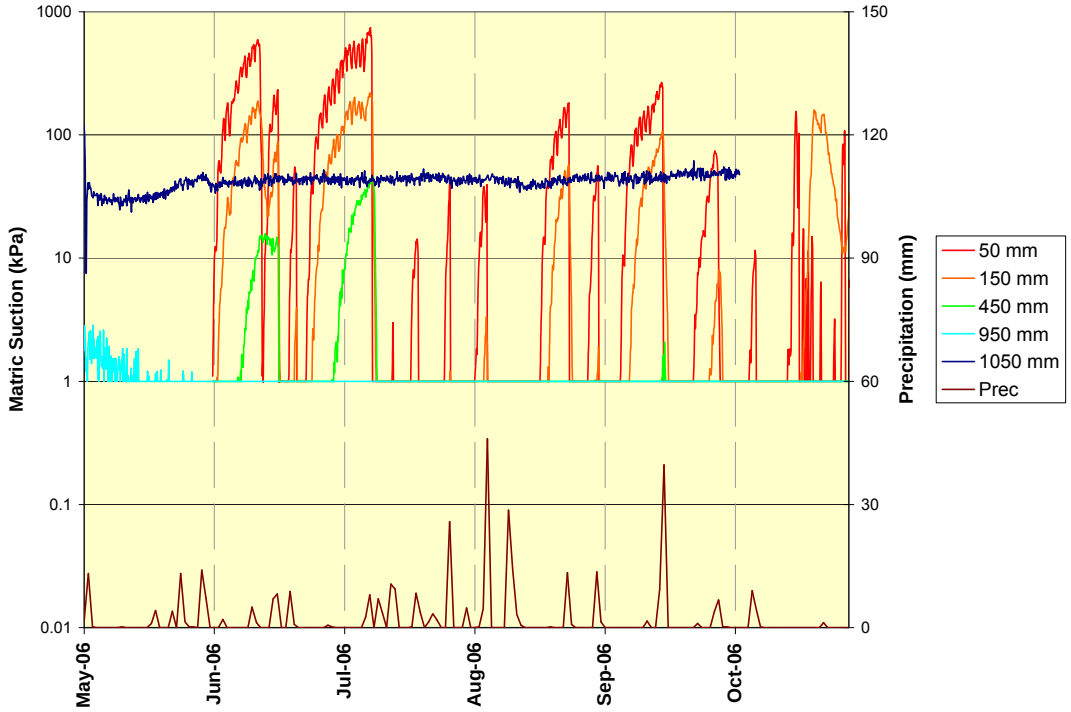

Figure 4-13 Matric suction readings for Plot A (1m cover soil over GCB)

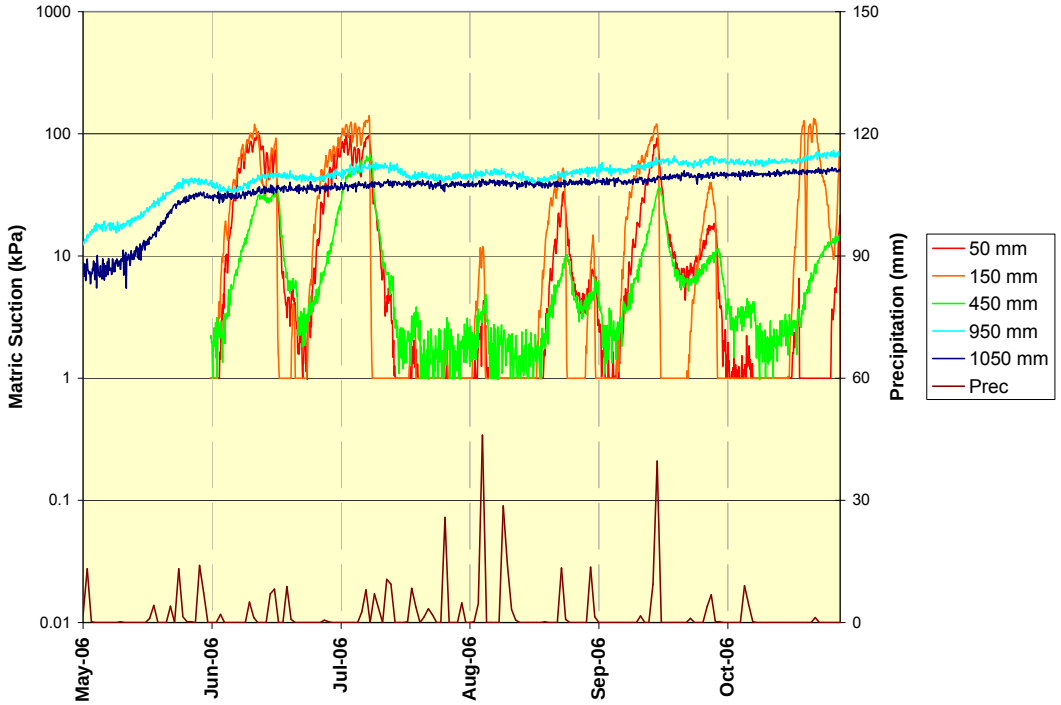

Figure 4-14 Matric suction readings for Plot B (1m cover soil only)

depth in Plot A is below the sensor's operating range of 1 kPa by early summer. This data confirms that the presence of the GCB is associated with the lowering of suction across the interface, and suggesting that a capillary break has been developed (as seen in works by Nicholson, 1989, and Park and Fleming, 2006).

The sensors installed in the middle of the soil covers also show a reduction in suction in the plot containing the GCB. The 450 mm deep sensor in Plot A reaches slightly above 10 kPa during June and July, but reduces to below the operating range during the late summer months of August and September. The 450 mm deep sensor on Plot B is well above 10 kPa during the same time periods in June and July, and ranges between 1 and 10 kPa in the late summer months.

The top three sensors in both plots show a clear response to rainfall events. In extended dry periods, the suctions climb toward the wilting point (suction of 1500 kPa) and then drop significantly following a rainfall event. The time delay in the reduction in suction with increasing depth can be seen as the wetting front moves through the cover soil.

4.8 Volumetric Water Content

Volumetric water content measurements were made using both the manual Diviner 2000® and the automated Tri-SCAN® sensors. Three access tubes were installed in each of the five plots to allow for measurements with the Diviner® system. One Tri-SCAN® access tube was installed in both Plots A and B. Each of these tubes contained a rail in which 5 sensors were installed at depths of 50, 150, 450, 950, and 1050 mm. These sensors were programmed to take readings at 3 hour intervals.

4.8.1 Diviner 2000®

The Diviner 2000® system was used to measure the volumetric water content profiles in each of the five plots. Fifteen access tubes, three in each plot, were installed to allow for measurements with the moisture probe. Figure 4-15 shows the numbering system that was used to label the different access tubes on the test site.

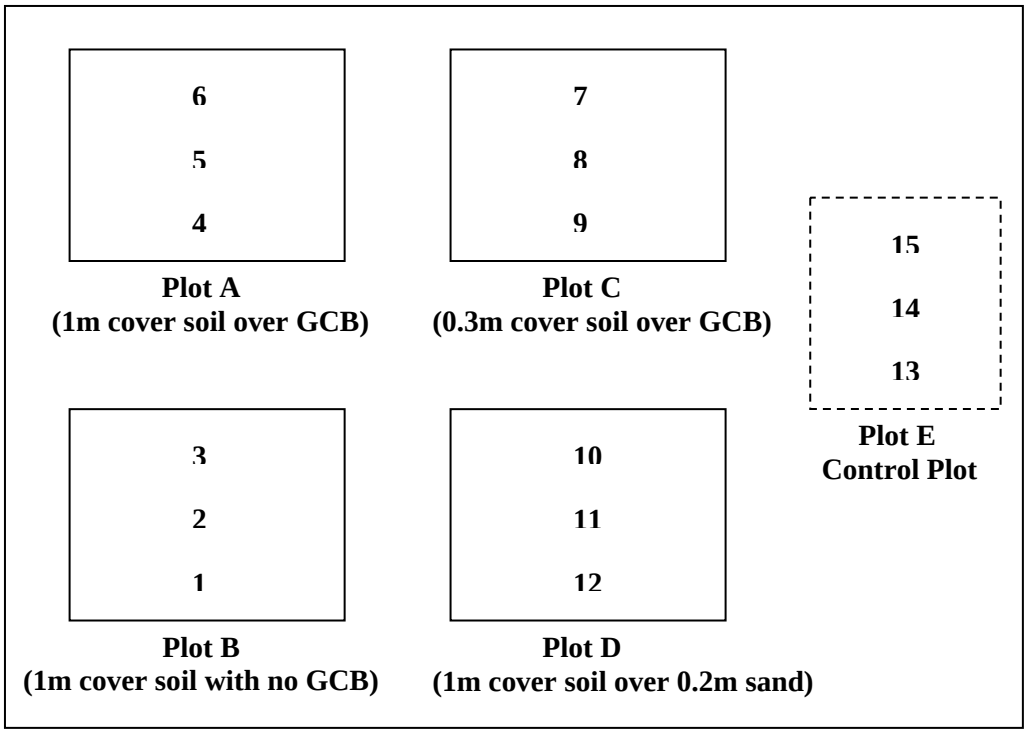

Figure 4-15 Numbering of Diviner® profiles

a) Depth Profiles

Figure 4-16 illustrates the volumetric water contents measured for profiles 4 through 6, all of which are on Plot A. Each of the profiles contain a line representing the average porosity of each plot (Section 4.3.1) of the cover material in blue, and the wilting point in red and the field capacity in green (volumetric water contents at 1500 and 30kPa, respectively, based on the estimated water retention function, Figure 4-3). For profiles 4 and 5, the volumetric water content at depths between 0.2 and 0.8 m varies from about

10% to 15%. At depths between 0.8 and 1.0 m, just above the GCB, the water content rises slightly to between 13% and 20%. Profile 6 has a fairly consistent profile between 0.2 and 1.0 m depths, ranging from 15% to 20%.

Figure 4-17 shows the results from profiles 2 and 3 on Plot B. The access tube for profile 1 was damaged sometime during construction; only allowing the probe to be inserted into the very top portion of the tube. The volumetric water content in profile 2 shows some similarity to profiles 4 and 5 at depths between 0.2 and 0.8 m. Below 0.8 m, profile 2 differs from those found in Plot A as there is a decrease in water content to between 6% and 9%. Profile 3 shows much lower water contents than the ones on Plot A. At depths between 0.2 and 0.8 m, the water content fluctuates between 8% and 12% and like profile 2, shows a decrease in water content above the tailings interface, dipping as low as 6%.

The differences seen just above the tailings/cover soil interface between Plots A and B indicate that the GCB is successful in enhancing water storage. There seems to be an increase in water content above the GCB, suggesting that a capillary break has developed. The lower water contents at the same depth on Plot B suggest that without the GCB, the tailings are drawing moisture out of the cover and into the tailings below.

Figure 4-18 illustrates the depth profiles on Plot C. The water content in the 0.3 m of cover soil varies quite considerably. This is to be expected as the wetting/drying front observed in Plots A and B reaches to a depth of just below 0.2 m. The GCB located at the .0.3 m depth shows a drop in water content, suggesting that a break has formed. In periods of heavier infiltration, the water content in the cover soil reaches as high as 15%

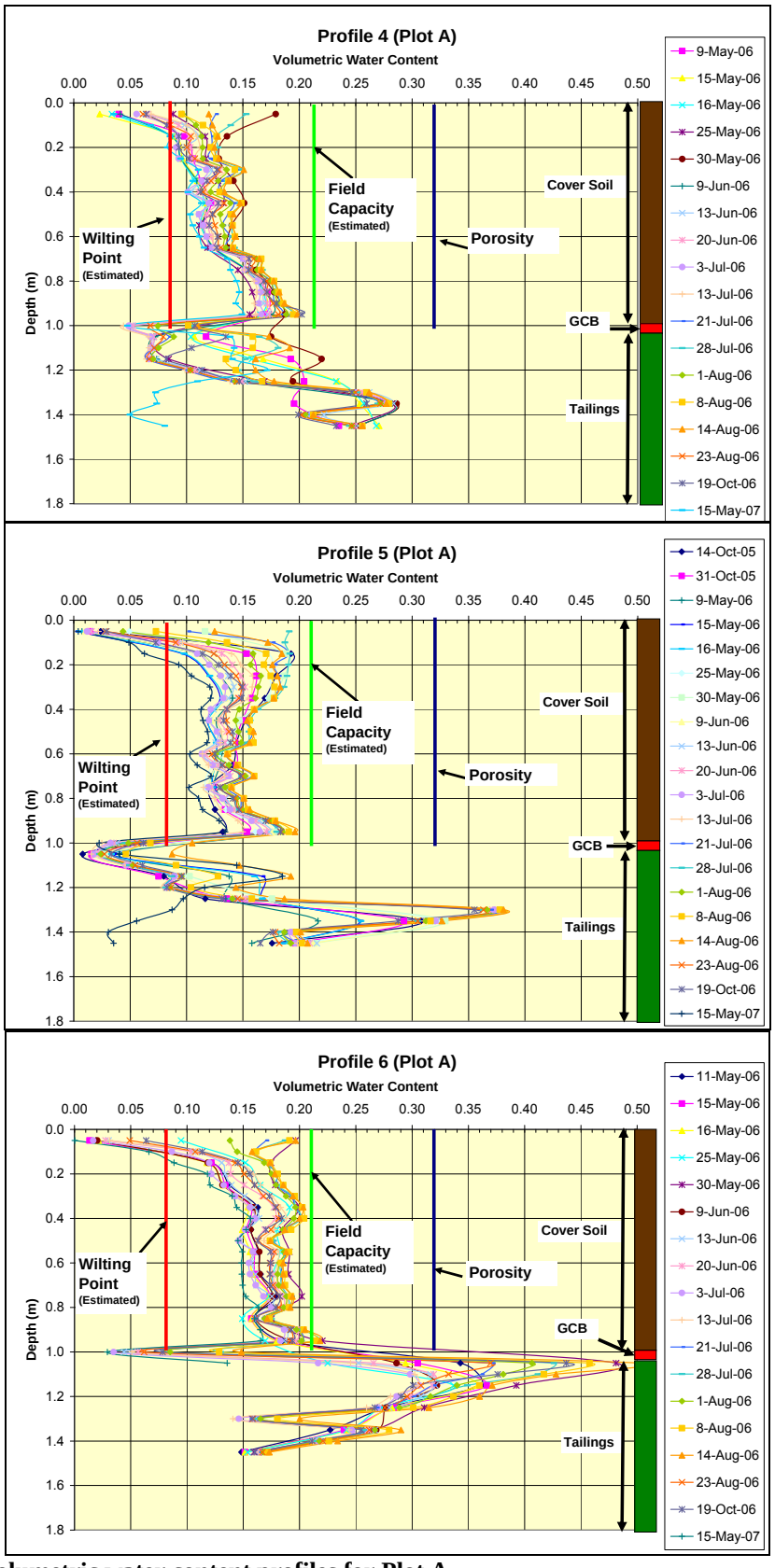

Figure 4-16 Volumetric water content profiles for Plot A

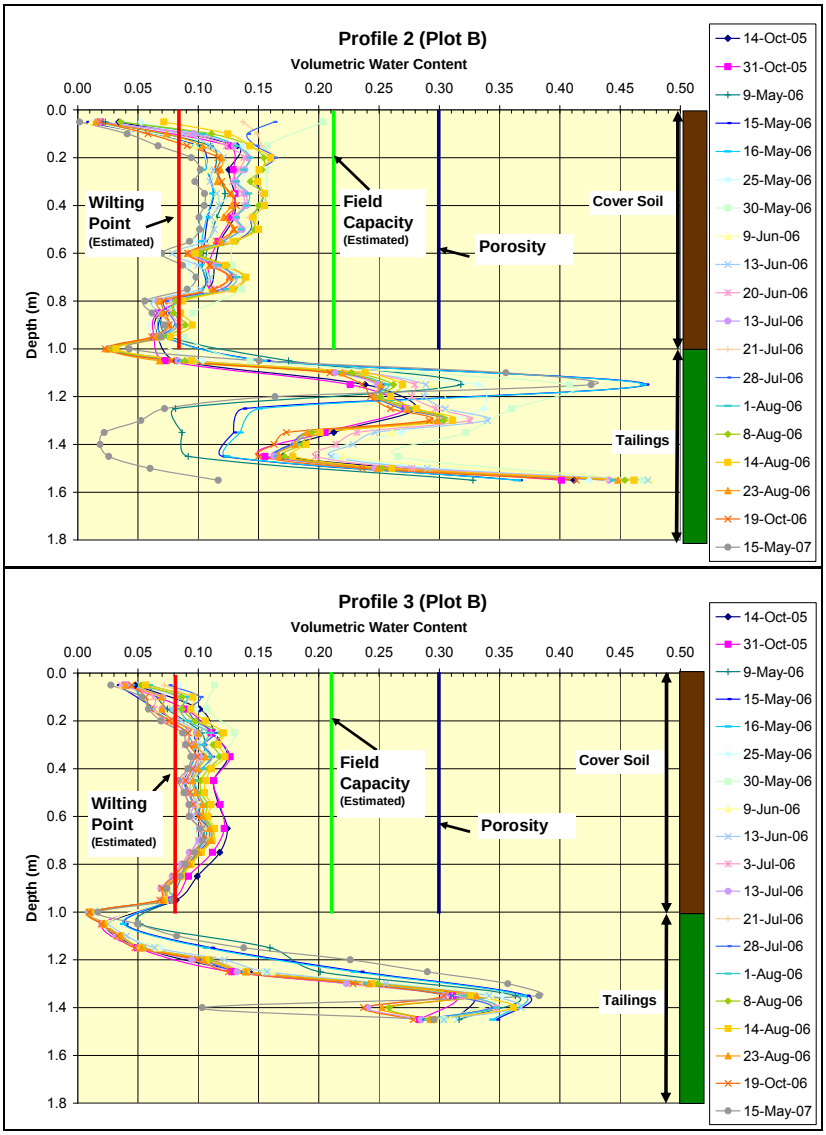

Figure 4-17 Volumetric water content profiles for Plot B

to 17%, higher than any water content measured in Plot B and similar to maximum water content in Plot A.

The volumetric water content measurements from Plot D can be found in Figure 4 19. The depth profiles 10 and 12 show that the water content is fairly steady at depths between 0.2 m and 1.0 m, with the water content varying between 11% and 16%. Profile 11 shows that at the same depths the water content varied between 13% and 18%.

At the cover soil/sand interface for all three profiles there is a break and a decrease in water content in the sand layer. In all three profiles the water content in the sand layer is between 5% and 9%. This decrease in water content suggests that at capillary break has developed. The measured water contents in Plot D in depths ranging from 0.2 to 0.8 m are comparable to those measured in the Plot A. The measured water content directly above the break sand are slightly less than those measured in Plot A.

Profiles 13 through 15 from Plot E are shown in Figure 4-20. The water content in the tailings varies greatly. Depth profiles 13 and 14 show a steady increase in water content from 0 % at the surface to a water content of 45 % at a depth of approximately 0.6 m. The water content decreases after a depth of 0.6 m. This increase in water content could be due to a layering affect of slimes or fine grained tailings. Profile 15 has a relatively steady water content profile. The wetting/drying front reaches to a depth of 0.4 m. Below the wetting/drying front the water content fluctuated between approximately 30% and 35%. The water content in the top 0.4 m of the control plot is higher than any of the plots containing a cover system. The water contents in the top 0.3 m of tailings in the plots A through D show water contents ranging from around 25% to 35%. This is approximately a 10% reduction from the control plot which contains no cover system.

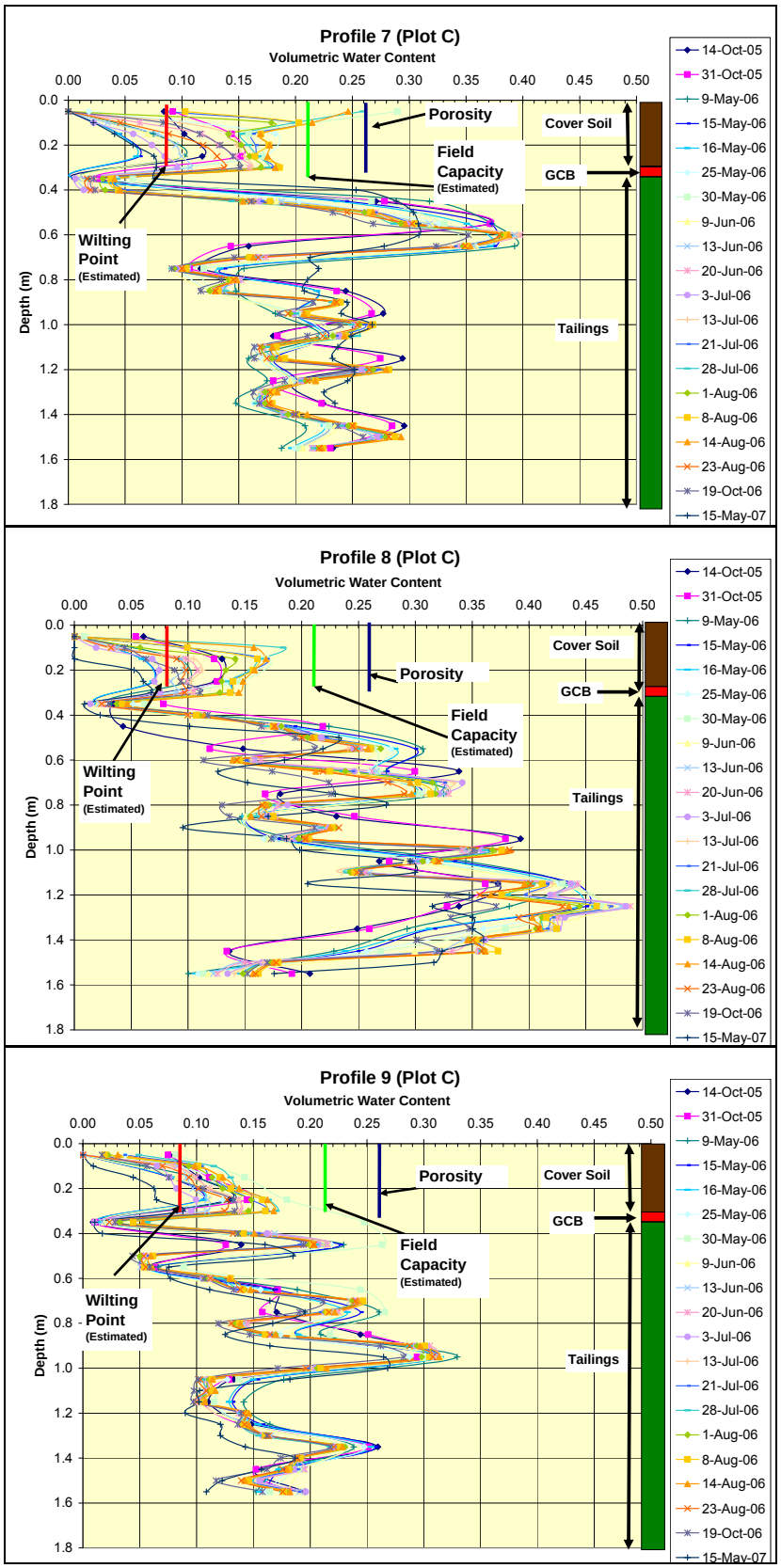

Figure 4-18 Volumetric water content profiles for Plot C

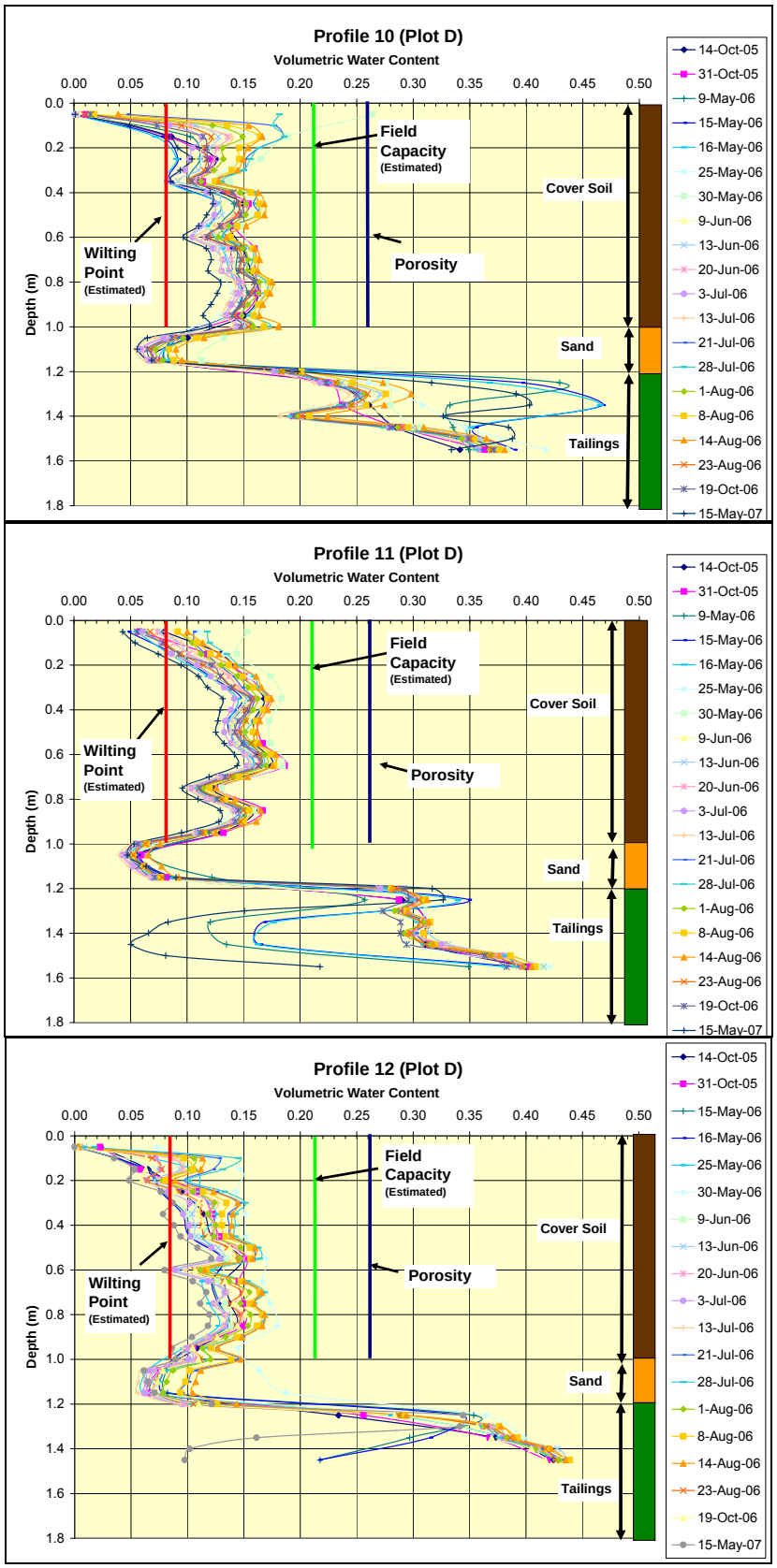

Figure 4-19 Volumetric water content profiles for Plot D

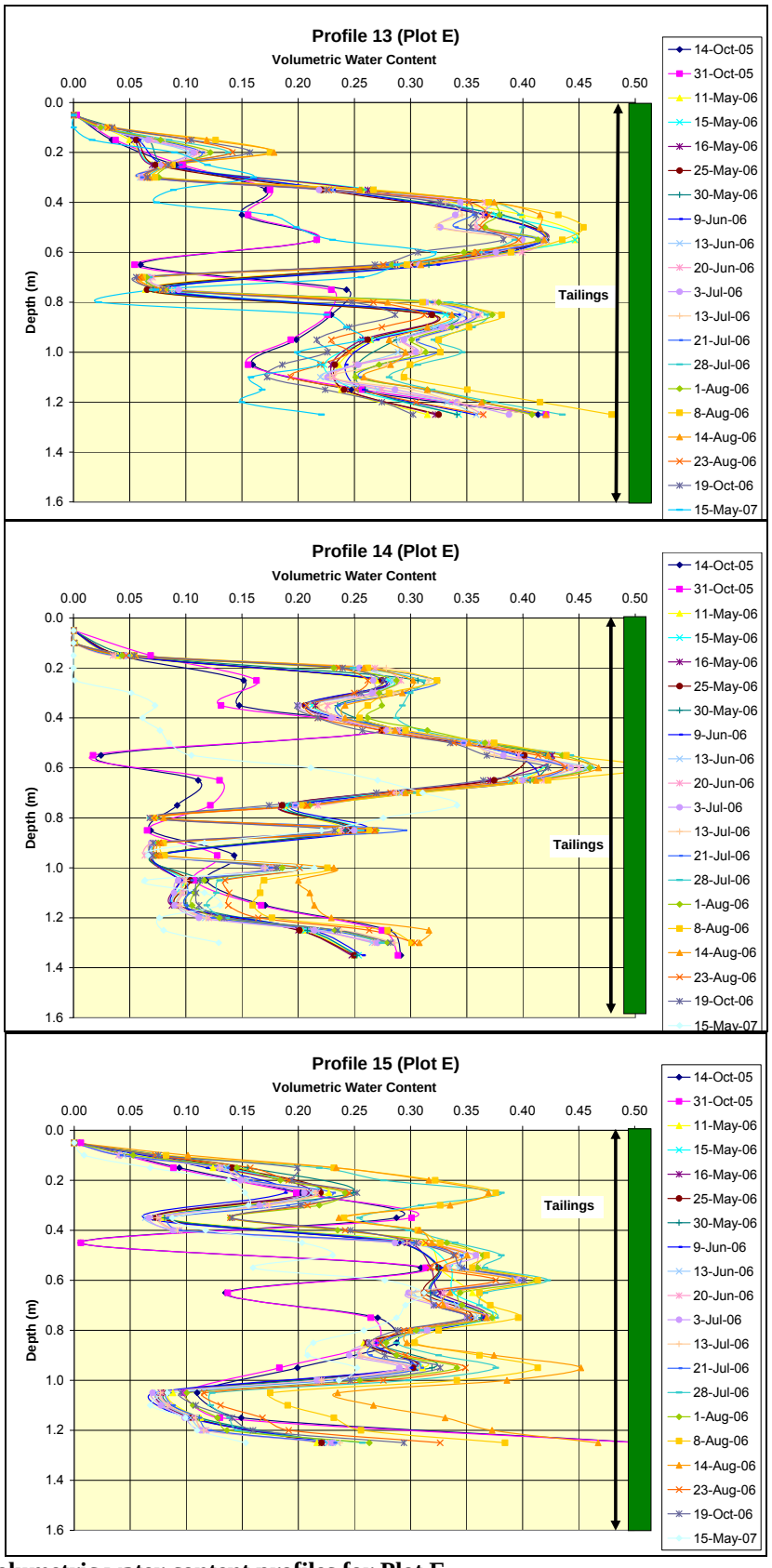

Figure 4-20 Volumetric water content profiles for Plot E

The average water contents for all dates measured from each of the different profiles are plotted in Figure 4-21 using the bottom of the cover soil as a datum. The bottom of the cover soil for each plot is represented by a depth of 0 m. The average water content for each cover plot is shown in Figure 4-22. It can be seen that Plot A has the highest average water content throughout the depth profile, averaging around 15% throughout the entire depth. The average profile for Plot A also shows an increase in water content above the GCB. Plot D has fairly high water contents, averaging around 13% to 14%. Plot B averages around 12% near the top of the soil cover, but drops dramatically just above the tailings/soil cover interface. Plot C also reaches an average water content of 13% in its 0.3 m of soil cover.

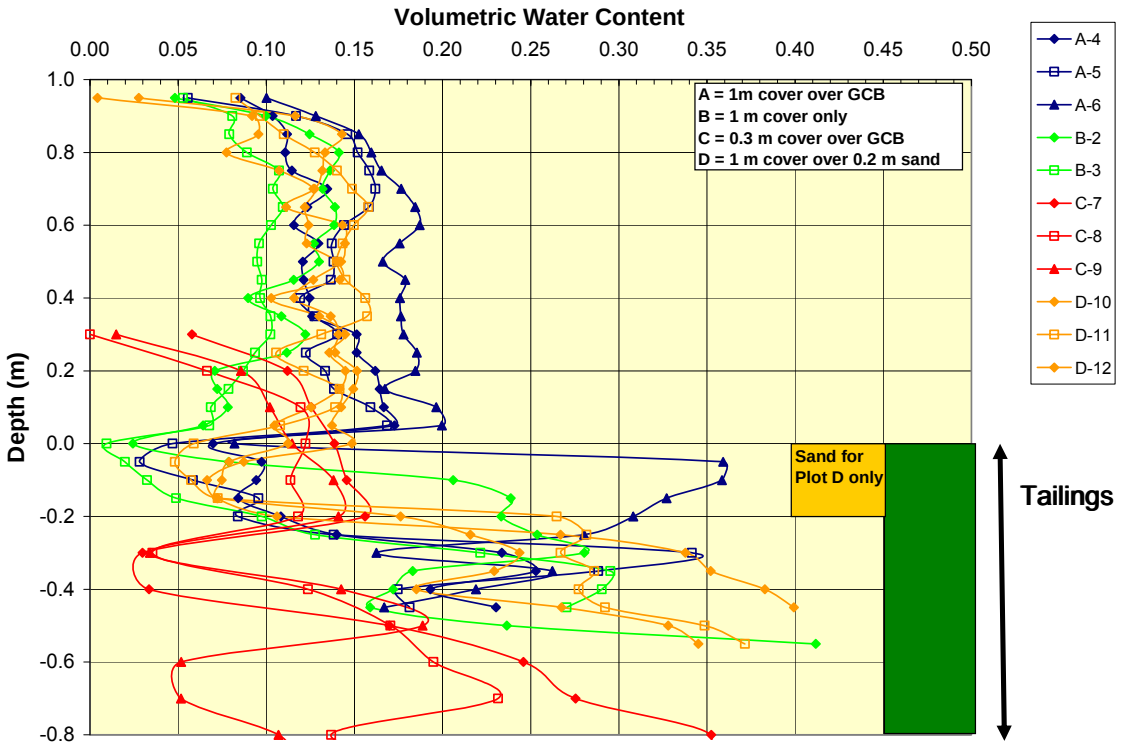

Figure 4-21 Average volumetric water content profiles for each individual access tube

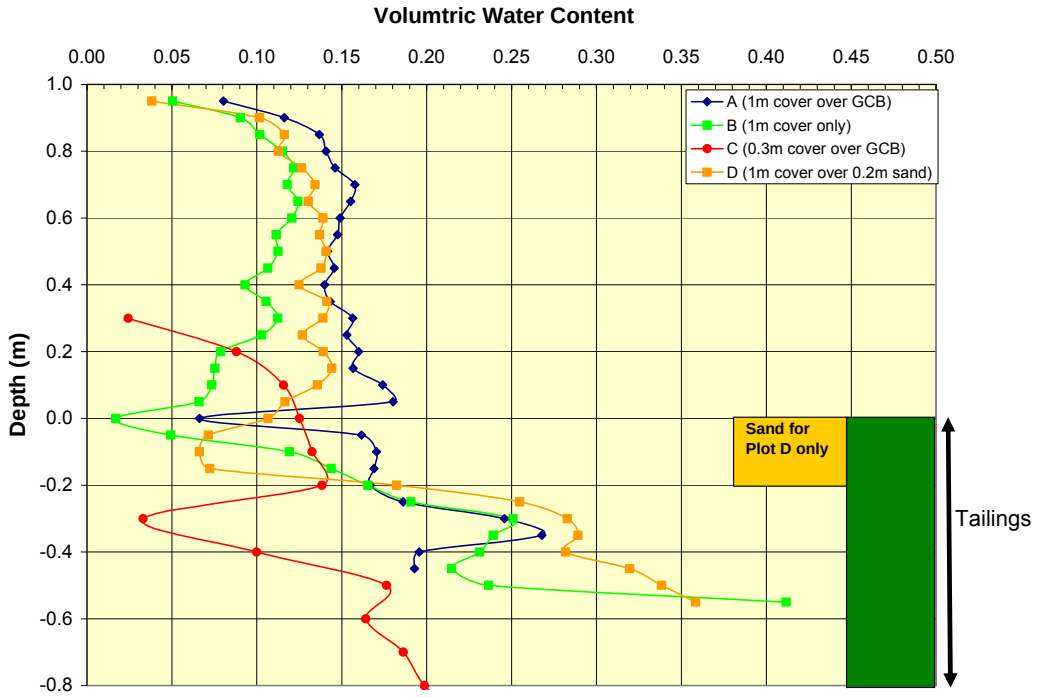

Figure 4-22 Average volumetric water content profile for each test plot

b) Water Volumes

The volume of water stored in each cover can be calculated from the water content profiles presented above. Figure 4-23 shows the volume of water stored in the soil covers for Plots A through D for the duration of the field trials. The portions of the year when the ground profiles were frozen are highlighted in grey. Figure 4-24 shows a zoomed in section of the water storage for the summer of 2006. From the graphs it can be seen that Plot A stores the largest volume of water. The water in Plot D is slightly less than Plot A. Plot B, without a CB, stores less water in the 1 m of cover soil than do Plots A and D. Plot C which contains only 0.3 m of soil cover stores the least amount of water, but normalized to the same 1 m thickness, the water volumes are comparable to Plot A during wet periods and Plot B in extended dry periods.

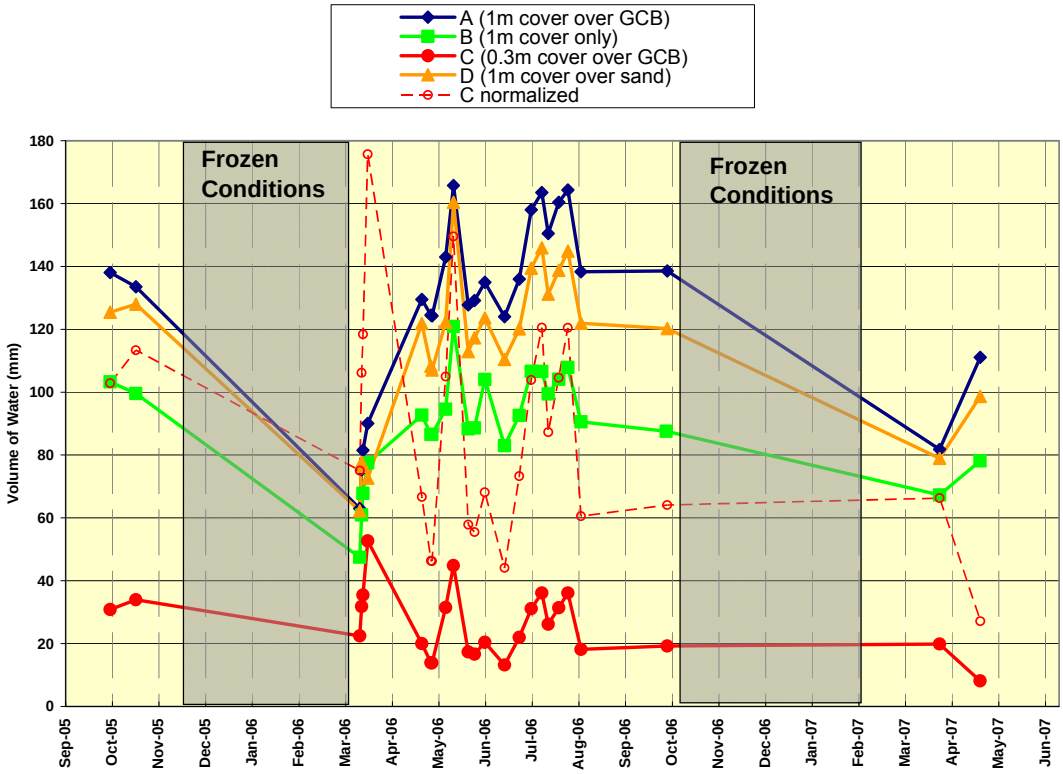

Figure 4-23 Water volume stored in each cover system

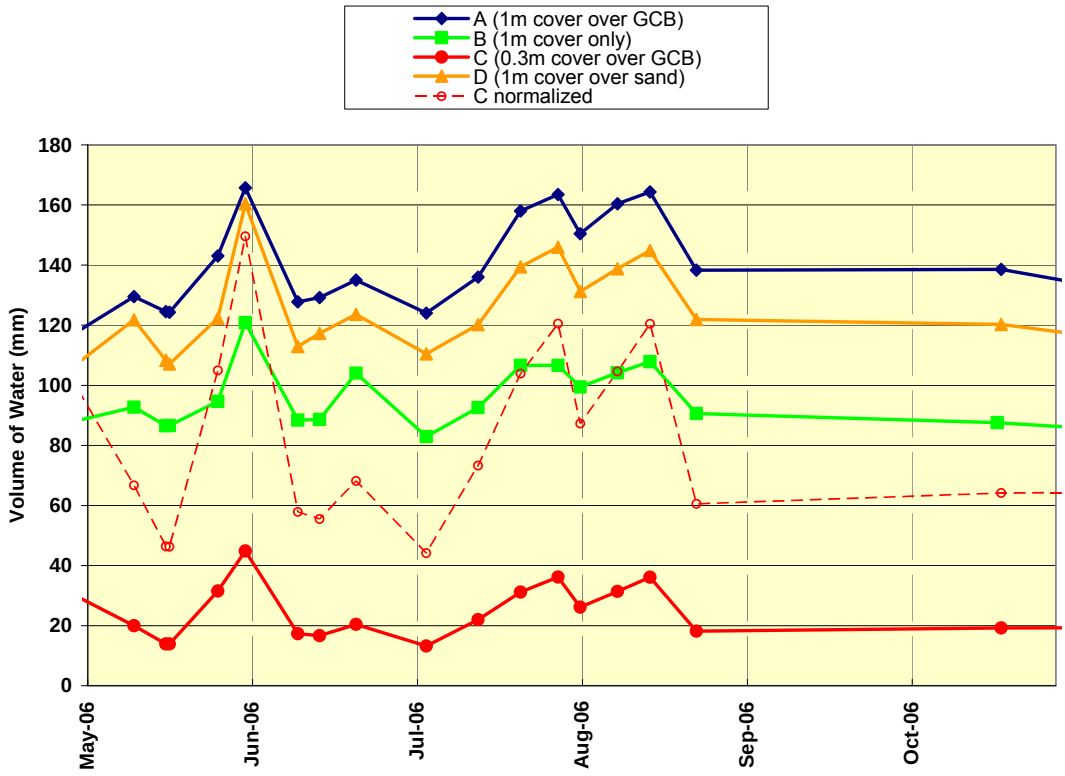

Figure 4-24 Water volume stored in each cover system for summer 2006

4.8.2 Tri-SCAN®

Five Tri-SCAN® sensors were installed in both Plots A and B. The sensors in each plot were installed at depths of 50, 150, 450, 950, and 1050 mm from the surface of the cover soil. Figures 4-25 and 4-26 show the data collected from Plots A and B respectively for the summer months of May through October of 2006 and Figure 4-27 shows the daily precipitation for the same time period.

When comparing the results of the Tri-SCAN® sensors and Diviner® system, there are some conflicting data. The sensor at 450 mm in both plots reads significantly lower than readings taken with the Diviner® system. This could be caused by layering produced during construction of the test plots or by the cover soil being built around the access tubes. The results can be used for comparison between sensors on plots A and B, as well as used to compare the change in storage observed from the response of the different sensors.

The sensors located at 950 mm show very different results than the observed results taken from the Diviner® system. The automated sensor shows elevated water contents in Plot B, with much lower water contents on Plot A. This is directly opposite from the manual probe which shows that the water contents at this depth is higher in Plot A than Plot B. One explanation for this is that the automated sensor is installed slightly below what was expected. The automated sensor might be affected by the presence of the GCB and tailings on Plot A, and by the tailings on Plot B.

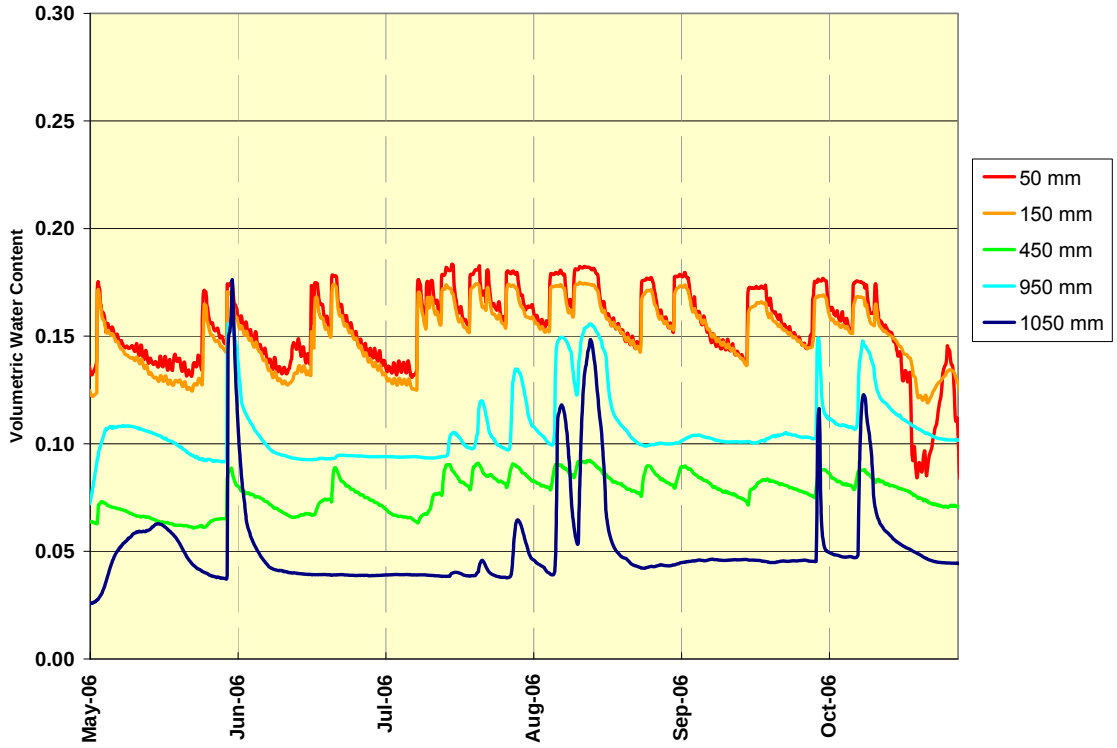

Figure 4-25 Water contents on Plot A (1m cover soil over GCB) as measured by automated sensor

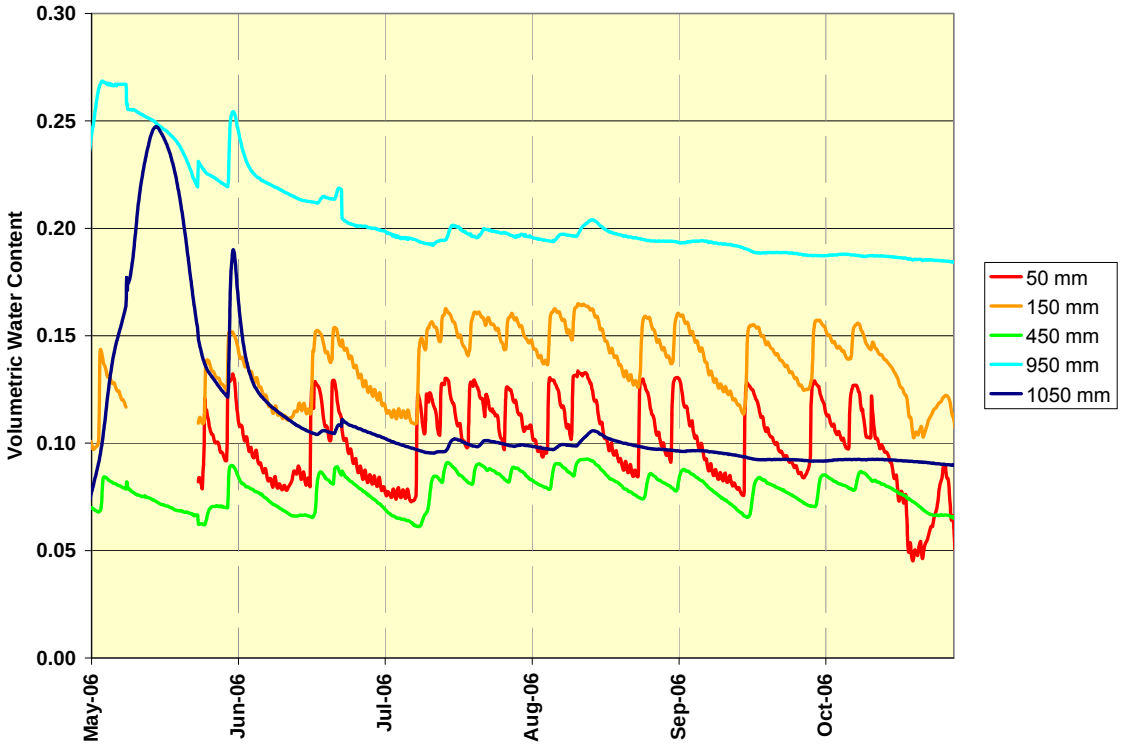

Figure 4-26 Water contents on Plot B (1m cover soil only) as measured by automated sensors

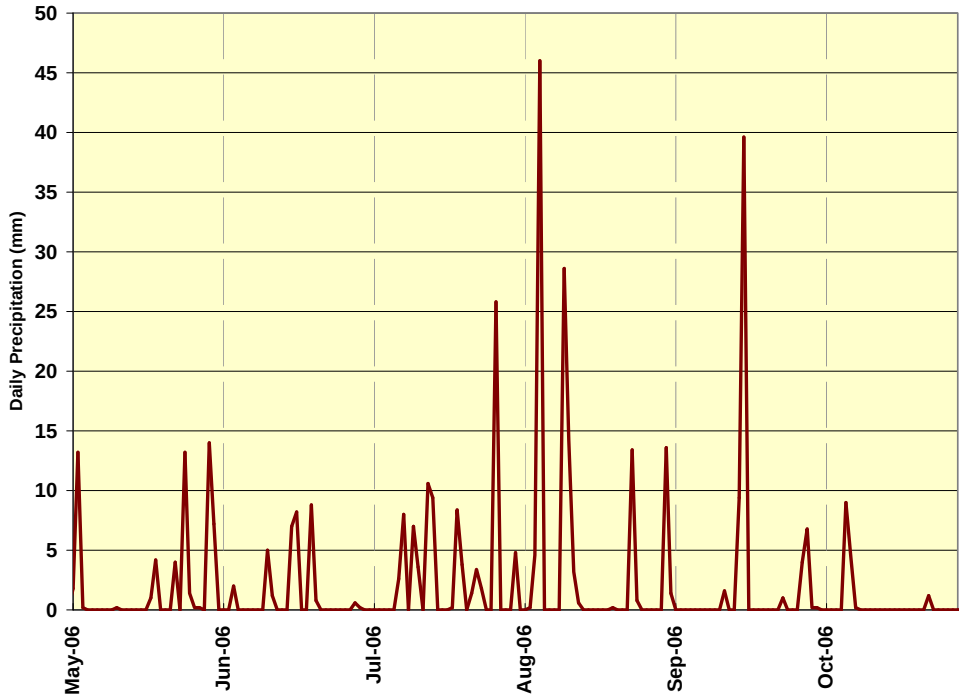

Figure 4-27 Daily precipitation for May through October 2006

The top three sensors in Plot A consistently show higher water contents than the sensors installed at the same depths in Plot B. A clear response to rainfall can be observed in the top sensors in both plots. A time delay and dampening can be seen as the higher water content moves from top sensor at 50 mm through the second sensor to the middle sensor located at 450 mm.

4.9 Change in Storage

The cumulative change in storage for each of the plots was calculated from the water volume data that was collected. Figure 4-28 shows the change in storage calculated from manual water content readings for the period of May through October of 2006. Figure 4-29 shows the same calculation using the automated sensors that were

installed in plots A and B. Both figures show that the Plot A, which contains the GCB, is the most responsive to precipitation events. Both sets of readings illustrate that Plot A stores more of the precipitation than the other plots.

The increase in storage can be used to compare the performance of each of the plots. The change in storage for each of the plots was calculated for the time period of July 3 to July 28, as shown in Figure 4-28. The storage in Plot A increased 40 mm, with Plot D increasing 35 mm, Plot B increasing 24 mm, and Plot C increasing 23 mm. It is also apparent that Plot A is storing more moisture when looking at the heavy rainfall event in Figure 4-29 that occurred at the beginning of August. The moisture storage in Plot A increases from 5 mm to 30 mm, resulting in an increase of 25 mm. During the same rainfall event, Plot B only increases 12 mm, going from -4.5 mm to 7.5 mm.

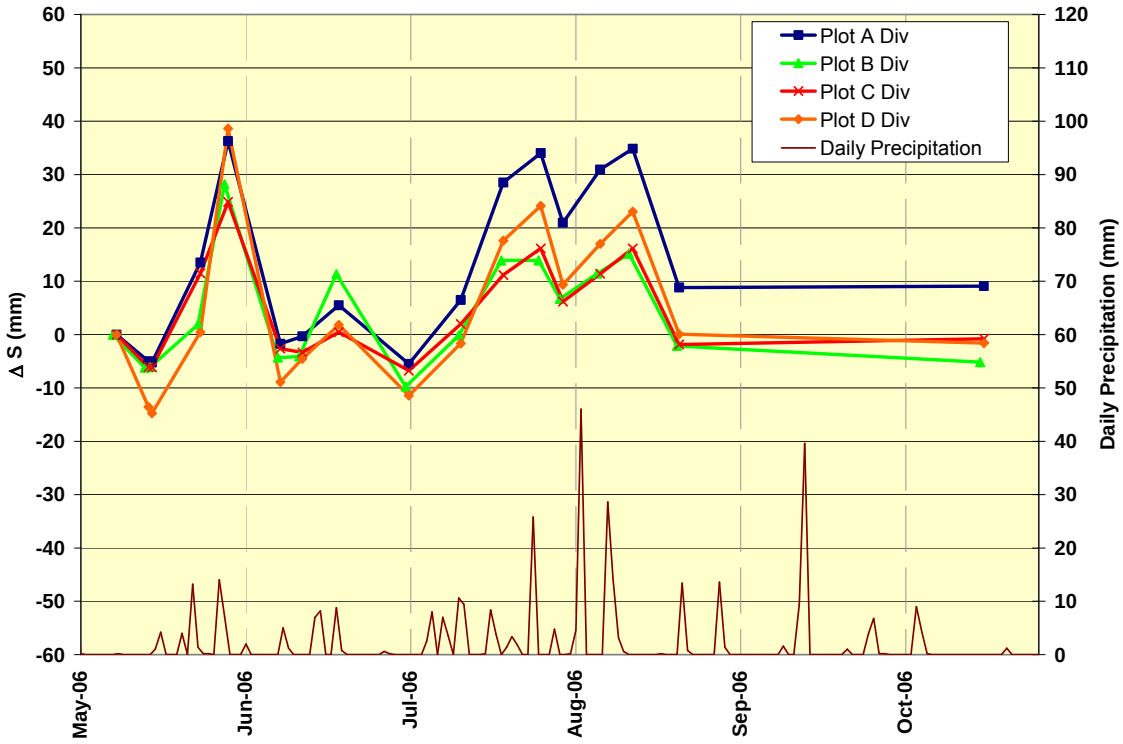

Figure 4-28 Change in Storage using Diviner® readings

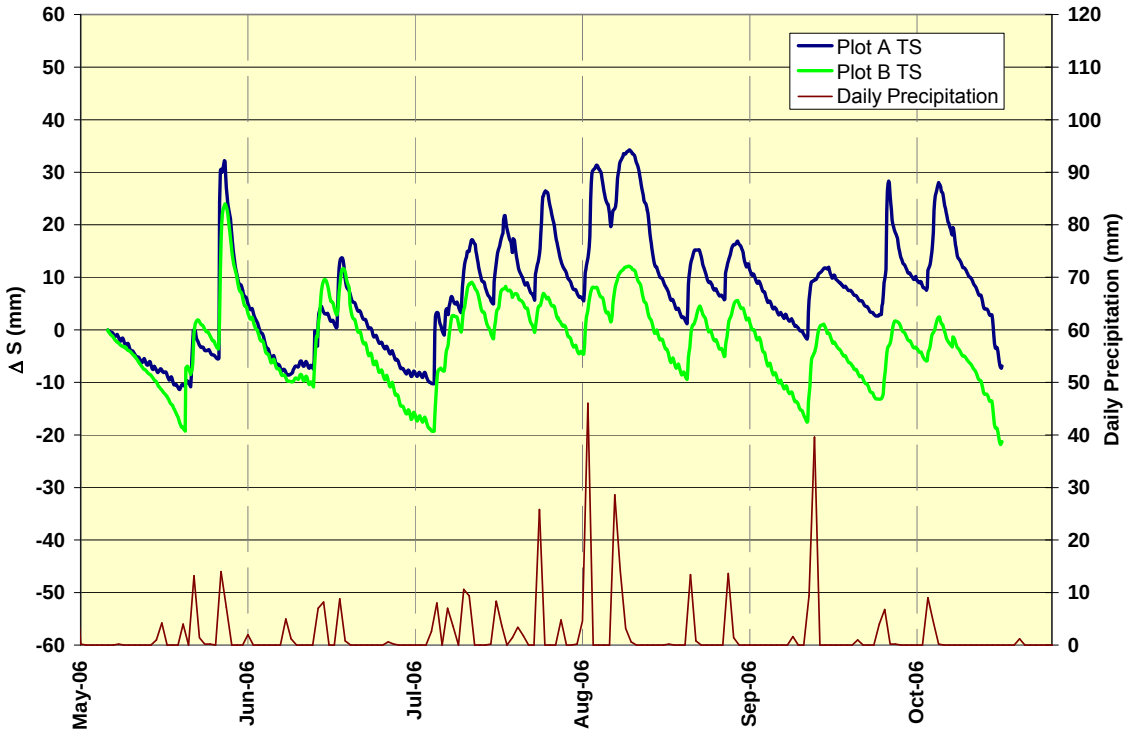

Figure 4-29 Change in storage using Tri-SCAN® readings

4.10 Water Balance

A water balance was completed for each plot for the months of May through October of 2006 for illustrative purposes. For Plots A and B the change in storage was calculated using both the manual and automated water content sensors. As Plots C and D only contained access tubes for the manual water content sensors, the change in storage was only calculated using those readings.

The components of the water balance have been discussed in Section 2.2.5. One of the goals of these field trials was to design the test plots so that the water balance would be as simple as possible. To achieve this goal, the test plots were constructed on a flat section of the TMA and built large enough that edge effects would be minimal. This design allows for the assumption the flow system is one dimensional flow and that the water balance components of runoff and interflow can be assumed to be zero. Most

likely some runoff would occur off of the test plots during heavy rainfall periods, but for this purpose it is assumed that runoff is negligible.

Figures 4-30 through Figure 4-35 show the cumulative water balance for Plots A through E. The precipitation (PPT) was recorded by the meteorological station installed on Plot B. The potential evapotranspiration (PE) was calculated from the other recorded meteorological measurements taken from the weather station. The AET/PE ratio was assumed to be 0.15 for all plots for this simplified illustration. The ratio of AET/PE will likely change under the varying conditions, but because the plots are not vegetated, the evapotranspiration would likely not be a considerable part of the water balance due to evaporation shutting down soon after rainfall events (the roots in a vegetated cover aid in drawing water up from within the soil cover).

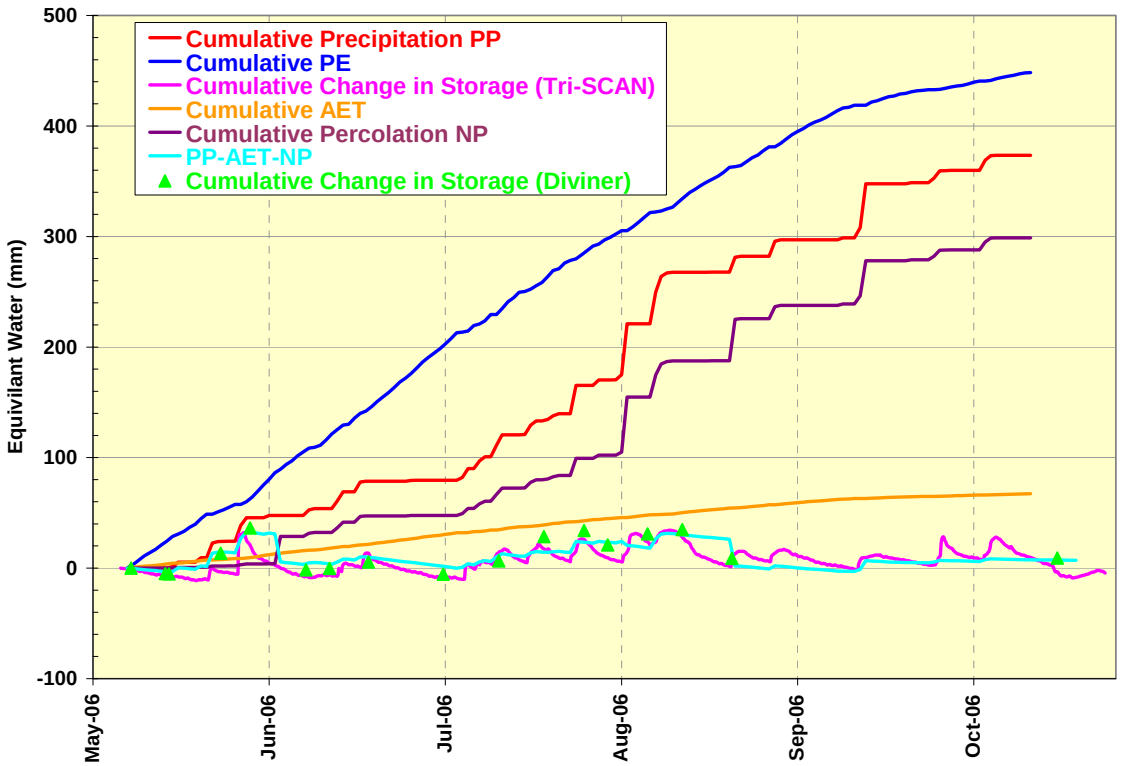

Figure 4-30 Cumulative water balance for Plot A (1m cover soil over GCB)

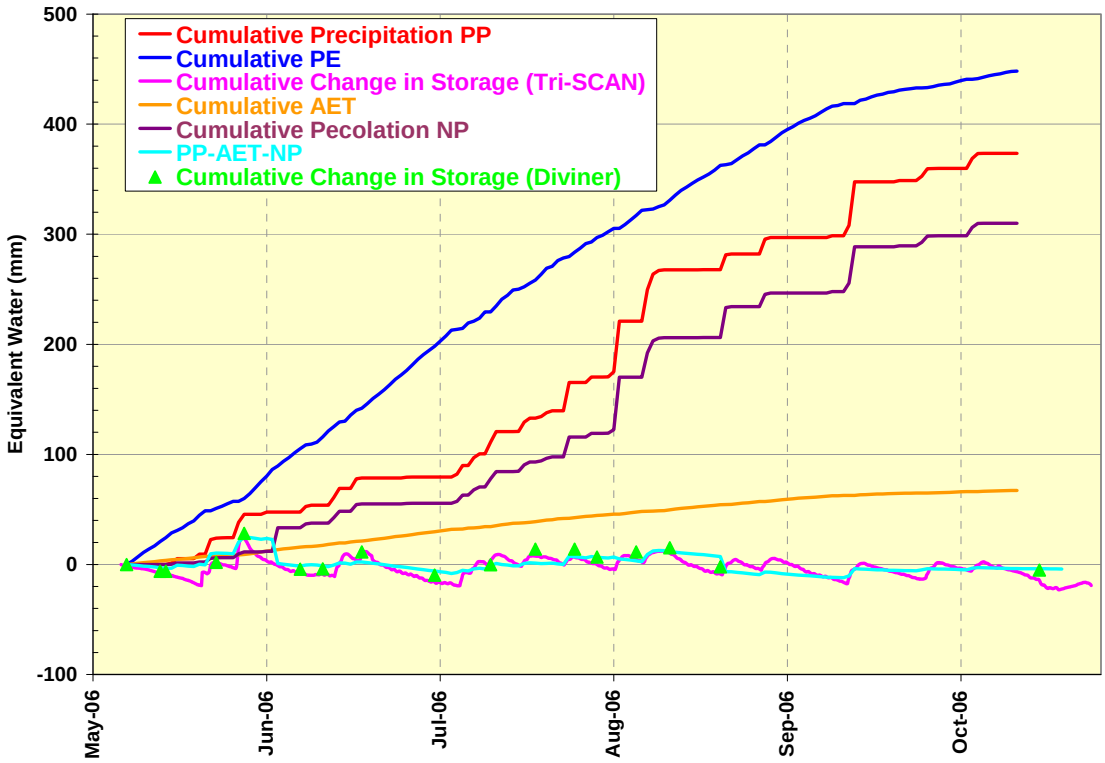

Figure 4-31 Cumulative water balance for Plot B (1m cover soil only)

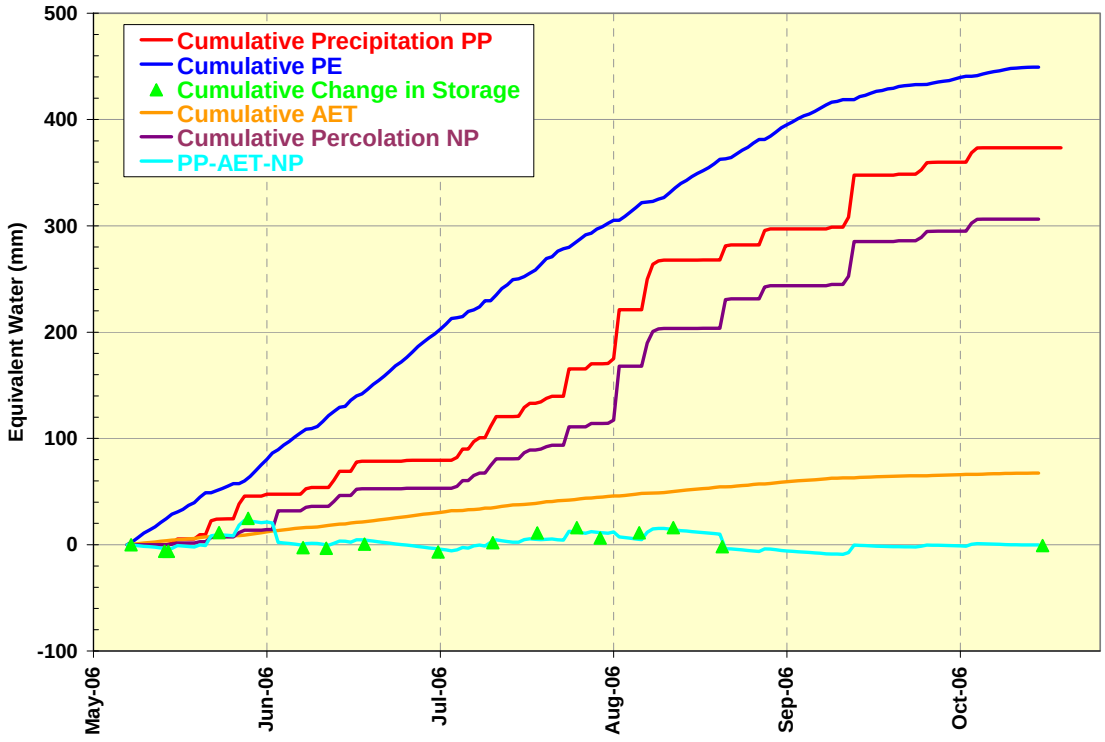

Figure 4-32 Cumulative water balance for Plot C (0.3 m cover soil over GCB)

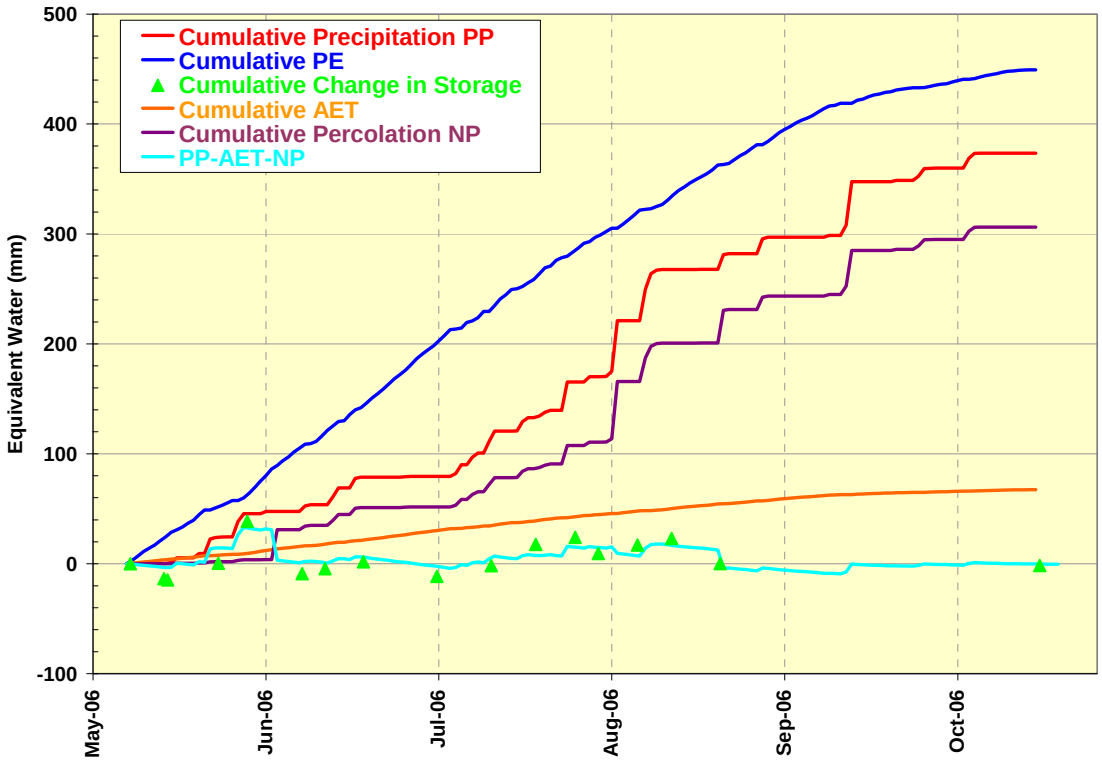

Figure 4-33 Cumulative water balance for Plot D (1m cover soil over 0.2 m sand)

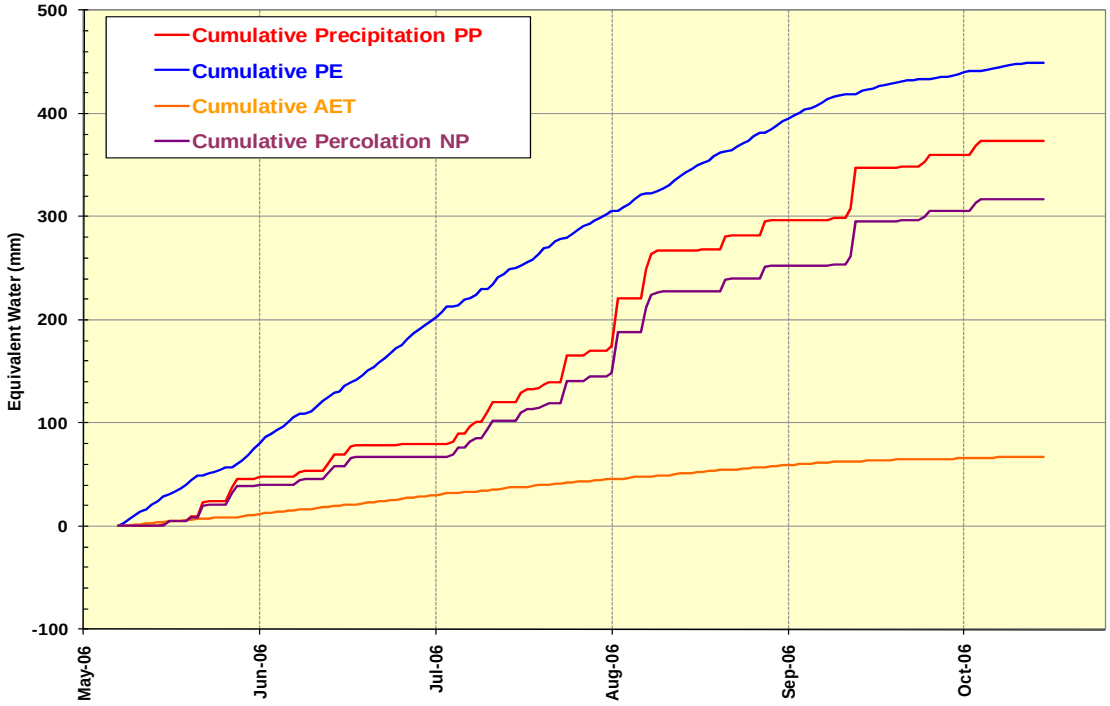

Figure 4-34 Cumulative water balance for Plot E (control plot)

The calculated change in storage was fitted to the measured change in storage by adjusting the value of net percolation. The net percolation (NP) was calculated by splitting the water balance time frame into sections and taking a percent of the precipitation. The theoretical change in storage (ΔS) was calculated using the water balance equation (ΔS = PPT-AET-NP) and compared to the measured change in storage from the water content sensors. Table 4-6 shows the net percolation response to match the measured change in storage.

The calculated change in storage is higher than measured right after heavy rainfall events. This is most likely caused by a change in the AET rate that occurs after rainfall events. The AET/PE ratio is assumed to be constant over the entire water balance to simplify the equation. This temporary increase in AET is not accounted for in the water balance analysis. Thus the estimates of net percolation are most likely high rather than low.

Table 4-6 Percolation data

	Cummlative Net Percolation (mm)				
	Plot A	**Plot B**	**Plot C**	**Plot D**	**Plot E**
May 9 -Jun 4	3.8	11.9	14.3	3.8	40.5
Jun 4 - Aug 4	101.2	110.6	103.0	110.0	108.3
Aug 4 - Aug 23	82.5	83.5	86.2	86.3	78.9
Aug 23 - Oct 19	111.3	104.0	102.7	106.1	89.8
Total	298.8	310.0	306.2	306.2	317.5

It can be seen that Plot A has the lowest amount of total net percolation. The total percolation for Plots C and D are very similar and are both slightly higher than Plot A. The total percolation for Plot B is the highest out of the four test plots and is the only plot that does not contain any type of CB.

The total precipitation and percolation for each of the plots for the time period of May through October of 2006 was used to calculate a total percolation percentage as

presented in Table 4-7. Plot A has the lowest percolation rate at 80%. Plots C and D have a net percolation of 82% of the measured precipitation. Plot B has the highest percentage of net percolation at 83%. Plot E has a percolation percent of approximately 85% of precipitation.

Table 4-7 Percolation summary

	Plot A	Plot B	Plot C	Plot D	Plot E
Total Precipitation (mm)	373	373	373	373	373
Total Percolation (mm)	298.8	310.0	306.2	306.2	317.5
% Percolation	80%	83%	82%	82%	85%

4.11 Oxygen and Carbon Dioxide Profiles

The oxygen and carbon dioxide ports described in Section 3.4.6 were read twice in August of 2006, once in October 2006 and finally again in April 2007. The results for Plot A can be seen in Figure 4-35. Only the top three ports in Plot A were working properly. The second reading in August did not work properly for this series of ports. The two ports that had needles on the end became plugged and would not allow enough air to be pumped to the oxygen sensor.

The readings for Plot B can be seen in Figure 4-36. It can be seen that the oxygen concentrations drop from near atmospheric at the surface to around 5 % at a depth of 1.3 m. From the measured oxygen concentration profiles, it appears that the oxygen level approaches zero somewhere in the tailings.

Figure 4-37 presents the data collected from the ports installed in Plot C. The oxygen gradient is significantly larger than that observed in Plot B. The concentration of oxygen is lower in the tailings than the readings taken in the tailings for Plot B, even with

less cover soil. The percent oxygen in two of the readings is around 2% at a depth of 0.4 m.

The results for the oxygen ports for Plot D can be seen in Figure 4-38. The oxygen concentrations decrease from near atmospheric near the surface to near 0% just above and including the sand layer. The oxygen concentrations in the tailings below the sand are also near 0%.

Figure 4-39 shows the data collected from the control plot, Plot E. It appears that the oxygen concentration decreases to a depth of 0.9 m and then starts to increase below that depth.

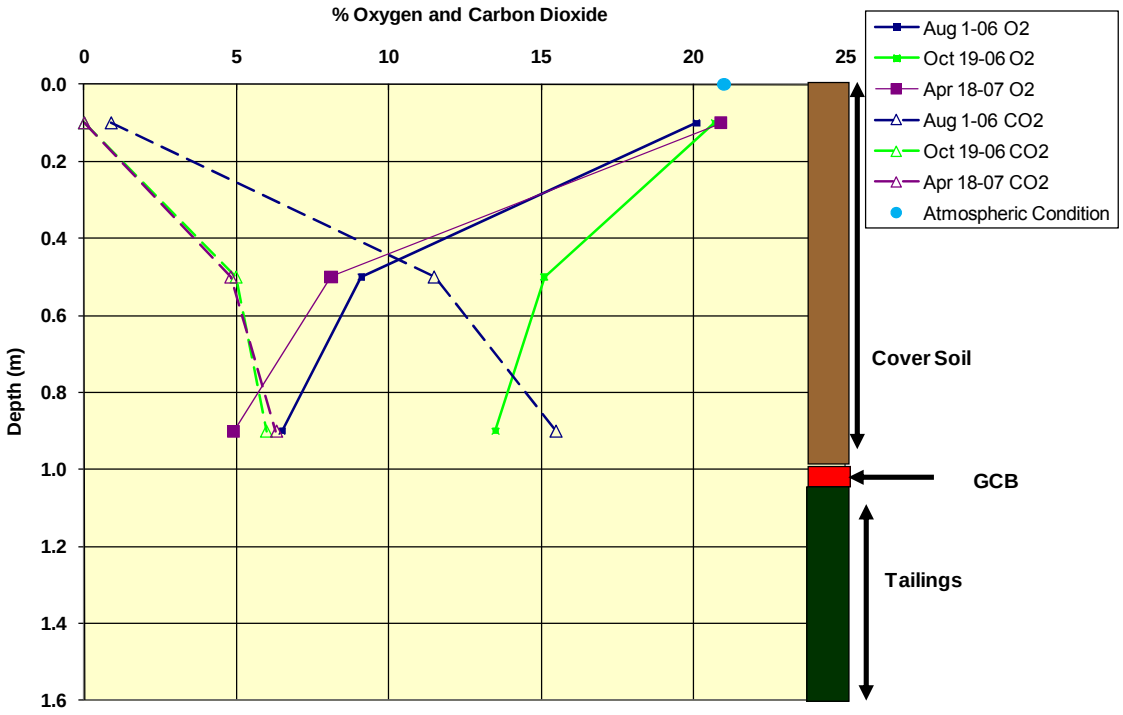

Figure 4-35 Plot A gas concentration

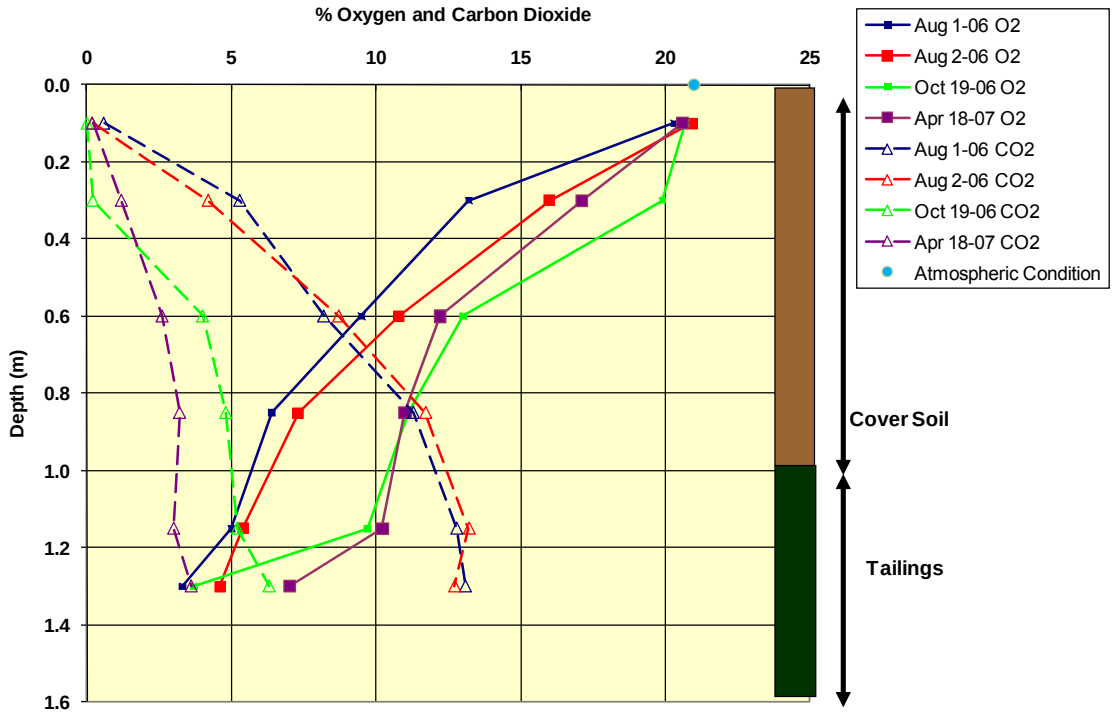

Figure 4-36 Plot B gas concentrations

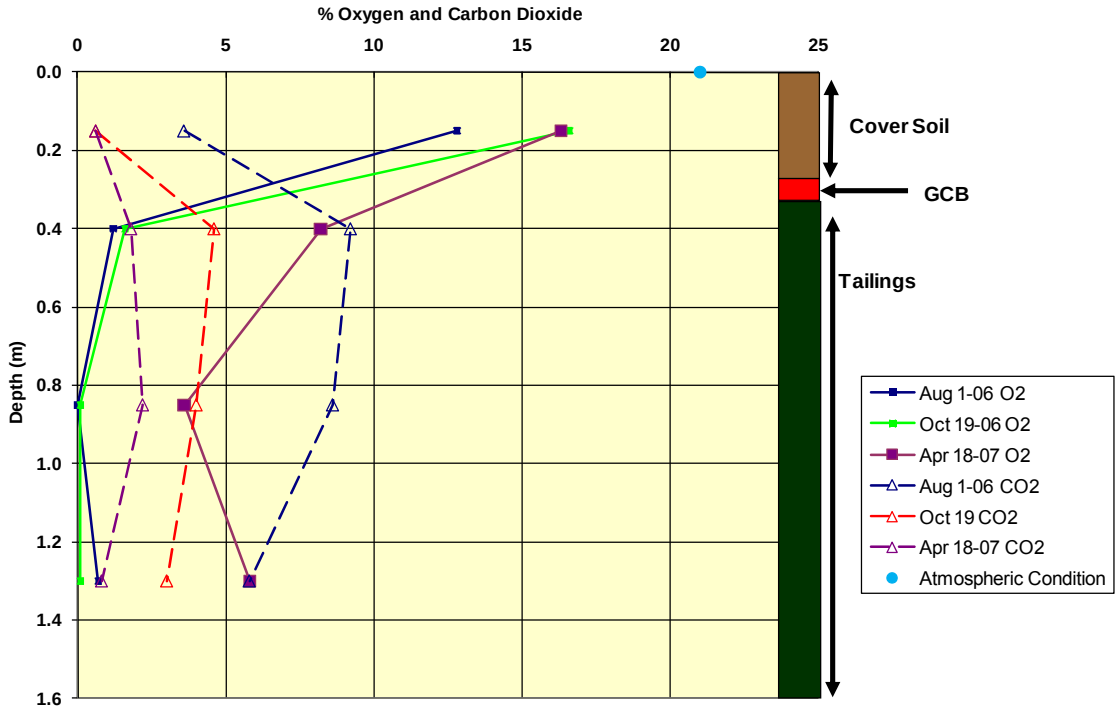

Figure 4-37 Plot C gas concentrations

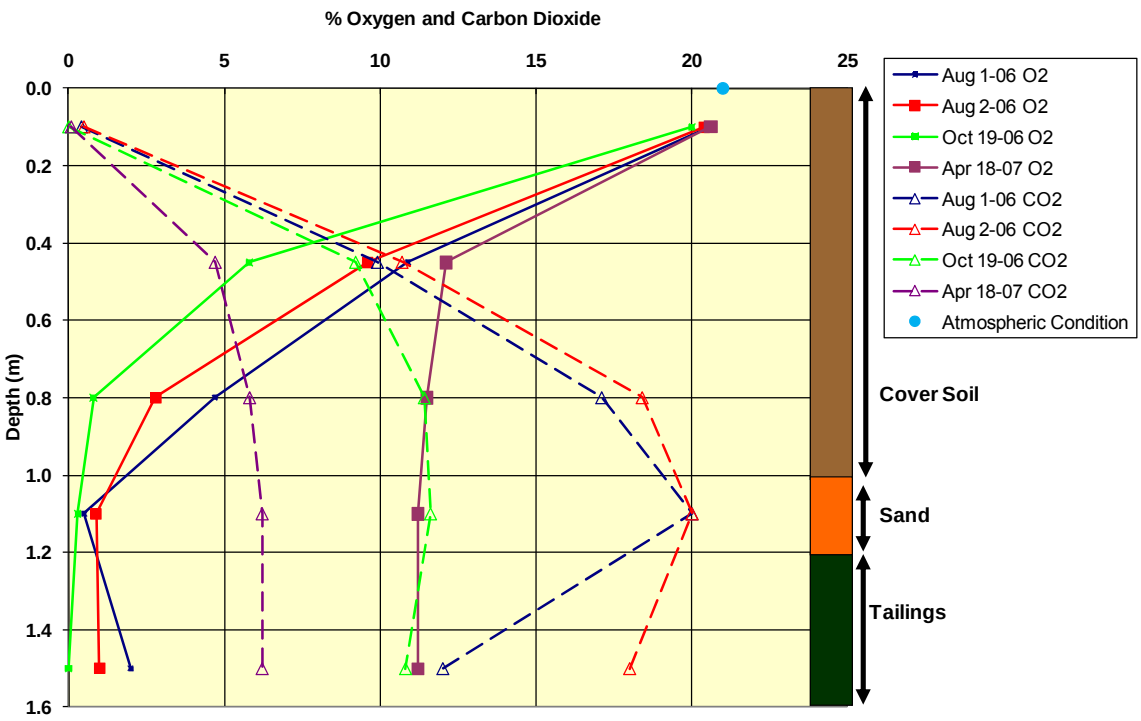

Figure 4-38 Plot D gas concentrations

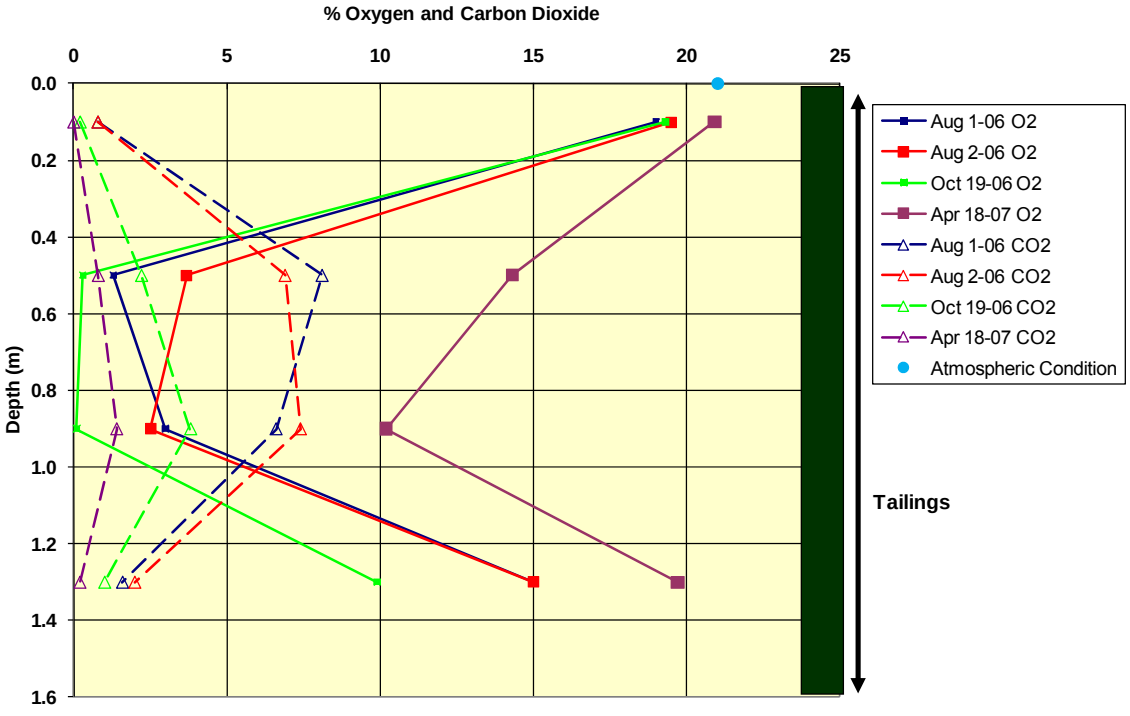

Figure 4-39 Plot E gas concentrations

As previously stated, the oxygen diffusion through an unsaturated soil is affected by the degree of saturation. The monitoring data from the water content sensors for the dates of August 1, 2006 and October 19, 2006 were analyzed for degree of saturation and a theoretical profile was developed. The cover soil profile was divided into 50 mm increments and the degree of saturation at each depth was calculated from the water content data from that day. The relationship between degree of saturation and oxygen diffusion coefficient discussed in Section 2.2.2.2 was used to calculate a diffusion coefficient (De) for each depth increment. From the values of diffusion coefficients, an equivalent series diffusion coefficient (De*) was calculated by using a harmonic mean. An overall mean gradient was calculated from the measured oxygen data (two separate gradients for Plot A and one gradient for Plots B, C, and D). The oxygen flux for the entire system was calculated using Fick's Law (Section 2.2.2) with the equivalent diffusion coefficient (De*) and the apparent overall gradient ($\delta C/\delta z^*$). The apparent overall flux was then used to calculate the concentrations at each depth interval using the calculated De for that depth. The values of calculated saturation and oxygen diffusion coefficients for each discrete depth in the test plots, as well as the oxygen monitoring data from the two dates (August 1, 2006 and October 19, 2006) and the theoretical profile for Plots A through D can be seen in Figures 4-40 through 4-47. The percent of saturation of the rock flour in the GCB (Plots A and C) was adjusted using trial and error in order for the calculated profile to fit the measured data. It was found that a degree of saturation ($S_r = 0.75$) of the rock flour was found to fit the measured data. A profile was also calculated assuming that the rock flour was completely saturated ($S_r = 1$ for 10 mm) in order to illustrate what the profile would look like with a completely saturated rock flour

in the GCB. In both cases the geotextile was assumed to have a diffusion coefficient of free air. This was taken from the high porosity (0.82) of the geotextile (assuming the geotextile is completely unsaturated).

A percent saturation envelope for Plots A, B, C, and D were calculated from the average density and water content data. Figure 4-48 shows the maximum and minimum percent saturation with depth for each of the plots using the bottom of the cover soil as a datum. It can be seen that the envelopes for Plots A and D are generally higher than Plot B.

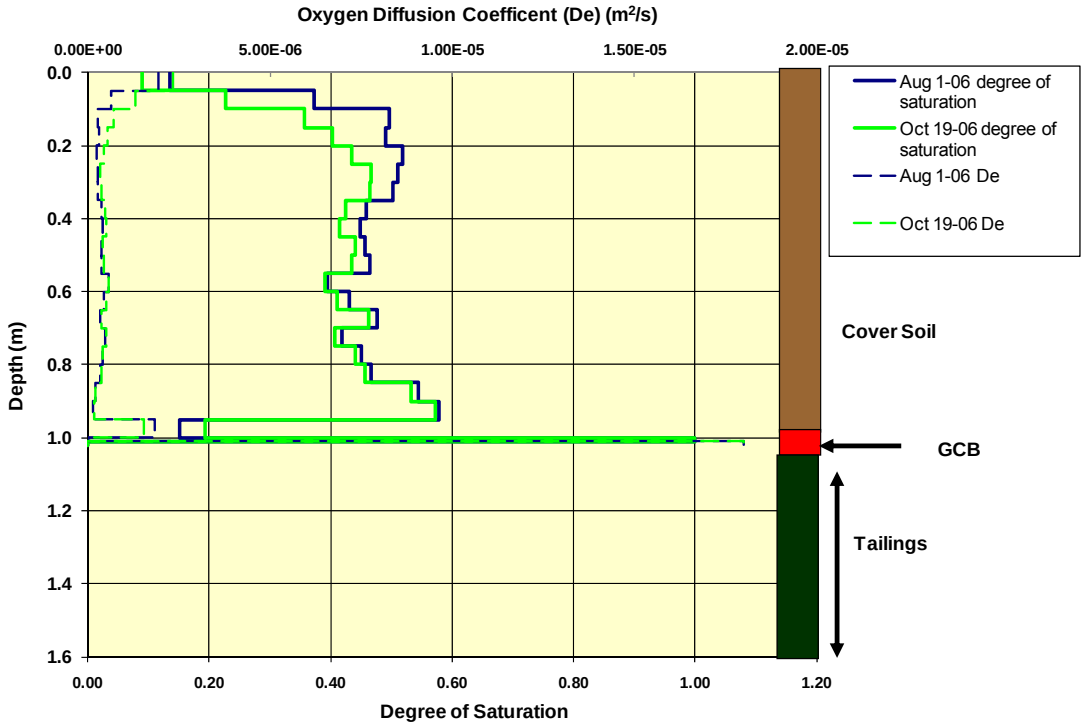

Figure 4-40 Degree of saturation and oxygen diffusion coefficients for Plot A

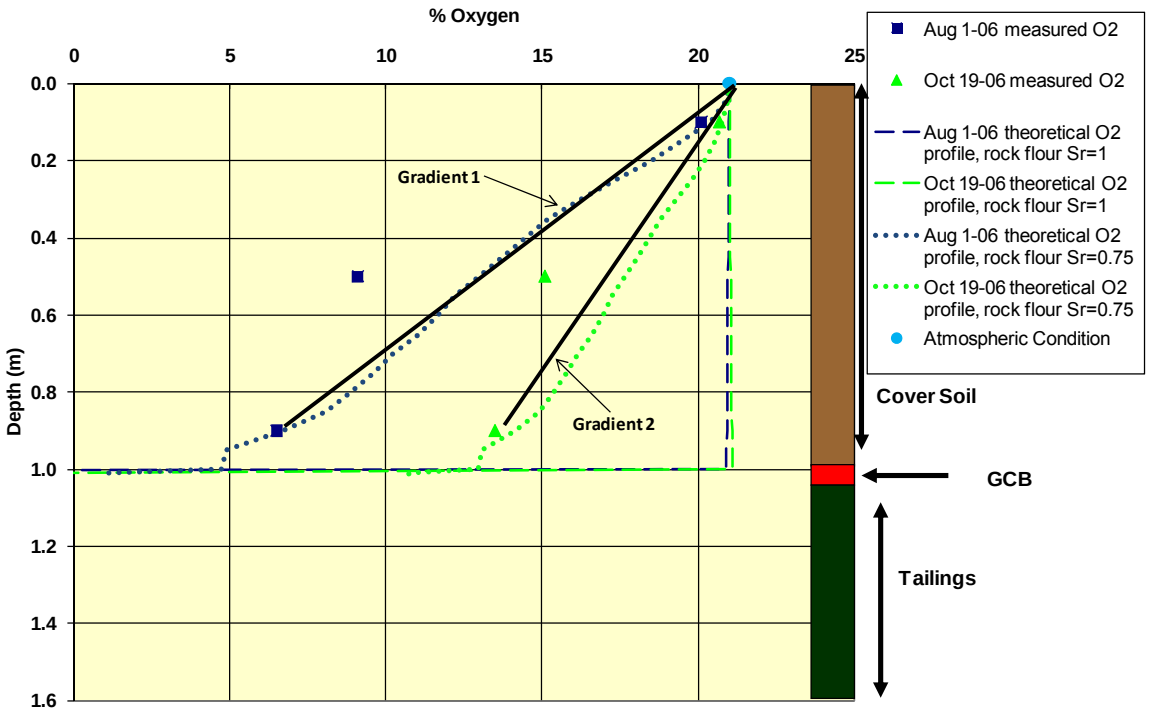

Figure 4-41 Measured and calculated oxygen profiles for Plot A

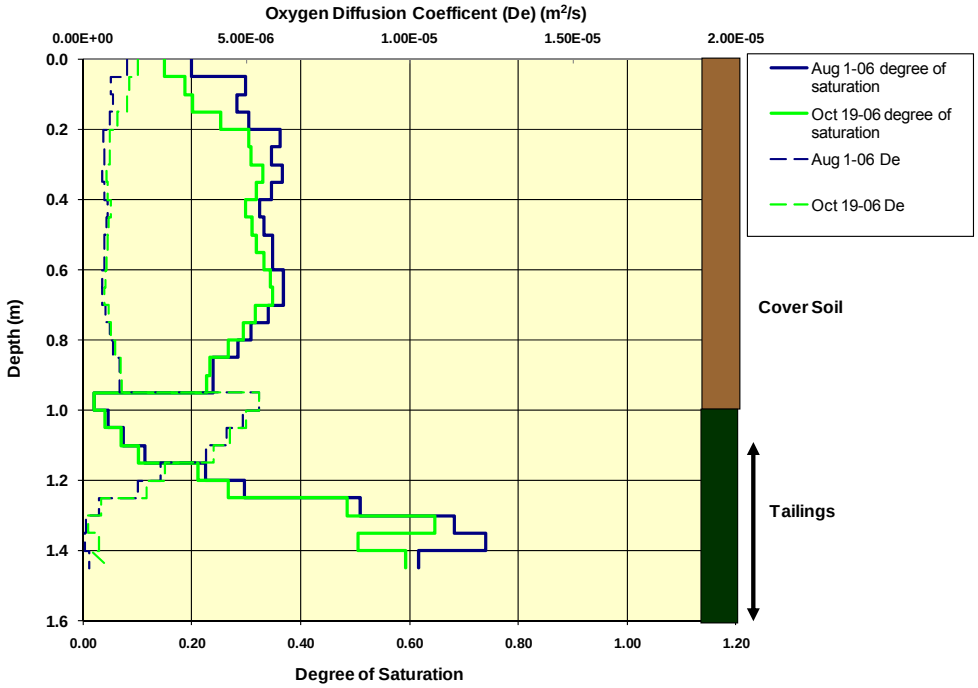

Figure 4-42 Degree of saturation and oxygen diffusion coefficients for Plot B

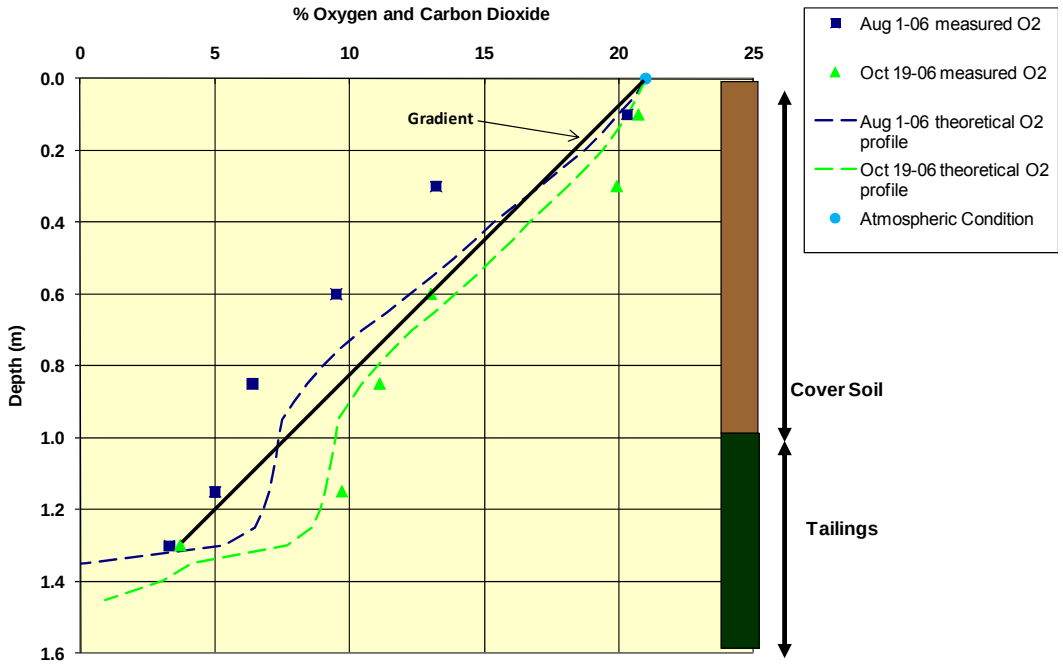

Figure 4-43 Measured and calculated oxygen profiles for Plot B

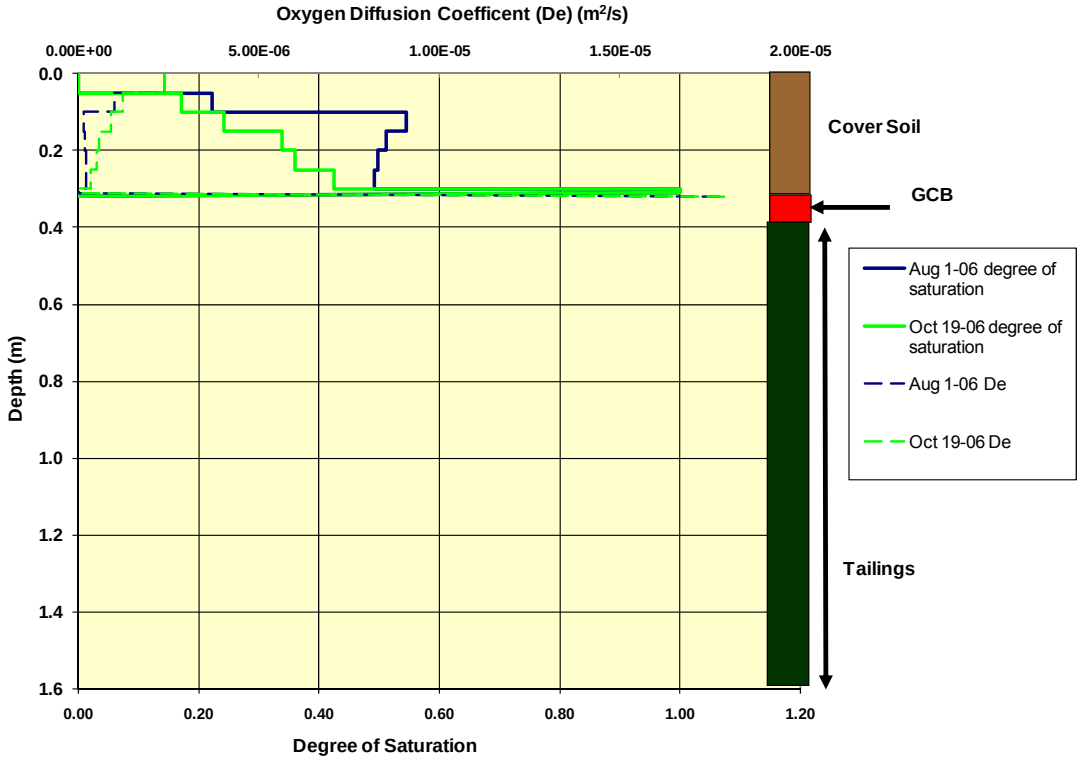

Figure 4-44 Degree of saturation and oxygen diffusion coefficients for Plot C

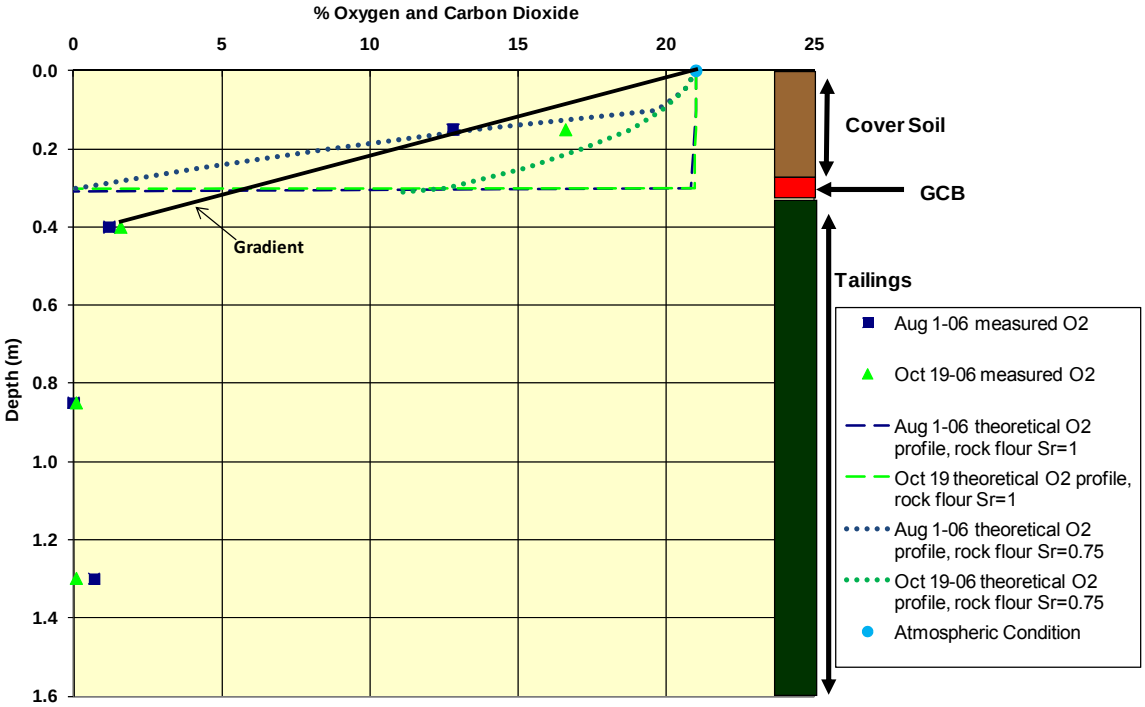

Figure 4-45 Measured and calculated oxygen profiles for Plot C

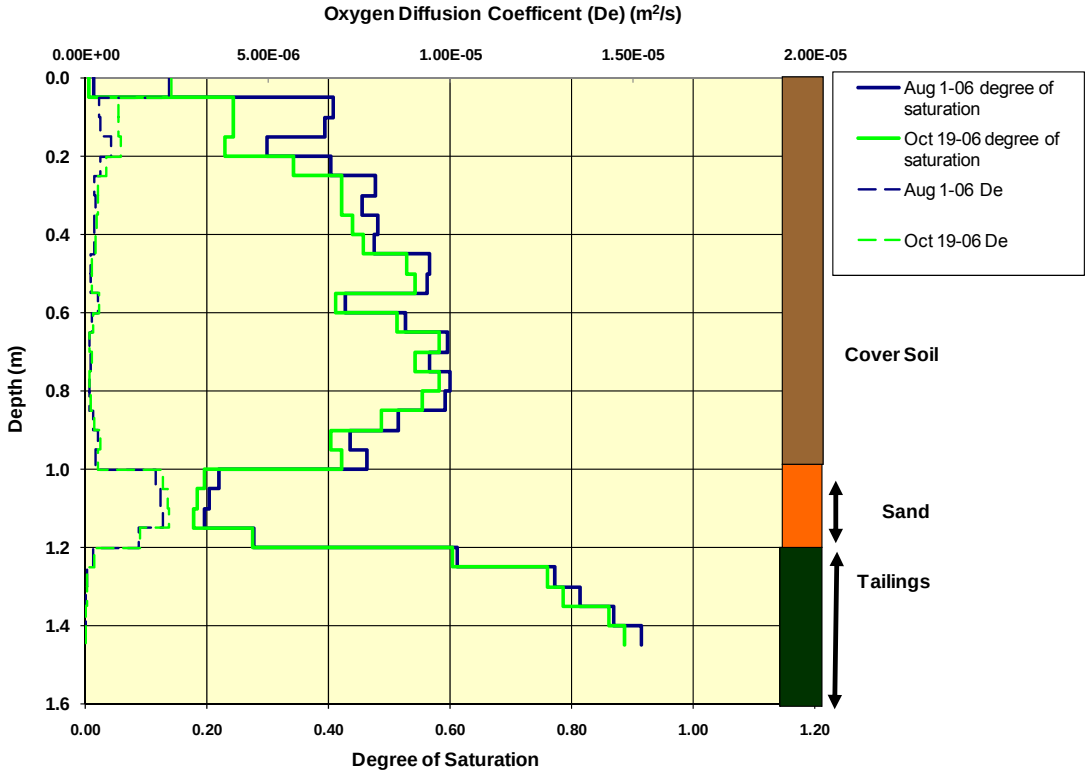

Figure 4-46 Degree of saturation and oxygen diffusion coefficients for Plot D

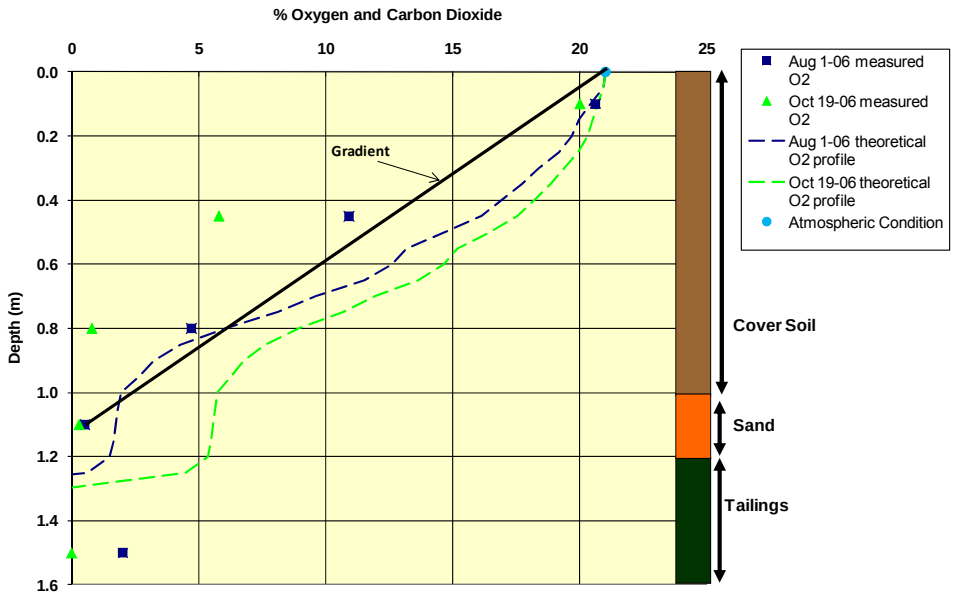

Figure 4-47 Measured and calculated oxygen profiles for Plot D

The average water content profiles seen in Figure 4-22 were used to develop an average saturation profile. The average saturation profile was used to calculate an average theoretical oxygen concentration profile, both of which are presented in Figure 4-49. The average theoretical oxygen profile was found using the same method as the calculated profiles seen above (dividing the cover system into 50 mm depth intervals, calculating an oxygen diffusion coefficient for each interval using the method of Aachib *et al.,* (2002) and calculating an equivalent series oxygen diffusion coefficient). The gradient was calculated by assuming the tailings are completely oxygen consuming (oxygen concentration atmospheric at surface and zero at the tailings interface). The gradient was used in calculating a mass flux across the cover system using the equivalent oxygen diffusion coefficient. The mass flux was then used to calculate the concentrations at each depth with the De for that depth. The same assumptions for the saturation of the GCB presented above were used in the analysis.

It can be seen in Figure 4-49 that the calculated oxygen concentrations profiles for Plots A and C differ substantially based on the degree of saturation of the rock flour. If the rock flour is completely saturated, the gradient across of the rock flour is very steep. If the degree of saturation in the rock flour is lower than 0.75 (which is assumed to be the case in the field measurements) the oxygen profile shifts significantly.

Table 4-8 shows the calculated flux rates of each of the plots (mg m^{-2} s^{-1}) from the analysis presented in Figure 4-49. Plots A and C were calculated with the rock flour have degrees of saturation of 0.75 and 1.0. It can be seen that the flux rates for Plots A and C (containing the GCB) are lower than the other plots, even when the rock flour has a degree of saturation of 0.75. If the rock flour in the GCB is assumed to be saturated, the calculated oxygen flux is two orders of magnitude lower than the other plots. The flux rate for Plot D (with the sand capillary break) is higher than the plots containing the GCB, but lower than Plot B. This decrease in flux rate compared to Plot B is due to the higher saturation that occurs in the capillary break formed by the sand.

Table 4-8 Calculated oxygen flux rates into the tailings (mg m^{-2} s^{-1})

Plot	A	A	B	C	C	D
Rock Flour Sr	1	0.75	n/a	1	0.75	n/a
Oxygen Flux Rate (mg/m2 *s)	-4.12E-10	-2.769E-08	-6.63E-08	-1.34E-09	-1.423E-07	-2.38E-08

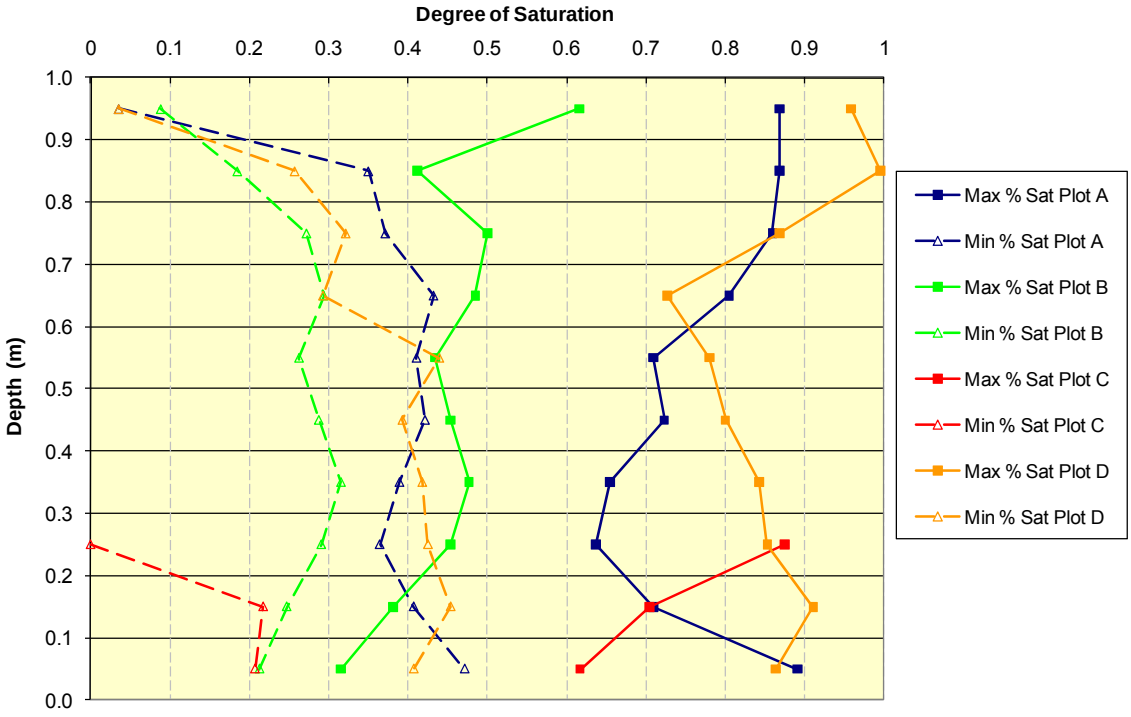

Figure 4-48 Saturation envelopes for each plot

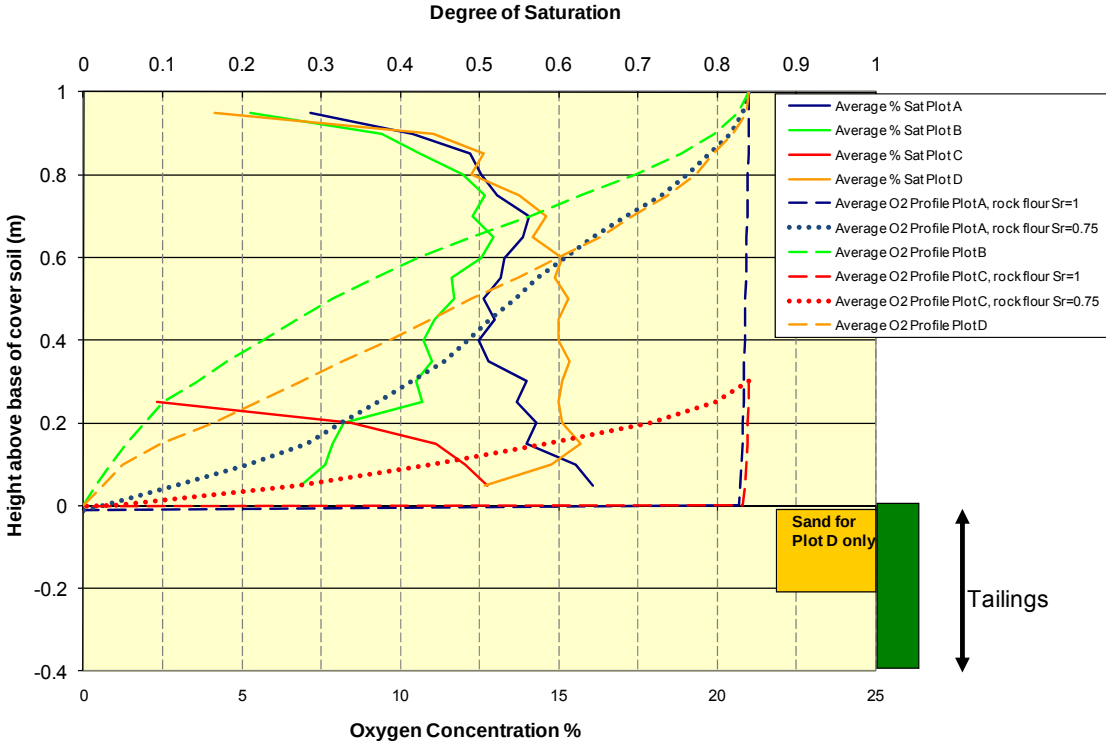

Figure 4-49 Average saturation profile and oxygen concentration profile for each plot

4.12 Chapter Summary

This chapter presents the collected data and analysis from the field trials of the geosynthetic capillary break. The findings of the laboratory program used to quantify basic geotechnical properties were presented in Section 4.2. Section 4.3 discusses the results of the *in-situ* testing that was used to measure the dry density and field saturated conductivity of the cover system materials. The field saturated hydraulic conductivity of the cover soil and tailings were found to be 6.6×10^{-7} m/s and 1.7×10^{-5} m/s respectively.

The data from the tipping bucket rain gauge showed the recorded rainfall for 2006 was 411 mm, which exceeds the yearly average of 343 mm. Data from the air temperature, net radiation, and relative humidity sensors was presented in Section 4.4. This data was used to calculate potential evapotranspiration (PE), is also presented in Section 4.4. The total cumulative PE for the 2006 calendar year was 560 mm.

Sections 4.5 and 4.6 describe the data collected from the soil temperature/matric suction sensors. A clear reduction in matric suction can be seen across the GCB when comparing the data with the plot that has no capillary break. The sensor located just above the GCB on Plot A at a depth of 950 mm recorded matric suction readings below the operating range of 1 kPa for the majority of the growing season of 2006. This is much lower than the sensor located at the same depth on Plot B, which recorded matric suction readings of between 40 and 60 kPa during the same time period.

Section 4.7 presents the volumetric water content data that was collected by both the manual Diviner 2000® system and the automated Tri-SCAN® sensors. The profiles developed from the manual readings show an increase in water content just above the GCB in Plot A. At the same depths on Plot B, the water content decreases suggesting

that the moisture is being pulled from the cover soil into the tailings. The average water contents throughout Plot A are higher than those recorded on Plot B. This data suggests that GCB is beneficial in increasing the moisture storage in the cover soil. The data from Plot C also shows an increase in water content above the GCB, but the there is quite a wide range of recorded water contents due to the relatively thin layer of cover soil. Plot D shows similar results to that of Plot A. The moisture contents throughout the cover soil profile are higher than Plot B, which contains no capillary break layer. A decrease in water content can be observed in the sand layer in Plot D, suggesting that the sand is successful in creating a break.

The water content readings were used to calculate storage in the form of water volume over time for each of the plots. From the calculations it can be seen that Plot A is storing the largest volume of water. Plot D has similar results to Plot A, but is storing slightly less. Plot B is storing the least amount when comparing the plots with 1 m of cover soil.

The manual and automated water content sensor data was used to calculate change in storage. It can be seen that Plot A containing the GCB has the greatest increase in storage after rainfall events. From the water content and meteorological measurements, a simplified water balance for each plot was developed and presented in Section 4.10. The illustrative water balance analysis was used to estimate percolation for each of the plots. Plot A had the lowest amount of percolation into the waste. Percolation rates for Plots C and D were intermediate in value, with Plot B having the worst percolation, although the range from “best” to “worst” was not large.

The data and discussion for the gas concentration probes is presented in Section 4.11. The results from the gas concentration data show that Plots A and C are the most effective in preventing oxygen influx into the tailings, as they have the lowest flux rates. Plot D is the next most effective in limiting oxygen into the tailings, followed by Plot B.

CHAPTER 5 CONCLUSIONS AND RECOMMENDATIONS

5.1 Study Objectives

The primary objective for this thesis was stated in Section 1.3. The goal of this thesis was to evaluate, at field scale, a prototype GCB as a moisture and oxygen limiting barrier in a soil cover system. In order to achieve this objective, the research was divided into three main parts:

- Construct and instrument a series of test plots on the TMA using GCB and conventional soil CB covers.
- Collect and interpret the monitoring data.
- Evaluate the test covers to store water, maximize saturation, and limit oxygen ingress to the tailings as compared to a conventional CB cover.

Chapter two provided a fundamental understanding of the mechanisms and design of engineered cover systems. Chapter two also described previous work in the development of the GCB through lab scale column tests and numerical simulations. The first two objectives were achieved in Chapter three, which described the constructing and instrumentation of the test plots. Chapter four discussed the results of the monitoring, which achieves the third objective.

5.2 Conclusions

The data collected from the field scale test plots show that the GCB was successful in developing a capillary break above the tailings. The data from the *in-situ* matric suction sensors show a clear drop in matric suction across the GCB when compared to the plot containing the same amount of cover soil with no GCB. The data from the water content sensors also show elevated water content above the GCB when compared with the plot that contains no capillary break. The average water content in the plots containing GCB was higher when compared to no capillary break. From the water content sensors the total volume of water stored within each of the plots was calculated. The results show that the test plot containing the GCB and 1 m of cover soil has the largest amount of water stored within the cover soil system.

The change in storage was also calculated using the water content sensors. The data shows that Plot A with the GCB had a higher increase in storage when compared to Plot B, which did not contain the GCB. This shows that Plot A is more effective in being able to store water within the cover soil profile resulting in less water reaching the tailings. A simplified water balance was completed using meteorological and the change in storage. The water balance shows that the GCB does slightly reduce the amount of water percolating into the tailings. The results show that the plot containing the GCB is comparable to that of a conventional capillary break using sand. Both types of capillary breaks performed better than the plot containing no capillary break at all (Plot B). It should be noted that the differences in moisture storage and net percolation rates are slight. It is anticipated that if the plots were vegetated that the observed differences would be more pronounced as the vegetation would take advantage of the increased

moisture storage and evapotranspiration would be a larger part of the water balance. The increased evapotranspiration in the plots with elevated moisture storage will decrease the net percolation significantly.

The higher water content in the plots containing the GCB resulted in a lower flux rate into the tailings. This was observed when analyzing the data from the gas probes. The plots containing the GCB (Plot A and C) and the conventional capillary break (Plot D) had the lowest oxygen flux rates when compared to the other plots. Plot B (containing no capillary break) had the next lowest flux rate.

5.3 Recommendations

The primary objective of this research was to evaluate at field scale the effectiveness of a newly developed GCB in mitigating water and oxygen influx into sulphide bearing tailings. The research program was to design, build, and instrument test plots to test the GCB in a "real world" situation. The design of the plots was developed to simplify the analysis in order to compare the results with a few of unknowns as possible. This section describes recommendations for future research in order to determine the long term performance of the GCB.

It is recommended that the test plots continue to be monitored in order to determine the long term performance of the cover systems. Long term monitoring will also provide information on how the cover systems perform under varying climatic conditions as they were only monitored over a relatively short period of time. During the continued monitoring it is recommended that the density and hydraulic conductivity be measured in order to quantify changes over time.

It is also recommended that the test plots be vegetated in order to determine the effects that vegetation will have on the performance of the cover systems. It is expected the vegetation will decrease the net percolation substantially. The increase in storage and increased water volumes observed in the capillary break cover systems (Plot A in particular) will aid in evapotranspiration and will decrease the net percolation rates.

It is recommended that a calibrated soil-atmospheric model be created in order to determine the long term performance of the cover systems in a variety of climatic conditions. The model will be used to design cover systems in other climatic conditions. It is also recommended that the GCB be tested with a variety of waste materials. The performance of the GCB has been proven with one type of waste material during one year and a half monitoring period. More extensive testing is warranted to prove that is works in a variety of conditions with a variety of waste material.

REFERENCES

Aachib M., Aubertin M., 2002, Laboratory measurements and predictive equations for gas diffusion coefficient of unsaturated soils. CGS-IAH conference proceedings, Niagara Falls, Canada

Adu-Wusu C., Yanful E. K., 2006, Performance of engineered test covers on acid generating waste rock at Whistle mine, Ontario, Canadian Geotechnical Journal, Vol. 43, pp. 1-18.

Akindunni, F.F., Gillham, R.W., and Nicholson, R.V. 1991. Numerical simulations to investigate moisture-retention characteristics in the design of oxygen-limiting covers for reactive mine tailings. Canadian Geotechnical Journal, Vol. 28, pp. 446-451.

American Society for Testing and Materials (ASTM). 1990. Standard test method for particle size analysis of soil (D422-63: reapproved 1990). In 1996 Annual Book of ASTM Standards, Vol. 4.08. ASTM. Philadelphia, Pa. pp. 10-16.

American Society for Testing and Materials (ASTM). 1992a. Standard test method for specific gravity of soils (D854-92) In 1996 Annual Book of ASTM Standards, Vol. 4.08. ASTM. Philadelphia, Pa. pp. 80-83.

American Society for Testing and Materials (ASTM). 1992b. Standard test method for density of soils and soil-aggregate in place by nuclear method (D2922-96)) In 1996 Annual Book of ASTM Standards, Vol. 4.08. ASTM. Philadelphia, Pa. pp. 80-83

American Society for Testing and Materials (ASTM). 2007. Standard test methods for laboratory compaction characteristics of soil using standard effort (12 400 ft-lbf/ft^3 (600 kN-m/m^3)) D698-07e1 In 2007 Annual Book of ASTM Standards, Vol. 4.08. ASTM. Philadelphia, Pa. pp. 71-84

Ayres, B.K. 1998. Soil-atmosphere fluxes at Cluff Lake, SK. M.Sc. Thesis, Department of Civil and Geological Engineering, University of Saskatchewan, Saskatoon, Saskatchewan, Canada

Barbour, S.L., 1990. Reduction of acid generation in mine tailings through the use of moisture-retaining cover layers as oxygen barriers: discussion. Canadian Geotechnical Journal, Vol. 27, pp. 398–401.

Boese, C.D., 2003, The design and installation of a field instrumentation program for the evaluation of soil-atmosphere water fluxes in a vegetated cover over saline/sodic shale overburden, M.Sc. Thesis, Department of Civil and Geological Engineering, University of Saskatchewan, Saskatoon, Saskatchewan, Canada.

Bussière, B., Aubertin, M., Chapuis R. P., 2003. The behavior of inclined covers used as oxygen barriers. Canadian Geotechnical Journal, Vol. 40, pp. 512-535

Campbell Scientific Inc. (CSI). 1993. CS 229 Matrix Water Potential Sensor, Operators Manual.

Campbell Scientific Inc. (CSI). 2003. NR-LITE Net Radiometer Instruction Manual.

Campbell Scientific Inc. (CSI). 2004. AM16/32 Relay Multiplexer Instruction Manual.

Campbell Scientific Inc. (CSI). 2004. CE4 Current Excitation Module Instruction Manual

Campbell Scientific Inc. (CSI). 2005. CR10X Measurement and Control System, Operators Manual.

Chapman D. 2005, Construction and monitoring of the Albian Sands Energy Inc. Slope Facet. 58th Canadian Geotechnical Conference, Saskatoon, September.

Crank J., 1975, The mathematics of diffusion. 2nd edition. Clarendon Press, Oxford, United Kindom

Fetter, C.W. Contaminant Hydrogeology. 2nd edition © 1993. Prentice-Hall, Upper Saddle River, New Jersey.

Fredlund, D.G. 2000. The 1999 R.M. Hardy Lecture: The implementation of unsaturated soil mechanics into to geotechnical engineering. Canadian Geotechnical Journal, Vol. 37, pp. 963-986.

Fredlund, D.G., Rahardjo, H. Soil Mechanics for Unsaturated Soils. © 1993. John Wiley and Sons Inc., New York, NY.

Fredlund, D.G., and Xing, A. 1994. Equations for the soil-water characteristic curve. Canadian Geotechnical Journal, Vol. 31, pp.521-532.

Fredlund, D.G., Xing, A., and Huang, S. 1994. Predicting the permeability function for unsaturated soil using the soil-water characteristic curve. Canadian Geotechnical Journal, Vol. 31, pp. 533-546.

Fredlund, M.D., Wilson, G.W., Fredlund, D.G. 2002. Use of the grain-size distribution for estimation of the soil-water characteristic curve. Canadian Geotechnical Journal, Vol. 39, pp. 1103-1117.

Freeze, R.A., and Cherry, J.A., Groundwater. © 1979. Prentice Hall, Englewood Cliffs, NJ.

Google Earth Internet Source, http://maps.google.com, accessed June 2006.

GeoStudio 2004. Version 6.13. GEO-SLOPE International, Ltd. © 1991-2005.

Henry, K.S. 1990. Geotextiles as capillary barriers. Geotechnical Fabrics Report, Vol. 8, No. 2, pp. 30-36.

Henry, K.S. 1995., The use of geosynthetic capillary barriers to reduce moisture migration in soils. Geosynthetics International, Vol. 2, No. 5. pp. 883-888.

Henry, K.S., Holtz, R.D., 2001. Geocomposite capillary barrier to reduce frost heave in soils. Canadian Geotechnical Journal, Vol. 38, pp. 678-694.

Hillel D., 1980. Fundamental of soil physics. University of Massachusetts. Academic Press. New York.

INAP, 2003, Evaluation of the long-term performance of dry cover systems, edited by O'Kane Consultants Inc.

Kovács, C., 1981, Seepage hydraulics, Elsevier Science Publishers, Amsterdam.

Khire M. V., Benson C. H., Bosscher P. J., 2000, Capillary barriers: design variables and water balance, Journal of Geotechnical and Geoenvironmental Engineering, Vol. 126, No. 8,

Lungren, T., 2000, The dynamics of oxygen transport into soil covered mining waste deposits in Sweden, Journal of Geochemical Exploration 74, 163-173

Mbonimpa M., Aubertin M., Dagenais A.M., Bussière B., Julien M., Kissiova M., 2002, Interpretation of field tests to determine the oxygen diffusion and reaction rate coefficients of tailings and soil covers. CGS-IAH conference proceedings, Niagara Falls, Canada

Meiers, G.P. 2002. The use of field measurements of hydraulic conductivity to characterize the performance of reclamation soil covers with time. M.Eng. Report, Department of Civil and Geological Engineering, University of Saskatchewan, Saskatoon, Saskatchewan, Canada

Melis, L.A. Uranium waste management in Canada. Paper presented o Canadian Uranium Producers Metallugical Committee Meeting, Toronto, Ont.

MEND 2.21.4, 2004, Design, construction, and performance monitoring of cover systems for waste rock and tailings, Vol 1, edited by O'Kane Consultants Inc.

National Climate Archive – Environment Canada. Internet source. http://www.climate.weatheroffice.ec.gc.ca. accessed: June, 2006.

National Resources Canada Atlas of Canada, Map of Prairie Provinces. Internet source. http://atlas.nrcan.gc.ca/site/index.html accessed: June 2007

Nicholson, R.V., Gillham, R.W., Cherry, J.A., Reardon, E.J., 1989. Reduction of acid generation in mine tailings through the use of moisture-retaining cover layers as oxygen barriers. Canadian Geotechnical Journal, Vol. 26, pp. 1–8.

Nicholson, R.V., Gillham, R.W., Cherry, J.A., Reardon, E.J., 1990. Reduction of acid generation in mine tailings through the use of moisture-retaining cover layers as oxygen barriers: Reply. Canadian Geotechnical Journal, Vol. 26, pp. 1–8.

APPENDIX A – MATERIAL CALIBRATIONS

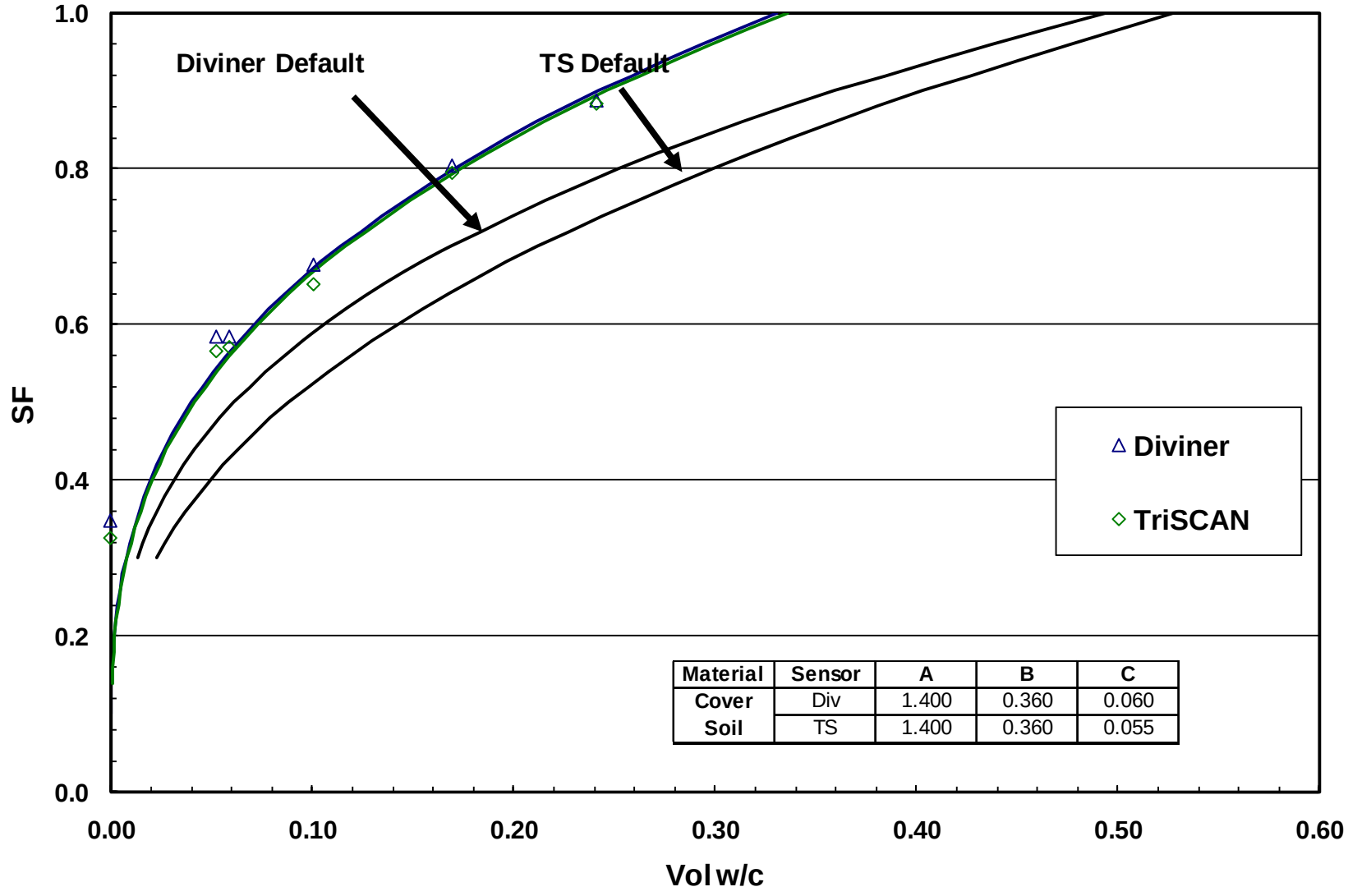

Material	Sensor	A	B	C
Cover	Div	1.400	0.360	0.060
Soil	TS	1.400	0.360	0.055

Figure A-1 Diviner and Tri-SCAN calibration for cover soil material

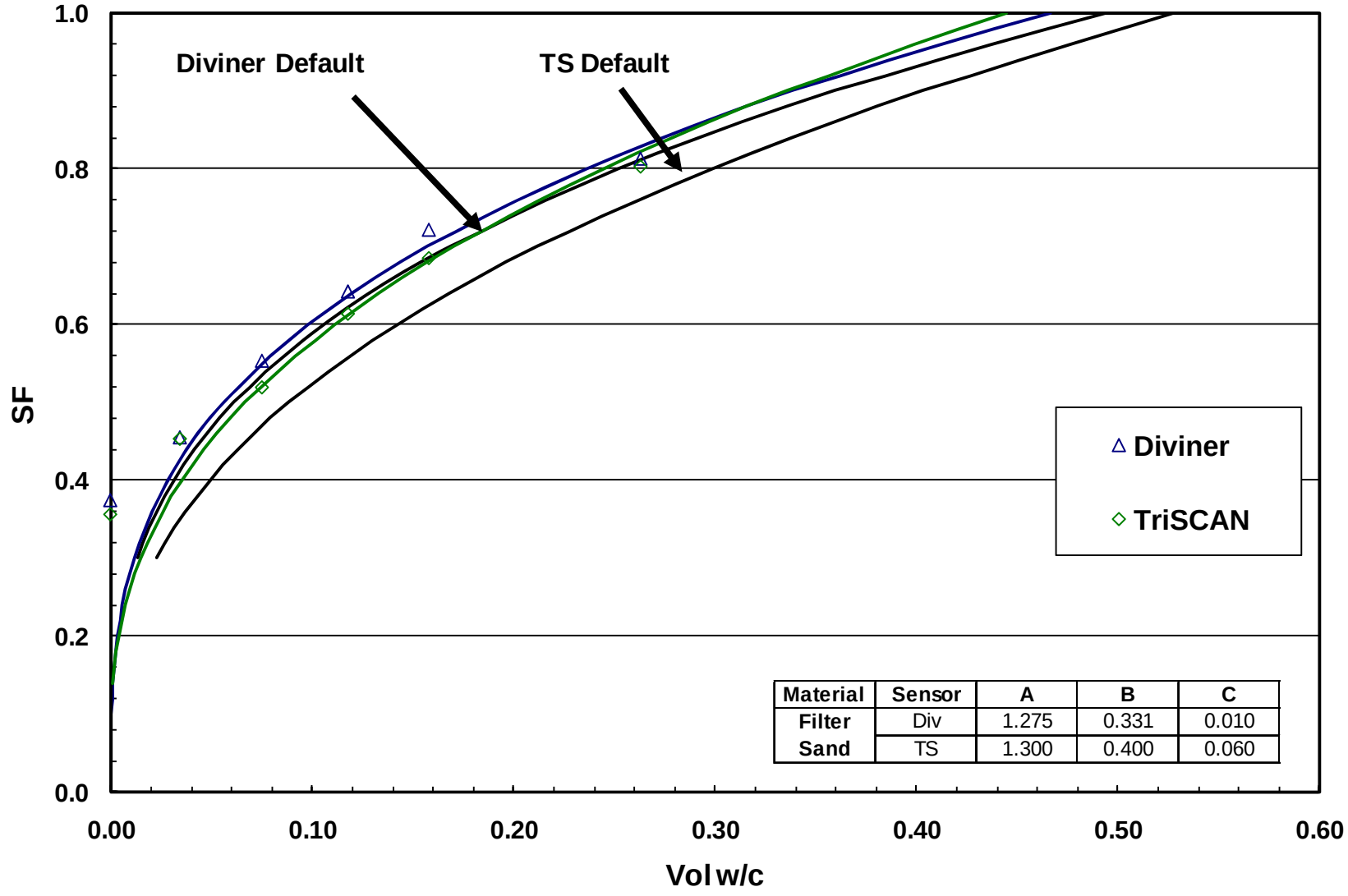

Figure A-2 Diviner and Tri-SCAN calibration for filter sand material

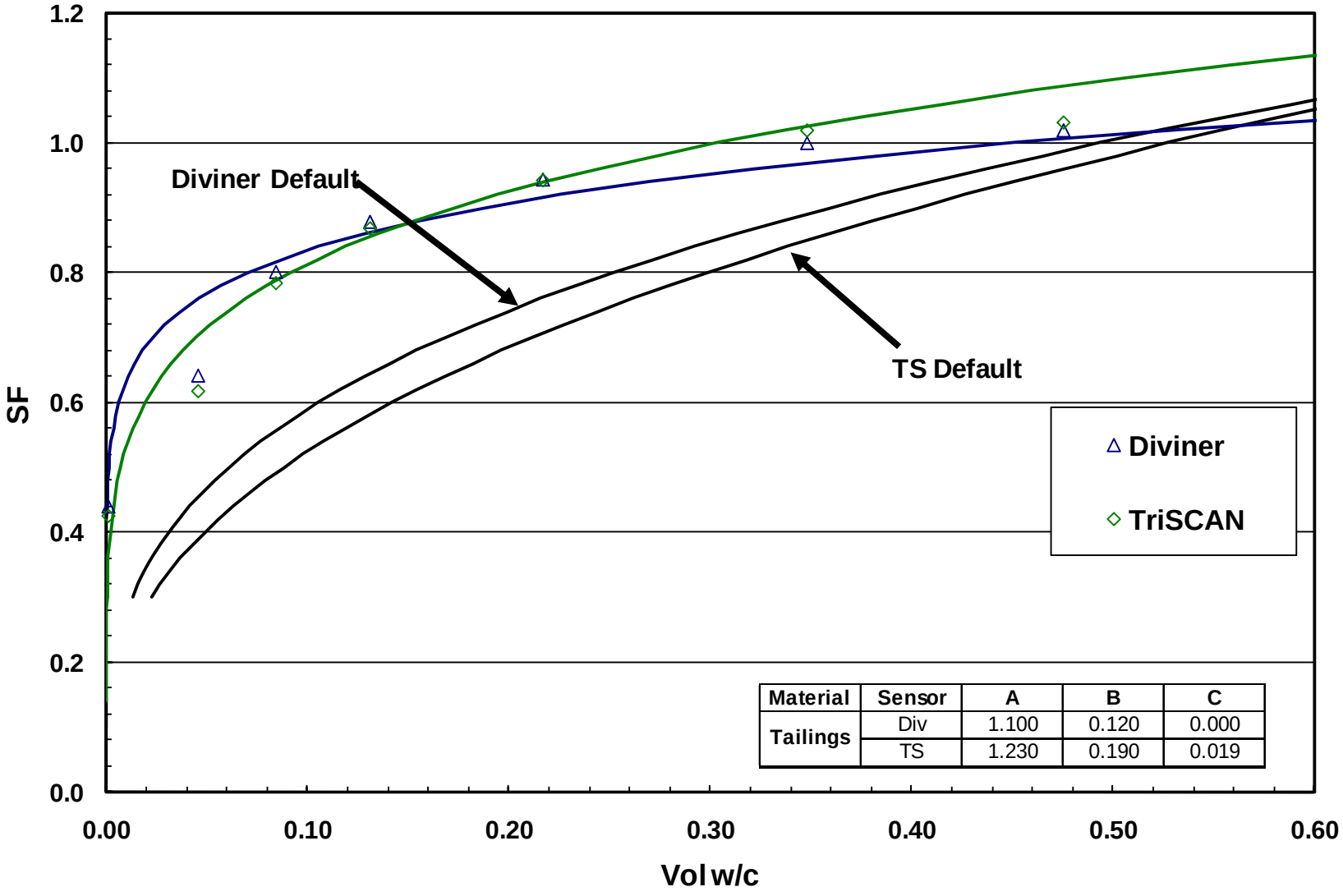

Material	Sensor	A	B	C
Tailings	Div	1.100	0.120	0.000
	TS	1.230	0.190	0.019

Figure A-3 Diviner and Tri-SCAN calibration for tailings material

APPENDIX B – METEROLOGICAL DATA

	Minium Daily Values			Maximum Daily Values			Daily Averages and Totals				
Date	**Min Daily Temp (^oC)**	**Min Daily RH (dec)**	**Min Wind Spd (m/s)**	**Max Daily Temp (^oC)**	**Max Daily RH (dec)**	**Max Wind Speed (m/s)**	**Avg Daily Temp (^oC)**	**Avg Daily RH (dec)**	**Avg Daily Wind Spd (m/s)**	**Total Daily Precip. (mm)**	**Total Net Radiaiton (MJ/m2)**
29-Nov-05	-14.1	0.76	3.8	-10.0	0.85	8.0	-11.7	0.80	8.0	0.0	-0.39
30-Nov-05	-14.7	0.81	3.8	-11.1	0.85	6.1	-13.2	0.83	6.1	0.0	-0.45
1-Dec-05	-16.0	0.72	3.1	-11.1	0.88	6.1	-12.8	0.81	6.1	0.0	-2.76
2-Dec-05	-21.0	0.75	0.4	-16.7	0.85	4.6	-18.6	0.80	4.6	0.0	-2.06
3-Dec-05	-25.2	0.75	0.0	-18.8	0.84	3.1	-20.6	0.81	3.1	0.0	-1.52
4-Dec-05	-26.1	0.77	0.4	-18.1	0.83	5.3	-21.9	0.80	5.3	0.0	-2.34
5-Dec-05	-18.8	0.79	3.4	-14.7	0.86	5.7	-17.0	0.81	5.7	0.0	-1.10
6-Dec-05	-22.6	0.78	0.0	-17.4	0.84	3.8	-19.3	0.82	3.8	0.0	-2.17
7-Dec-05	-23.4	0.74	0.8	-14.7	0.82	6.5	-19.4	0.79	6.5	0.0	-2.02
8-Dec-05	-14.1	0.71	1.5	-10.0	0.87	6.1	-12.0	0.81	6.1	0.0	-2.77
9-Dec-05	-12.9	0.88	0.0	-4.3	0.96	5.0	-8.4	0.93	5.0	0.0	-1.04
10-Dec-05	-11.7	0.86	0.0	-4.3	0.97	5.7	-9.2	0.92	5.7	0.0	-1.39
11-Dec-05	-9.5	0.93	0.0	-2.0	0.98	4.2	-4.2	0.95	4.2	0.0	-2.78
12-Dec-05	-11.1	0.86	0.0	-4.8	0.96	4.2	-8.5	0.92	4.2	0.0	-0.22
13-Dec-05	-8.9	0.91	2.3	-6.8	0.95	5.7	-8.1	0.94	5.7	0.0	-0.02
14-Dec-05	-15.4	0.85	4.6	-8.9	0.91	5.7	-12.4	0.87	5.7	0.0	-0.34
15-Dec-05	-16.0	0.86	4.2	-14.7	0.88	6.1	-15.3	0.87	6.1	0.0	-0.62
16-Dec-05	-21.8	0.81	3.8	-15.4	0.86	6.1	-17.7	0.83	6.1	0.0	-0.65
17-Dec-05	-27.1	0.79	0.0	-20.2	0.82	3.1	-23.7	0.81	3.1	0.0	-0.31
18-Dec-05	-25.2	0.79	1.5	-10.0	0.82	8.4	-17.3	0.80	8.4	0.0	-0.39
19-Dec-05	-18.8	0.78	0.0	-5.3	0.91	6.1	-9.7	0.85	6.1	0.0	-0.31
20-Dec-05	-23.4	0.82	0.0	-5.3	0.96	3.4	-9.9	0.92	3.4	0.0	-1.74
21-Dec-05	-10.0	0.92	0.4	-5.8	0.96	3.8	-8.4	0.93	3.8	0.0	-2.69
22-Dec-05	-8.4	0.89	0.8	-4.3	0.96	4.6	-6.1	0.93	4.6	0.0	-2.91
23-Dec-05	-8.4	0.94	0.0	-2.4	1.00	3.1	-5.3	0.96	3.1	0.0	-1.81
24-Dec-05	-6.8	0.95	0.0	-2.4	1.00	2.7	-5.2	0.97	2.7	0.0	-0.27
25-Dec-05	-7.3	0.95	0.8	-2.9	0.99	4.2	-5.8	0.97	4.2	0.0	-0.97
26-Dec-05	-3.4	0.99	0.0	-1.1	1.00	0.0	-2.4	1.00	0.0	0.0	-0.26
27-Dec-05	-5.3	0.98	0.0	-1.5	1.00	1.9	-2.8	0.99	1.9	0.0	0.16
28-Dec-05	-7.9	0.95	1.5	-3.4	0.99	2.7	-6.1	0.97	2.7	0.0	-0.37
29-Dec-05	-10.6	0.93	0.8	-7.9	0.95	2.3	-9.4	0.94	2.3	0.0	-0.14
30-Dec-05	-8.4	0.95	0.0	-4.8	0.97	0.4	-6.1	0.96	0.4	0.0	-0.26
31-Dec-05	-6.8	0.96	0.0	-5.3	0.97	0.8	-6.4	0.96	0.8	0.0	-0.68
1-Jan-06	-7.9	0.95	0.8	-4.8	0.97	4.6	-6.4	0.96	2.2	0.0	-0.53
2-Jan-06	-6.3	0.96	0.0	-4.8	0.98	3.8	-5.5	0.97	2.2	0.0	-0.60
3-Jan-06	-4.8	0.92	0.0	-2.4	0.98	2.3	-3.8	0.96	0.6	0.0	-0.78
4-Jan-06	-4.3	0.92	0.0	-2.9	0.98	3.8	-3.7	0.96	1.7	0.0	-0.98
5-Jan-06	-6.3	0.92	0.4	-3.9	0.98	3.8	-5.0	0.95	2.3	0.0	-0.75
6-Jan-06	-5.8	0.89	0.0	-4.8	0.98	3.8	-5.3	0.94	2.0	0.0	-0.88
7-Jan-06	-8.9	0.89	1.1	-4.3	0.98	3.8	-6.2	0.94	2.3	0.0	-0.86
8-Jan-06	-14.7	0.80	0.0	-9.5	0.92	3.4	-11.7	0.89	2.0	0.0	-1.94
9-Jan-06	-11.1	0.87	0.8	-3.9	0.97	5.7	-5.5	0.94	2.9	0.0	-0.88
10-Jan-06	-5.8	0.97	0.0	-3.4	0.98	3.4	-5.0	0.97	1.0	0.0	-0.58
11-Jan-06	-8.9	0.94	0.4	-5.3	0.97	1.5	-7.5	0.96	1.0	0.0	-0.43
12-Jan-06	-10.6	0.92	0.0	-6.3	0.95	5.3	-8.7	0.94	1.4	0.0	-1.16
13-Jan-06	-19.5	0.82	0.0	-7.9	0.90	6.9	-14.3	0.87	1.8	0.0	-2.19

	Minium Daily Values			Maximum Daily Values			Daily Averages and Totals				
Date	Min Daily Temp (^oC)	Min Daily RH (dec)	Min Wind Spd (m/s)	Max Daily Temp (^oC)	Max Daily RH (dec)	Max Wind Speed (m/s)	Avg Daily Temp (^oC)	Avg Daily RH (dec)	Avg Daily Wind Spd (m/s)	Total Daily Precip. (mm)	Total Net Radiaiton (MJ/m2)
14-Jan-06	-16.0	0.83	1.5	-11.7	0.88	5.3	-14.0	0.86	3.9	0.0	-1.84
15-Jan-06	-16.0	0.88	1.9	-13.5	0.90	3.4	-14.5	0.89	2.6	0.0	-0.27
16-Jan-06	-13.5	0.89	3.1	-11.1	0.92	6.1	-12.6	0.91	4.5	0.0	-1.24
17-Jan-06	-22.6	0.81	0.0	-13.5	0.88	6.5	-17.9	0.85	3.0	0.0	-2.85
18-Jan-06	-27.1	0.79	0.0	-16.0	0.88	3.1	-20.2	0.85	1.1	0.0	-1.21
19-Jan-06	-23.4	0.78	0.0	-16.0	0.89	5.7	-18.3	0.84	3.2	0.0	-2.06
20-Jan-06	-28.1	0.76	0.0	-21.8	0.83	2.7	-25.0	0.80	0.9	0.0	-2.43
21-Jan-06	-35.1	0.71	0.0	-20.2	0.83	2.3	-27.6	0.78	0.5	0.0	-2.86
22-Jan-06	-24.3	0.82	1.1	-8.9	0.91	5.3	-14.6	0.88	3.9	0.0	-1.05
23-Jan-06	-10.6	0.82	0.0	-0.6	0.94	10.3	-6.1	0.90	3.4	0.0	-1.45
24-Jan-06	-14.7	0.78	0.0	-4.8	0.86	10.3	-11.0	0.82	5.0	0.0	-0.78
25-Jan-06	-12.9	0.77	1.9	-6.3	0.92	5.0	-9.8	0.84	3.7	0.0	-1.97
26-Jan-06	-11.1	0.77	0.0	-1.5	0.95	8.0	-6.7	0.89	2.0	0.6	-1.88
27-Jan-06	-23.4	0.66	1.9	-8.4	0.92	8.4	-17.6	0.80	4.9	0.0	-1.90
28-Jan-06	-25.2	0.73	1.1	-16.0	0.88	5.0	-20.3	0.81	3.3	0.0	-0.46
29-Jan-06	-16.0	0.88	0.0	-11.7	0.92	1.5	-14.1	0.90	0.8	0.0	-0.37
30-Jan-06	-11.7	0.92	0.8	-4.3	0.98	3.1	-7.4	0.96	1.7	0.0	0.02
31-Jan-06	-16.0	0.89	1.9	-5.3	0.97	4.6	-9.0	0.94	2.9	0.0	-0.58
1-Feb-06	-21.8	0.85	0.4	-14.1	0.91	2.7	-18.0	0.87	1.5	0.0	-2.09
2-Feb-06	-28.1	0.79	0.0	-14.7	0.89	1.9	-21.6	0.84	0.9	0.0	-2.05
3-Feb-06	-29.1	0.78	0.0	-12.9	0.91	1.9	-21.0	0.85	0.7	0.0	-1.80
4-Feb-06	-16.7	0.88	0.0	-11.7	0.92	3.8	-14.3	0.90	1.6	0.0	-1.74
5-Feb-06	-11.1	0.75	4.6	-7.3	0.89	6.5	-8.6	0.80	5.7	0.0	-0.47
6-Feb-06	-10.6	0.83	2.3	-7.3	0.95	4.6	-8.9	0.92	3.3	0.0	-0.27
7-Feb-06	-23.4	0.83	0.0	-6.8	0.94	2.3	-13.1	0.89	0.5	0.8	-2.13
8-Feb-06	-22.6	0.76	0.0	-7.9	0.93	5.3	-14.5	0.85	1.9	0.0	-1.01
9-Feb-06	-10.6	0.76	0.0	-3.4	0.97	8.8	-7.0	0.90	4.6	0.0	-0.34
10-Feb-06	-15.4	0.75	0.8	-6.8	0.92	8.4	-9.9	0.85	5.1	0.0	-1.52
11-Feb-06	-18.1	0.73	1.1	-6.8	0.90	8.0	-11.3	0.81	4.6	0.0	-1.67
12-Feb-06	-18.8	0.71	0.0	-7.3	0.87	4.2	-13.5	0.80	2.2	0.0	-1.75
13-Feb-06	-18.1	0.51	0.8	-13.5	0.86	4.6	-16.1	0.75	2.6	0.0	-0.34
14-Feb-06	-28.1	0.57	1.9	-19.5	0.77	6.5	-23.6	0.67	4.3	0.0	-3.72
15-Feb-06	-32.5	0.62	0.8	-24.3	0.79	5.0	-27.2	0.73	3.3	0.0	-2.51
16-Feb-06	-36.5	0.59	2.3	-27.1	0.74	4.2	-31.8	0.69	3.4	0.0	-2.90
17-Feb-06	-30.2	0.51	0.4	-18.1	0.75	3.8	-24.8	0.66	2.4	0.0	-2.18
18-Feb-06	-26.1	0.67	1.1	-13.5	0.89	5.3	-19.5	0.78	2.9	0.0	-1.18
19-Feb-06	-14.1	0.71	1.1	-8.9	0.89	5.7	-10.9	0.80	3.3	0.0	-0.24
20-Feb-06	-18.1	0.63	0.0	-11.1	0.84	5.3	-14.9	0.73	2.9	0.0	-1.03
21-Feb-06	-20.2	0.73	0.0	-10.0	0.90	4.2	-15.1	0.82	1.6	0.0	-1.22
22-Feb-06	-18.1	0.66	0.0	-10.0	0.90	7.2	-13.3	0.79	3.5	0.0	-1.11
23-Feb-06	-18.1	0.67	0.0	-7.3	0.89	3.4	-13.3	0.80	1.6	0.0	-2.34
24-Feb-06	-26.1	0.54	0.0	-16.0	0.86	3.4	-20.4	0.74	2.2	0.0	-3.30
25-Feb-06	-30.2	0.76	0.0	-12.3	0.86	5.0	-21.1	0.81	2.1	0.0	-1.74
26-Feb-06	-32.5	0.47	0.0	-15.4	0.82	3.8	-21.7	0.66	1.2	0.0	-2.90
27-Feb-06	-26.1	0.50	0.0	-16.0	0.82	7.2	-20.6	0.64	3.8	0.2	-1.61
28-Feb-06	-17.4	0.67	2.7	-11.7	0.84	7.2	-14.2	0.75	4.6	0.0	0.46

	Minium Daily Values			Maximum Daily Values			Daily Averages and Totals				
Date	Min Daily Temp (^oC)	Min Daily RH (dec)	Min Wind Spd (m/s)	Max Daily Temp (^oC)	Max Daily RH (dec)	Max Wind Speed (m/s)	Avg Daily Temp (^oC)	Avg Daily RH (dec)	Avg Daily Wind Spd (m/s)	Total Daily Precip. (mm)	Total Net Radiaiton (MJ/m2)
1-Mar-06	-12.9	0.44	2.3	-9.5	0.66	5.0	-11.3	0.55	3.5	0.0	0.27
2-Mar-06	-12.3	0.56	1.9	-8.9	0.76	3.8	-10.5	0.67	3.1	0.0	0.18
3-Mar-06	-17.4	0.62	0.0	-6.8	0.90	2.3	-12.9	0.79	0.9	0.0	-1.23
4-Mar-06	-21.0	0.58	0.0	-3.9	0.86	3.8	-11.9	0.71	1.7	0.0	-1.81
5-Mar-06	-8.9	0.92	0.8	-4.3	0.95	3.8	-5.6	0.93	2.4	0.0	0.05
6-Mar-06	-4.8	0.90	0.4	-2.0	0.99	5.3	-3.4	0.95	2.8	0.0	-0.17
7-Mar-06	-5.3	0.88	1.5	-2.0	0.99	3.1	-3.5	0.95	2.1	0.8	-0.17
8-Mar-06	-6.3	0.80	0.4	-2.4	1.01	3.1	-3.6	0.93	1.9	0.6	-0.32
9-Mar-06	-14.1	0.85	0.0	-3.4	1.00	5.0	-6.0	0.92	2.9	0.0	-0.43
10-Mar-06	-7.3	0.66	3.4	-3.4	0.89	5.0	-5.3	0.79	4.2	0.0	-0.66
11-Mar-06	-12.9	0.52	3.1	-6.8	0.91	6.9	-9.9	0.73	5.6	0.0	-0.32
12-Mar-06	-18.8	0.53	1.9	-6.8	0.89	5.0	-12.7	0.73	3.4	0.0	-1.48
13-Mar-06	-16.7	0.62	0.0	-8.4	0.86	2.3	-12.5	0.73	0.9	0.0	-0.70
14-Mar-06	-21.0	0.47	0.0	-3.9	0.90	1.1	-12.4	0.74	0.3	0.2	-1.20
15-Mar-06	-21.8	0.58	0.0	-5.3	0.90	2.7	-12.8	0.76	0.8	0.0	-2.28
16-Mar-06	-18.1	0.44	0.0	-6.8	0.91	3.4	-12.5	0.65	1.9	0.0	-2.44
17-Mar-06	-18.1	0.45	1.9	-6.3	0.78	5.7	-12.1	0.59	3.7	0.0	-2.27
18-Mar-06	-15.4	0.35	1.9	-2.9	0.70	8.0	-9.1	0.53	4.4	0.0	-1.94
19-Mar-06	-13.5	0.32	1.1	-0.6	0.63	5.0	-7.5	0.48	2.7	0.0	-1.85
20-Mar-06	-11.7	0.28	0.8	1.2	0.53	5.3	-2.9	0.38	3.5	0.0	-0.83
21-Mar-06	-9.5	0.30	0.4	0.7	0.49	5.3	-4.6	0.41	3.2	0.0	-1.30
22-Mar-06	-12.3	0.25	0.0	3.7	0.72	5.0	-4.2	0.44	1.5	0.0	-0.73
23-Mar-06	-16.0	0.22	0.0	4.6	0.80	1.1	-5.0	0.54	0.3	0.0	-0.20
24-Mar-06	-14.7	0.23	0.0	3.7	0.84	2.3	-4.9	0.54	0.6	0.0	-0.15
25-Mar-06	-10.0	0.38	0.0	3.3	0.67	5.3	-3.0	0.56	1.9	0.0	-0.09
26-Mar-06	-6.8	0.59	0.8	3.7	0.97	6.1	-2.0	0.82	3.4	0.0	0.80
27-Mar-06	-0.6	0.47	1.1	7.4	1.02	6.1	1.6	0.83	3.2	0.8	0.03
28-Mar-06	-3.4	0.29	0.4	9.4	0.85	5.3	2.6	0.61	2.5	0.0	3.31
29-Mar-06	-4.8	0.30	1.5	9.0	0.91	5.0	0.9	0.59	3.3	0.0	3.08
30-Mar-06	-6.3	0.40	0.0	2.9	0.79	3.1	-1.3	0.57	1.5	0.0	3.96
31-Mar-06	-7.3	0.34	0.0	6.6	0.81	4.2	-0.1	0.58	2.0	0.0	5.93
1-Apr-06	-0.6	0.45	1.1	9.4	0.74	5.0	3.4	0.63	2.3	0.0	5.49
2-Apr-06	-6.3	0.50	2.3	2.0	0.70	7.6	-2.0	0.60	4.6	0.0	7.13
3-Apr-06	-8.4	0.34	0.0	7.8	0.90	3.8	0.4	0.58	1.8	0.0	8.96
4-Apr-06	-1.5	0.42	0.0	11.0	0.87	3.4	4.2	0.61	1.1	0.0	5.85
5-Apr-06	-1.1	0.39	0.0	9.0	0.95	4.2	3.4	0.63	2.2	0.0	7.40
6-Apr-06	-7.3	0.40	2.3	1.6	0.65	5.0	-2.2	0.51	3.7	0.0	8.34
7-Apr-06	-7.3	0.32	0.4	4.6	0.72	3.4	-1.1	0.49	2.0	0.0	7.48
8-Apr-06	-1.1	0.46	0.4	12.2	0.80	2.7	4.7	0.60	1.3	0.0	9.67
9-Apr-06	0.3	0.34	1.1	11.8	0.94	6.5	6.3	0.61	3.5	0.0	8.75
10-Apr-06	2.9	0.52	0.4	13.3	0.82	2.7	7.1	0.65	1.9	0.0	6.22
11-Apr-06	0.7	0.44	0.0	13.3	1.00	4.2	7.1	0.70	1.7	0.0	5.00
12-Apr-06	-0.2	0.34	0.8	11.4	0.95	3.1	5.7	0.62	2.0	0.0	8.46
13-Apr-06	1.6	0.65	0.0	4.2	1.03	8.0	2.4	0.92	4.8	5.6	-0.26
14-Apr-06	-1.5	0.43	0.0	11.4	1.10	6.5	4.7	0.82	2.8	0.2	6.98
15-Apr-06	3.7	0.37	1.5	19.8	0.85	5.3	10.9	0.60	4.0	0.0	9.47

	Minium Daily Values			Maximum Daily Values			Daily Averages and Totals				
Date	Min Daily Temp (^oC)	Min Daily RH (dec)	Min Wind Spd (m/s)	Max Daily Temp (^oC)	Max Daily RH (dec)	Max Wind Speed (m/s)	Avg Daily Temp (^oC)	Avg Daily RH (dec)	Avg Daily Wind Spd (m/s)	Total Daily Precip. (mm)	Total Net Radiaiton (MJ/m2)
16-Apr-06	5.4	0.45	0.4	15.6	0.89	3.8	9.3	0.73	2.2	0.0	5.92
17-Apr-06	2.5	0.86	0.8	8.2	1.01	5.7	5.8	0.96	2.7	8.8	0.13
18-Apr-06	2.0	0.64	1.1	8.6	0.99	4.6	4.6	0.84	3.0	0.0	4.32
19-Apr-06	4.6	0.48	0.8	12.9	0.83	5.0	9.2	0.62	3.8	0.0	7.29
20-Apr-06	0.3	0.41	0.0	17.1	0.99	3.4	9.4	0.67	1.1	0.0	9.71
21-Apr-06	3.7	0.30	0.0	20.6	1.00	5.0	13.4	0.57	2.3	0.0	9.70
22-Apr-06	5.8	0.26	1.5	22.5	0.74	8.4	14.4	0.51	4.8	0.0	8.10
23-Apr-06	-1.5	0.42	1.9	5.4	0.97	9.9	2.0	0.67	6.8	0.2	7.30
24-Apr-06	-2.9	0.24	0.0	16.4	0.85	6.1	6.8	0.49	3.0	0.0	7.91
25-Apr-06	2.5	0.16	1.1	21.0	0.65	6.1	12.9	0.35	3.6	0.0	8.80
26-Apr-06	3.3	0.37	4.2	12.9	0.79	6.5	8.5	0.53	5.4	0.0	8.56
27-Apr-06	2.5	0.25	1.1	18.3	0.52	5.3	10.3	0.38	3.9	0.0	8.59
28-Apr-06	12.6	0.27	0.0	21.0	0.50	3.4	18.6	0.35	2.1	0.0	8.62
29-Apr-06	7.4	0.21	0.0	24.0	0.72	6.9	16.0	0.45	3.6	0.0	8.90
30-Apr-06	7.4	0.42	1.1	17.1	0.99	6.1	12.9	0.68	3.9	0.0	5.96
1-May-06	7.0	0.62	0.0	11.0	1.02	3.4	9.3	0.88	1.9	1.8	0.17
2-May-06	3.7	1.00	0.4	11.0	1.04	6.1	8.5	1.02	2.9	13.2	0.85
3-May-06	-2.4	0.68	5.0	3.3	1.00	8.0	0.0	0.91	6.9	0.2	3.21
4-May-06	-3.9	0.33	0.8	7.4	0.82	5.7	1.8	0.55	2.7	0.0	10.66
5-May-06	2.5	0.49	1.5	12.2	0.79	4.2	7.1	0.63	2.6	0.0	9.49
6-May-06	5.0	0.52	3.1	13.3	0.92	8.8	8.9	0.69	5.6	0.0	8.09
7-May-06	7.0	0.55	0.4	14.9	0.82	6.1	11.2	0.69	3.9	0.0	5.67
8-May-06	7.4	0.88	2.3	10.2	1.04	3.4	8.7	0.98	2.9	0.0	1.73
9-May-06	2.9	0.94	3.8	6.2	0.99	5.3	4.3	0.96	4.8	0.0	1.74
10-May-06	1.6	0.68	1.9	6.6	1.03	5.7	3.5	0.92	4.3	0.2	11.01
11-May-06	-0.6	0.27	1.5	11.4	0.81	5.0	5.4	0.54	3.3	0.0	10.61
12-May-06	0.7	0.14	0.0	16.8	0.87	3.1	9.9	0.40	1.4	0.0	10.69
13-May-06	4.2	0.21	0.0	17.1	0.85	6.5	11.8	0.44	2.9	0.0	4.64
14-May-06	6.2	0.21	0.0	15.2	0.89	7.2	11.1	0.47	3.5	0.0	4.52
15-May-06	6.2	0.41	1.9	11.0	0.81	3.8	8.5	0.67	3.0	0.0	11.47
16-May-06	4.2	0.40	0.8	18.7	0.92	3.1	10.6	0.67	1.8	0.0	10.05
17-May-06	9.8	0.20	0.4	20.6	0.95	7.6	15.2	0.53	4.4	1.0	7.67
18-May-06	7.0	0.27	0.4	16.8	0.85	3.1	12.6	0.52	1.7	4.2	3.89
19-May-06	8.6	0.53	0.0	12.2	1.02	7.6	8.7	0.80	4.3	0.0	6.42
20-May-06	1.2	0.32	1.1	11.0	0.75	6.5	5.5	0.53	2.9	0.0	9.94
21-May-06	2.0	0.36	0.0	11.4	0.94	7.2	7.4	0.59	3.9	0.0	5.68
22-May-06	7.4	0.39	2.3	22.5	0.84	7.2	14.2	0.61	4.4	4.0	11.55
23-May-06	12.2	0.38	0.8	27.5	0.86	3.8	19.5	0.61	2.1	0.0	9.30
24-May-06	6.6	0.48	1.9	21.3	1.01	8.0	11.2	0.81	5.0	13.2	-0.78
25-May-06	6.2	0.76	0.0	9.8	1.03	3.8	7.5	0.93	2.2	1.4	7.29
26-May-06	4.2	0.69	1.9	8.2	1.00	3.8	6.2	0.83	3.0	0.2	5.35
27-May-06	5.0	0.50	1.5	12.6	0.94	3.8	8.4	0.74	2.5	0.2	6.17
28-May-06	5.8	0.39	0.4	14.1	0.91	6.1	11.1	0.62	3.5	0.0	4.31
29-May-06	9.0	0.55	1.1	12.9	1.03	5.3	9.9	0.95	3.0	14.0	-0.01
30-May-06	4.2	0.58	1.5	15.6	1.03	9.1	8.9	0.90	5.7	7.2	7.46
31-May-06	5.8	0.41	0.4	16.4	0.99	4.6	10.9	0.72	2.1	0.0	12.92

	Minium Daily Values			Maximum Daily Values			Daily Averages and Totals				
Date	Min Daily Temp (^oC)	Min Daily RH (dec)	Min Wind Spd (m/s)	Max Daily Temp (^oC)	Max Daily RH (dec)	Max Wind Speed (m/s)	Avg Daily Temp (^oC)	Avg Daily RH (dec)	Avg Daily Wind Spd (m/s)	Total Daily Precip. (mm)	Total Net Radiaiton (MJ/m2)
1-Jun-06	9.8	0.28	1.4	24.0	0.74	3.8	17.3	0.50	2.0	0.0	12.66
2-Jun-06	13.7	0.21	0.0	28.7	0.84	6.1	21.4	0.52	2.7	0.0	12.24
3-Jun-06	17.5	0.30	4.1	30.7	0.79	6.9	22.8	0.57	3.8	2.0	9.26
4-Jun-06	14.5	0.20	4.1	26.0	0.99	4.2	20.5	0.53	3.0	0.0	13.09
5-Jun-06	17.9	0.47	4.1	22.9	0.72	5.7	19.8	0.60	4.0	0.0	4.75
6-Jun-06	12.9	0.45	1.4	21.7	0.91	10.3	17.0	0.68	4.4	0.0	9.25
7-Jun-06	9.0	0.55	9.6	13.7	0.77	8.4	11.5	0.64	6.2	0.0	6.22
8-Jun-06	5.8	0.21	0.0	18.3	0.94	3.1	12.3	0.53	2.0	0.0	11.27
9-Jun-06	8.6	0.30	5.5	16.0	0.64	5.3	12.5	0.44	3.6	0.0	6.05
10-Jun-06	11.0	0.34	0.0	19.0	0.67	6.1	14.8	0.49	3.2	5.0	6.25
11-Jun-06	10.6	0.47	5.5	15.6	0.97	5.0	12.5	0.80	2.8	1.2	0.16
12-Jun-06	11.0	0.60	4.1	17.5	1.00	4.2	13.5	0.85	2.9	0.0	4.83
13-Jun-06	10.6	0.26	0.0	23.2	0.99	3.1	18.0	0.59	1.4	0.0	12.17
14-Jun-06	11.4	0.37	0.0	25.2	0.85	6.1	20.7	0.47	1.6	0.0	12.15
15-Jun-06	14.5	0.39	0.0	25.6	0.85	4.2	20.8	0.58	2.3	7.0	8.28
16-Jun-06	16.8	0.43	1.4	27.5	1.01	5.7	21.0	0.75	2.6	8.2	9.95
17-Jun-06	15.6	0.92	5.5	17.9	1.02	4.6	16.1	0.98	3.0	0.0	2.33
18-Jun-06	12.9	0.27	4.1	25.2	1.02	3.8	18.9	0.63	2.9	0.0	13.55
19-Jun-06	17.1	0.40	1.4	27.1	0.89	4.2	21.8	0.61	2.2	8.8	9.32
20-Jun-06	16.4	0.46	0.0	26.0	1.00	5.3	19.2	0.81	1.9	0.8	4.34
21-Jun-06	11.4	0.39	4.1	18.7	0.98	6.1	15.1	0.73	3.9	0.0	10.46
22-Jun-06	7.8	0.28	1.4	19.8	0.81	3.8	13.8	0.49	2.0	0.0	11.17
23-Jun-06	11.0	0.25	0.0	24.8	0.88	3.8	18.7	0.55	1.8	0.0	8.45
24-Jun-06	13.7	0.31	1.4	26.0	0.90	5.7	20.5	0.54	2.6	0.0	8.21
25-Jun-06	15.2	0.25	2.7	26.3	0.69	8.4	21.4	0.46	3.9	0.0	6.83
26-Jun-06	13.7	0.29	4.1	22.9	0.76	4.6	18.9	0.46	3.3	0.0	9.22
27-Jun-06	11.8	0.27	0.0	26.7	0.87	1.9	20.5	0.49	1.2	0.0	7.78
28-Jun-06	14.9	0.30	0.0	27.5	0.85	5.3	22.2	0.54	2.5	0.6	8.24
29-Jun-06	19.4	0.32	5.5	30.7	0.84	6.5	24.1	0.62	3.8	0.2	9.39
30-Jun-06	16.8	0.16	1.4	28.3	0.99	6.9	22.5	0.57	3.7	0.0	10.57
1-Jul-06	15.6	0.34	0.0	23.6	0.74	9.5	19.4	0.52	4.5	0.0	6.05
2-Jul-06	12.6	0.48	12.3	19.8	0.82	9.1	16.3	0.66	6.1	0.0	6.68
3-Jul-06	12.9	0.40	8.2	22.5	0.96	5.7	18.1	0.67	3.4	0.0	8.08
4-Jul-06	16.8	0.28	0.0	27.5	0.80	3.1	26.3	0.53	2.2	0.0	8.84
5-Jul-06	19.0	0.27	1.5	30.7	0.76	6.5	24.1	0.53	4.0	0.0	7.70
6-Jul-06	20.2	0.25	1.1	32.8	0.75	5.0	26.4	0.50	3.0	0.0	9.37
7-Jul-06	15.6	0.67	1.9	25.6	1.00	4.2	18.2	0.91	3.3	2.6	1.11
8-Jul-06	8.6	0.78	2.3	16.0	1.03	6.5	12.9	0.97	4.4	8.0	2.79
9-Jul-06	7.4	0.46	0.0	22.1	1.01	5.7	14.3	0.75	2.9	0.0	14.06
10-Jul-06	16.0	0.64	0.4	19.8	1.01	5.7	17.6	0.90	2.6	7.0	3.55
11-Jul-06	14.1	0.53	1.9	25.2	1.01	8.0	18.4	0.85	5.5	3.6	6.51
12-Jul-06	15.2	0.34	0.8	28.3	0.78	4.6	21.4	0.56	2.3	0.0	13.05
13-Jul-06	16.4	0.45	1.1	24.8	1.00	6.5	19.4	0.76	3.4	10.6	-0.04
14-Jul-06	14.9	0.30	0.0	25.2	1.01	8.8	19.3	0.76	4.4	9.4	13.30
15-Jul-06	13.3	0.23	1.1	26.0	0.91	8.4	20.5	0.52	4.4	0.0	11.93
16-Jul-06	14.1	0.37	0.0	23.6	0.92	6.9	18.8	0.64	3.0	0.0	7.66

	Minium Daily Values			Maximum Daily Values			Daily Averages and Totals				
Date	Min Daily Temp (^oC)	Min Daily RH (dec)	Min Wind Spd (m/s)	Max Daily Temp (^oC)	Max Daily RH (dec)	Max Wind Speed (m/s)	Avg Daily Temp (^oC)	Avg Daily RH (dec)	Avg Daily Wind Spd (m/s)	Total Daily Precip. (mm)	Total Net Radiaiton (MJ/m2)
17-Jul-06	12.9	0.26	1.9	27.5	0.96	6.1	20.4	0.61	4.0	0.0	9.80
18-Jul-06	16.8	0.46	0.0	23.2	0.90	2.3	19.7	0.75	1.1	0.2	0.66
19-Jul-06	15.2	0.70	1.1	20.2	1.00	4.6	17.1	0.89	3.1	8.4	5.33
20-Jul-06	11.8	0.40	0.0	25.6	1.00	5.0	18.9	0.76	2.1	3.8	7.98
21-Jul-06	15.2	0.38	0.0	27.9	0.99	5.0	17.2	0.87	0.2	0.0	8.77
22-Jul-06	16.8	0.29	0.4	30.7	0.96	6.5	24.2	0.62	3.0	1.4	11.30
23-Jul-06	17.9	0.35	0.4	27.1	1.01	6.9	22.7	0.66	3.9	3.4	11.99
24-Jul-06	16.4	0.48	0.0	26.3	1.00	4.2	20.6	0.77	1.5	1.8	3.39
25-Jul-06	16.0	0.32	1.1	27.5	1.00	4.2	21.8	0.65	2.8	0.0	11.73
26-Jul-06	17.1	0.68	1.9	20.2	0.86	4.6	18.9	0.75	3.3	0.0	4.65
27-Jul-06	9.8	0.85	1.1	19.8	1.02	6.5	13.9	0.94	4.1	25.8	3.69
28-Jul-06	8.6	0.43	0.0	20.2	1.01	3.4	14.9	0.71	2.0	0.0	10.04
29-Jul-06	12.9	0.40	0.0	23.6	0.85	4.6	18.2	0.63	2.0	0.0	8.73
30-Jul-06	14.9	0.41	0.0	24.8	0.84	4.2	19.8	0.62	2.0	0.0	9.50
31-Jul-06	12.9	0.65	0.4	18.7	1.02	9.1	15.7	0.89	4.5	4.8	3.59
1-Aug-06	11.4	0.39	1.1	21.7	0.97	7.6	16.3	0.70	4.1	0.0	8.84
2-Aug-06	9.8	0.49	0.8	18.3	1.01	6.1	14.0	0.77	3.1	0.0	5.08
3-Aug-06	11.0	0.42	0.4	21.7	0.97	5.0	16.0	0.70	2.2	0.2	7.42
4-Aug-06	13.3	0.41	0.0	22.9	0.98	4.2	17.6	0.75	2.0	4.6	7.29
5-Aug-06	13.3	0.79	2.7	16.0	1.01	7.6	14.3	0.93	4.2	46.0	-2.21
6-Aug-06	13.7	0.57	0.4	19.8	0.99	6.1	16.4	0.81	3.8	0.0	9.19
7-Aug-06	12.2	0.36	0.0	26.3	1.00	5.3	19.2	0.69	2.6	0.0	9.60
8-Aug-06	15.2	0.32	0.0	27.5	0.97	4.6	21.8	0.63	2.1	0.0	9.52
9-Aug-06	16.4	0.28	0.8	26.7	0.70	5.0	21.6	0.53	2.6	0.0	8.84
10-Aug-06	17.1	0.73	0.0	21.7	1.03	6.1	18.9	0.93	3.4	28.6	1.24
11-Aug-06	15.6	0.85	0.0	21.3	1.05	3.8	18.2	0.99	1.8	14.2	2.07
12-Aug-06	12.9	0.66	0.0	22.1	1.04	6.5	17.3	0.94	3.7	3.2	5.70
13-Aug-06	11.8	0.73	1.5	16.4	1.00	7.2	14.1	0.90	5.6	0.6	3.73
14-Aug-06	11.0	0.36	0.0	23.6	1.00	5.0	16.4	0.50	2.1	0.0	9.62
15-Aug-06	14.5	0.37	0.4	26.7	0.92	6.9	21.0	0.62	3.4	0.0	9.54
16-Aug-06	14.5	0.37	0.4	23.2	0.86	5.7	19.0	0.60	3.8	0.0	8.27
17-Aug-06	12.6	0.46	1.9	19.0	0.89	8.4	15.7	0.69	4.6	0.0	5.20
18-Aug-06	8.6	0.37	0.0	18.7	1.01	3.4	12.8	0.42	1.2	0.0	8.56
19-Aug-06	16.0	0.42	0.0	24.8	0.79	5.3	20.2	0.65	3.1	0.0	5.26
20-Aug-06	12.6	0.49	0.4	19.8	0.89	8.0	16.4	0.72	4.5	0.2	4.53
21-Aug-06	8.6	0.40	0.8	19.4	1.04	3.4	14.1	0.71	1.9	0.0	7.13
22-Aug-06	11.8	0.37	0.8	22.5	0.97	5.0	17.5	0.66	3.1	0.0	7.49
23-Aug-06	12.2	0.59	2.7	22.5	0.96	5.3	14.0	0.35	3.7	0.0	7.00
24-Aug-06	14.5	0.69	0.8	19.4	1.03	6.9	16.6	0.90	2.3	13.4	0.68
25-Aug-06	13.7	0.70	0.0	19.8	1.04	6.1	16.8	0.92	3.4	0.8	2.84
26-Aug-06	11.8	0.40	0.8	21.7	1.01	4.2	16.5	0.71	2.9	0.0	7.95
27-Aug-06	11.8	0.44	2.3	21.7	0.86	9.1	16.6	0.66	5.3	0.0	6.00
28-Aug-06	8.2	0.45	0.0	19.4	1.02	5.3	14.2	0.72	1.9	0.0	6.78
29-Aug-06	13.3	0.45	3.4	24.8	0.85	8.0	18.3	0.65	6.0	0.0	6.09
30-Aug-06	16.4	0.46	3.8	26.0	0.77	6.9	20.7	0.62	5.4	0.0	4.41
31-Aug-06	10.6	0.79	1.1	19.4	1.02	6.9	14.2	0.95	3.1	13.6	-1.62

	Minium Daily Values			Maximum Daily Values			Daily Averages and Totals				
Date	Min Daily Temp (^oC)	Min Daily RH (dec)	Min Wind Spd (m/s)	Max Daily Temp (^oC)	Max Daily RH (dec)	Max Wind Speed (m/s)	Avg Daily Temp (^oC)	Avg Daily RH (dec)	Avg Daily Wind Spd (m/s)	Total Daily Precip. (mm)	Total Net Radiaiton (MJ/m2)
1-Sep-06	10.6	0.45	1.1	18.7	1.01	6.5	13.8	0.76	4.5	1.4	6.72
2-Sep-06	11.0	0.24	1.9	26.3	0.85	5.7	18.1	0.55	3.4	0.0	7.69
3-Sep-06	12.6	0.21	1.5	27.1	0.74	4.6	19.5	0.47	2.9	0.0	6.62
4-Sep-06	12.2	0.21	0.0	27.9	0.83	4.2	20.4	0.52	1.3	0.0	5.69
5-Sep-06	12.2	0.47	0.8	21.0	0.92	4.6	16.4	0.73	3.0	0.0	5.65
6-Sep-06	11.4	0.31	0.4	27.1	1.02	7.2	19.4	0.67	3.5	0.0	6.03
7-Sep-06	6.6	0.42	0.0	17.9	0.93	7.2	10.5	0.62	4.1	0.0	4.31
8-Sep-06	4.2	0.38	0.0	15.2	0.99	2.7	9.9	0.67	0.9	0.0	4.71
9-Sep-06	5.8	0.38	0.0	17.1	0.90	5.3	12.1	0.63	2.9	0.0	5.00
10-Sep-06	9.0	0.36	1.9	21.3	0.86	6.9	15.2	0.63	4.3	0.0	5.23
11-Sep-06	11.8	0.21	0.8	26.3	0.90	6.9	18.4	0.61	2.9	0.0	5.36
12-Sep-06	12.9	0.25	0.0	21.7	0.96	6.1	16.5	0.62	2.7	1.6	4.28
13-Sep-06	7.8	0.48	0.0	16.8	0.96	3.1	12.9	0.71	1.3	0.0	0.54
14-Sep-06	7.8	0.63	2.7	12.6	0.81	6.5	10.2	0.74	5.2	0.0	2.82
15-Sep-06	5.0	0.76	5.3	7.4	0.94	9.1	6.0	0.84	7.2	9.4	-1.71
16-Sep-06	3.7	0.78	5.3	6.2	0.99	9.5	4.9	0.93	8.1	39.6	-1.77
17-Sep-06	2.0	0.65	4.2	7.8	0.87	9.1	5.7	0.75	7.1	0.0	6.79
18-Sep-06	3.3	0.56	0.4	11.8	0.95	3.8	7.0	0.79	2.3	0.0	2.36
19-Sep-06	2.9	0.38	0.4	14.9	0.96	4.6	9.0	0.70	2.3	0.0	4.85
20-Sep-06	2.5	0.32	0.0	16.4	0.97	2.3	9.9	0.65	0.7	0.0	4.49
21-Sep-06	9.0	0.55	0.0	14.5	0.99	4.2	11.1	0.80	2.0	0.0	1.10
22-Sep-06	7.4	0.46	0.0	15.2	0.89	3.8	11.2	0.70	1.5	0.0	3.44
23-Sep-06	7.4	0.69	0.0	12.2	0.97	3.8	9.7	0.86	1.9	0.0	1.25
24-Sep-06	7.4	0.40	2.3	16.0	0.97	7.6	10.7	0.77	4.4	1.0	2.24
25-Sep-06	5.4	0.51	0.0	13.7	1.01	4.6	9.3	0.77	3.0	0.0	0.77
26-Sep-06	4.2	0.56	1.1	10.6	1.00	5.7	7.1	0.85	3.7	0.0	0.53
27-Sep-06	0.7	0.52	0.0	7.8	0.97	5.7	4.4	0.75	2.9	0.0	0.39
28-Sep-06	1.2	0.92	0.0	6.2	1.04	4.6	5.0	1.00	2.3	4.0	-0.10
29-Sep-06	5.8	0.90	0.0	11.8	1.10	3.4	8.6	1.02	1.5	6.8	0.91
30-Sep-06	3.3	0.59	0.0	16.0	1.10	2.7	10.1	0.89	1.4	0.2	2.83
1-Oct-06	7.0	0.53	0.0	16.0	1.04	6.5	11.0	0.85	3.1	0.2	2.59
2-Oct-06	4.2	0.55	2.3	11.4	1.01	6.9	7.3	0.83	4.1	0.0	1.18
3-Oct-06	1.6	0.62	0.0	9.8	1.04	3.8	5.4	0.89	2.0	0.0	1.06
4-Oct-06	5.0	0.37	0.0	12.6	0.96	4.6	9.1	0.64	2.4	0.0	2.48
5-Oct-06	4.2	0.48	1.5	18.3	1.02	6.9	11.2	0.76	3.6	0.0	2.54
6-Oct-06	7.0	0.45	0.0	14.9	1.04	4.6	10.8	0.75	2.0	0.0	2.07
7-Oct-06	1.2	0.68	1.5	8.2	1.02	6.5	6.1	0.82	4.1	9.0	-1.28
8-Oct-06	0.7	0.73	0.8	6.2	1.04	5.3	3.0	0.91	3.7	4.4	1.48
9-Oct-06	0.7	0.47	2.3	9.8	0.99	7.6	5.7	0.71	4.9	0.2	2.09
10-Oct-06	-3.4	0.60	6.1	2.9	0.85	9.5	-1.7	0.68	7.9	0.0	0.80
11-Oct-06	-5.3	0.59	5.7	0.3	1.03	11.0	-2.6	0.78	8.3	0.0	1.21
12-Oct-06	-0.6	0.66	5.3	5.0	1.03	8.4	1.3	0.84	6.6	0.0	1.13
13-Oct-06	-2.4	0.33	1.9	4.2	0.82	7.6	0.2	0.61	5.8	0.0	0.74
14-Oct-06	-2.4	0.42	0.4	7.4	0.89	6.1	1.7	0.67	2.7	0.0	1.34
15-Oct-06	-2.9	0.71	0.4	0.7	1.03	3.4	-1.4	0.84	2.2	0.0	0.36
16-Oct-06	-2.9	0.69	2.3	-1.5	0.87	4.2	-2.1	0.78	3.3	0.0	0.35

	Minium Daily Values			Maximum Daily Values			Daily Averages and Totals				
Date	Min Daily Temp (^oC)	Min Daily RH (dec)	Min Wind Spd (m/s)	Max Daily Temp (^oC)	Max Daily RH (dec)	Max Wind Speed (m/s)	Avg Daily Temp (^oC)	Avg Daily RH (dec)	Avg Daily Wind Spd (m/s)	Total Daily Precip. (mm)	Total Net Radiaiton (MJ/m2)
17-Oct-06	-4.8	0.64	0.4	0.3	0.92	3.4	-1.6	0.79	2.3	0.0	0.17
18-Oct-06	-4.8	0.79	0.0	-1.1	0.97	2.3	-2.5	0.91	1.6	0.0	0.12
19-Oct-06	-4.3	0.62	0.8	-0.6	1.04	3.4	-2.7	0.94	2.7	0.0	-0.10
20-Oct-06	-7.9	0.68	1.9	-2.4	0.99	5.0	-5.2	0.84	3.5	0.0	-0.42
21-Oct-06	-6.3	0.70	3.8	-1.5	1.00	6.9	-4.0	0.85	5.6	0.0	2.09
22-Oct-06	-3.9	0.79	0.0	1.6	1.00	5.0	-1.7	0.91	3.0	0.0	1.24
23-Oct-06	-5.8	0.72	0.0	1.6	1.10	4.2	-1.7	0.90	2.0	0.0	0.04
24-Oct-06	-0.6	0.82	1.5	4.6	1.10	3.4	1.1	1.01	2.2	1.2	0.25
25-Oct-06	-0.2	0.71	0.0	5.8	1.01	5.0	2.2	0.89	2.8	0.0	0.95
26-Oct-06	-0.6	0.61	0.0	7.0	1.10	6.5	2.7	0.87	3.0	0.0	-0.68
27-Oct-06	-0.2	0.46	3.1	6.2	0.83	8.4	2.4	0.68	4.8	0.0	-0.39
28-Oct-06	-2.0	0.62	2.3	0.7	0.78	6.9	-1.0	0.68	4.7	0.0	-0.43
29-Oct-06	-5.8	0.63	2.3	-1.5	0.84	5.3	-3.1	0.74	3.8	0.0	0.13
30-Oct-06	-6.3	0.62	1.1	-2.9	0.95	4.6	-4.8	0.77	3.2	0.0	-0.78
31-Oct-06	-7.9	0.71	1.1	-4.3	1.02	4.6	-5.2	0.79	2.8	0.0	-0.09
1-Nov-06	-5.8	0.81	2.7	-2.9	1.03	6.5	-4.2	0.90	4.7	0.0	-0.13
2-Nov-06	-7.9	0.78	2.3	-3.9	0.99	5.7	-5.1	0.88	4.2	0.0	-0.41
3-Nov-06	-14.1	0.70	0.0	-5.8	0.95	3.4	-8.4	0.82	1.9	0.0	-0.74
4-Nov-06	-9.5	0.86	1.9	-6.8	0.99	3.4	-8.0	0.91	2.6	0.0	-0.14
5-Nov-06	-6.3	0.89	1.9	-1.1	1.04	8.0	-3.1	1.00	4.7	0.0	-0.49
6-Nov-06	-12.3	0.71	1.9	-2.9	0.94	5.7	-9.0	0.83	3.8	0.0	-3.64
7-Nov-06	-12.3	0.87	2.7	-8.9	0.99	5.7	-10.2	0.94	4.0	0.0	-0.41
8-Nov-06	-10.6	0.93	1.9	-7.9	0.99	5.0	-9.3	0.97	3.5	0.0	-0.56
9-Nov-06	-12.3	0.74	4.2	-7.9	0.93	6.5	-10.2	0.83	5.0	0.0	-0.89
10-Nov-06	-15.4	0.83	0.0	-12.3	0.94	4.2	-13.4	0.88	2.1	0.0	-1.08
11-Nov-06	-14.7	0.94	1.5	-6.8	1.00	6.5	-10.1	0.97	4.3	0.0	-0.14
12-Nov-06	-18.1	0.85	0.0	-7.9	1.00	4.2	-10.8	0.94	2.2	0.0	-1.90
13-Nov-06	-21.8	0.86	0.0	-6.8	1.01	5.0	-13.0	0.95	1.8	0.0	-0.58
14-Nov-06	-11.7	0.97	4.2	-6.8	1.01	6.5	-9.0	0.99	5.1	0.0	-0.88
15-Nov-06	-19.5	0.89	0.0	-8.9	0.98	5.3	-13.7	0.95	2.0	0.0	-2.97
16-Nov-06	-9.5	0.95	1.5	-1.5	1.10	9.9	-4.7	1.02	6.5	0.0	0.21
17-Nov-06	-11.7	0.73	0.0	-2.0	0.97	6.9	-6.9	0.88	3.0	0.0	-1.61
18-Nov-06	-15.4	0.79	0.0	-2.9	0.98	5.3	-9.1	0.91	1.4	0.2	-1.94
19-Nov-06	-17.4	0.70	0.0	-7.9	0.91	7.6	-12.4	0.81	2.6	0.0	-1.79
20-Nov-06	-6.8	0.78	0.0	-0.2	1.01	7.2	-4.1	0.88	3.2	1.0	-0.88
21-Nov-06	-10.6	0.77	0.0	0.3	1.01	5.0	-5.8	0.93	1.8	0.4	-2.03
22-Nov-06	-21.0	0.78	1.9	-10.6	0.93	7.2	-15.5	0.87	5.1	0.0	-0.72
23-Nov-06	-24.3	0.84	0.0	-16.0	0.91	5.7	-20.1	0.88	2.8	0.0	-1.70
24-Nov-06	-18.8	0.89	0.0	-14.1	0.94	5.0	-15.8	0.92	3.1	0.0	-1.16
25-Nov-06	-20.2	0.87	1.5	-13.5	0.93	8.0	-16.3	0.91	5.3	0.0	-2.62
26-Nov-06	-22.6	0.85	1.1	-18.8	0.87	2.3	-20.2	0.86	1.8	0.0	-1.65
27-Nov-06	-24.3	0.82	1.5	-18.8	0.88	5.0	-20.7	0.85	2.8	0.0	-0.60
28-Nov-06	-18.8	0.86	5.0	-16.7	0.89	8.4	-17.5	0.88	6.5	0.0	0.12
29-Nov-06	-22.6	0.85	0.0	-15.4	0.88	7.2	-18.2	0.86	5.1	0.0	-1.70
30-Nov-06	-26.1	0.81	0.0	-14.1	0.92	4.2	-19.9	0.86	2.0	0.0	-2.02
1-Dec-06	-20.2	0.85	3.1	-14.1	0.92	6.1	-16.2	0.90	4.7	0.0	-0.85

Date	Minium Daily Values			Maximum Daily Values			Daily Averages and Totals				
	Min Daily Temp (^oC)	Min Daily RH (dec)	Min Wind Spd (m/s)	Max Daily Temp (^oC)	Max Daily RH (dec)	Max Wind Speed (m/s)	Avg Daily Temp (^oC)	Avg Daily RH (dec)	Avg Daily Wind Spd (m/s)	Total Daily Precip. (mm)	Total Net Radiaiton (MJ/m2)
2-Dec-06	-30.2	0.77	0.0	-20.2	0.86	5.0	-23.5	0.82	2.2	0.0	-2.01
3-Dec-06	-27.1	0.79	0.0	-20.2	0.86	3.8	-23.6	0.83	2.2	0.0	-1.58
4-Dec-06	-26.1	0.81	1.1	-15.4	0.92	3.1	-19.9	0.87	2.3	0.0	-2.90
5-Dec-06	-19.5	0.80	0.8	-13.5	0.92	6.9	-15.5	0.88	3.6	0.0	-1.43
6-Dec-06	-24.3	0.74	0.8	-19.5	0.85	6.5	-22.0	0.81	3.2	0.0	-3.73
7-Dec-06	-23.4	0.79	2.3	-8.4	0.97	5.3	-14.0	0.86	4.2	0.0	-0.50
8-Dec-06	-8.9	0.88	0.8	-4.3	0.99	3.4	-6.6	0.96	1.9	0.0	-1.19
9-Dec-06	-4.8	0.85	1.5	0.7	0.99	5.3	-1.9	0.94	3.9	1.2	-1.45
10-Dec-06	-11.7	0.94	2.3	-5.8	0.99	4.6	-9.7	0.96	3.0	0.0	-0.06
11-Dec-06	-10.0	0.94	2.3	-2.9	1.02	5.0	-6.1	1.00	3.8	0.0	-1.27
12-Dec-06	-11.7	0.93	0.0	-6.8	1.01	4.2	-9.6	0.98	2.0	0.0	-1.99
13-Dec-06	-10.6	0.97	0.8	-1.1	1.02	3.4	-4.4	0.99	2.6	0.0	-0.46
14-Dec-06	-6.8	0.95	0.8	-2.0	1.02	4.6	-5.3	1.00	2.3	0.0	-0.09
15-Dec-06	-9.5	0.99	0.4	-6.3	1.02	5.0	-7.6	1.00	2.0	0.0	-0.38
16-Dec-06	-16.7	0.83	5.0	-5.3	1.02	6.5	-9.8	0.95	5.7	0.0	-0.59
17-Dec-06	-28.1	0.79	0.0	-16.7	0.87	4.2	-21.5	0.83	1.5	0.0	-2.22
18-Dec-06	-28.1	0.79	0.0	-7.9	0.97	5.3	-16.0	0.88	2.7	0.0	-1.12
19-Dec-06	-9.5	0.79	0.8	1.6	0.97	8.4	-3.3	0.91	4.8	0.6	-1.67
20-Dec-06	-7.9	0.68	1.1	-0.6	0.87	9.1	-3.6	0.78	4.6	0.0	-4.09
21-Dec-06	-10.6	0.78	0.4	-3.4	0.97	3.4	-7.4	0.87	1.7	0.0	-2.93
22-Dec-06	-11.7	0.65	0.0	-0.6	0.98	6.1	-5.4	0.80	3.2	0.0	-3.46
23-Dec-06	-11.1	0.63	0.4	-5.8	0.87	5.0	-8.8	0.78	3.3	0.0	-3.72
24-Dec-06	-16.0	0.79	0.0	-7.3	0.97	4.6	-10.0	0.85	1.8	0.0	-1.26
25-Dec-06	-16.0	0.92	0.0	-7.9	0.98	6.5	-11.1	0.94	2.8	0.0	-0.91
26-Dec-06	-16.0	0.92	0.0	-8.9	0.98	1.9	-11.3	0.96	0.5	0.0	-0.43
27-Dec-06	-21.0	0.86	0.0	-11.7	0.94	0.8	-17.0	0.90	0.2	0.0	0.54
28-Dec-06	-22.6	0.85	0.0	-16.0	0.91	2.7	-18.9	0.88	0.9	0.0	-0.04
29-Dec-06	-22.6	0.85	0.0	-11.1	0.95	3.4	-17.0	0.90	1.1	0.0	-0.23
30-Dec-06	-16.7	0.85	0.0	-6.8	0.92	6.1	-10.8	0.89	3.7	0.0	-3.08
31-Dec-06	-12.9	0.80	1.5	-5.3	0.91	4.2	-9.1	0.86	3.2	0.0	-3.02
1-Jan-07	-14.1	0.65	0.4	-4.3	0.92	4.2	-8.8	0.79	3.0	0.0	-2.69
2-Jan-07	-9.5	0.76	0.8	-3.4	0.99	5.7	-5.9	0.85	3.6	0.0	-2.66
3-Jan-07	-5.8	0.82	0.8	2.0	1.02	4.2	-1.0	0.95	2.4	0.2	-1.50
4-Jan-07	-7.9	0.93	2.3	-2.0	1.02	6.9	-5.4	0.97	4.6	0.0	-0.48
5-Jan-07	-9.5	0.92	0.8	-5.3	1.01	2.7	-7.3	0.97	2.0	0.0	-0.57
6-Jan-07	-15.4	0.85	0.0	-6.8	0.97	3.8	-11.6	0.93	0.9	0.0	-1.60
7-Jan-07	-19.5	0.80	0.0	-8.4	0.97	4.6	-12.9	0.90	2.0	0.0	-2.04
8-Jan-07	-19.5	0.77	0.8	-13.5	0.93	7.6	-15.9	0.87	3.6	0.0	-1.89
9-Jan-07	-27.1	0.75	0.0	-19.5	0.85	4.6	-23.0	0.82	1.1	0.0	-2.90
10-Jan-07	-29.1	0.74	2.7	-23.4	0.84	6.1	-25.6	0.78	4.3	0.0	-1.34
11-Jan-07	-36.5	0.70	0.0	-28.1	0.76	4.6	-31.9	0.74	2.4	0.0	-2.94
12-Jan-07	-36.5	0.59	0.0	-22.6	0.78	3.4	-29.8	0.70	1.6	0.0	-2.59
13-Jan-07	-30.2	0.55	1.9	-21.8	0.79	8.0	-26.9	0.69	4.1	0.0	-2.30
14-Jan-07	-32.5	0.56	0.0	-24.3	0.76	4.2	-29.6	0.69	2.0	0.0	-2.49
15-Jan-07	-29.1	0.59	0.0	-18.1	0.79	1.9	-23.2	0.72	0.7	0.0	-1.27
16-Jan-07	-21.8	0.79	0.8	-6.3	0.98	4.2	-12.6	0.90	2.7	0.0	-0.86

	Minium Daily Values			Maximum Daily Values			Daily Averages and Totals				
Date	Min Daily Temp (^oC)	Min Daily RH (dec)	Min Wind Spd (m/s)	Max Daily Temp (^oC)	Max Daily RH (dec)	Max Wind Speed (m/s)	Avg Daily Temp (^oC)	Avg Daily RH (dec)	Avg Daily Wind Spd (m/s)	Total Daily Precip. (mm)	Total Net Radiaiton (MJ/m2)
17-Jan-07	-16.0	0.66	1.9	-5.3	0.97	6.5	-10.1	0.85	4.5	0.0	-1.53
18-Jan-07	-25.2	0.65	0.0	-16.0	0.82	6.1	-21.8	0.74	2.8	0.0	-1.72
19-Jan-07	-27.1	0.66	0.0	-16.7	0.83	1.9	-21.0	0.77	0.8	0.0	-1.60
20-Jan-07	-17.4	0.83	0.0	-7.9	0.93	5.0	-11.2	0.87	2.3	0.0	-0.04
21-Jan-07	-16.0	0.82	0.0	-9.5	0.98	1.9	-13.4	0.92	0.3	0.0	-1.62
22-Jan-07	-16.7	0.86	0.0	-10.6	0.95	3.1	-12.8	0.91	1.5	0.0	-0.41
23-Jan-07	-21.0	0.85	0.4	-10.0	0.95	3.4	-17.0	0.88	1.8	0.0	0.19
24-Jan-07	-16.0	0.79	0.0	-10.0	0.94	3.4	-13.8	0.87	1.9	0.0	-1.25
25-Jan-07	-14.1	0.90	0.0	-6.8	0.99	6.1	-11.9	0.95	3.2	0.0	0.08
26-Jan-07	-19.5	0.79	3.8	-4.3	1.00	9.1	-13.3	0.88	6.4	0.0	-0.40
27-Jan-07	-29.1	0.72	0.0	-18.1	0.85	4.6	-22.6	0.80	2.1	0.0	-1.78
28-Jan-07	-20.2	0.81	1.5	-11.7	0.92	8.4	-16.1	0.87	5.1	0.0	-0.61
29-Jan-07	-23.4	0.75	0.8	-18.8	0.85	6.5	-21.1	0.82	3.8	0.0	-2.70
30-Jan-07	-22.6	0.78	0.0	-14.1	0.88	5.7	-18.9	0.84	2.4	0.0	-1.75
31-Jan-07	-26.1	0.74	1.5	-10.6	0.94	8.8	-19.0	0.84	4.6	0.0	-1.99
1-Feb-07	-25.2	0.76	2.3	-18.8	0.85	7.6	-22.8	0.80	4.8	0.0	-2.80
2-Feb-07	-33.7	0.63	0.0	-24.3	0.80	7.2	-28.4	0.72	4.6	0.0	-2.69
3-Feb-07	-35.1	0.64	0.0	-24.3	0.80	5.0	-30.3	0.73	2.1	0.0	-2.06
4-Feb-07	-39.6	0.58	0.0	-22.6	0.77	1.5	-33.1	0.70	0.2	0.0	-2.36
5-Feb-07	-41.3	0.57	0.0	-22.6	0.77	1.5	-32.4	0.68	0.2	0.0	-2.23
6-Feb-07	-36.5	0.67	0.0	-20.2	0.81	4.6	-28.6	0.74	2.0	0.0	-2.64
7-Feb-07	-30.2	0.57	1.9	-18.8	0.79	5.7	-24.6	0.70	4.0	0.0	-2.77
8-Feb-07	-28.1	0.65	1.5	-21.8	0.79	5.3	-24.7	0.74	3.8	0.0	-2.29
9-Feb-07	-29.1	0.68	1.5	-21.0	0.79	5.0	-25.5	0.75	3.5	0.0	-2.22
10-Feb-07	-25.2	0.56	1.9	-16.0	0.75	6.1	-21.3	0.67	4.3	0.0	-2.51
11-Feb-07	-32.5	0.60	1.1	-21.8	0.79	4.2	-27.6	0.72	2.4	0.0	-2.22
12-Feb-07	-28.1	0.68	1.5	-16.7	0.83	4.2	-22.1	0.76	3.1	0.0	-0.49
13-Feb-07	-28.1	0.66	0.0	-15.4	0.85	3.1	-21.9	0.79	1.2	0.0	-1.99
14-Feb-07	-31.3	0.59	0.0	-12.9	0.85	5.7	-21.8	0.73	2.2	0.0	-1.61
15-Feb-07	-19.5	0.69	0.8	-9.5	0.91	6.1	-13.1	0.82	3.5	0.0	0.51
16-Feb-07	-21.8	0.67	1.9	-8.4	0.96	6.1	-12.1	0.81	4.1	0.0	-1.20
17-Feb-07	-29.1	0.56	0.0	-17.4	0.81	2.7	-23.5	0.72	1.7	0.0	-2.09
18-Feb-07	-30.2	0.72	0.0	-16.0	0.91	6.5	-20.2	0.84	3.4	0.0	-0.07
19-Feb-07	-18.8	0.89	0.4	-14.7	0.92	3.4	-17.1	0.90	1.4	0.2	-0.29
20-Feb-07	-23.4	0.83	0.4	-16.0	0.89	3.4	-19.4	0.85	2.1	0.0	-1.24
21-Feb-07	-19.5	0.85	0.0	-14.1	0.91	2.7	-17.0	0.87	1.0	0.0	0.07
22-Feb-07	-21.0	0.66	0.0	-7.9	0.91	1.5	-16.1	0.85	0.5	0.4	-2.67
23-Feb-07	-20.2	0.76	1.1	-7.9	0.96	6.1	-13.9	0.87	3.8	0.0	-0.57
24-Feb-07	-16.0	0.92	0.0	-4.3	1.01	4.6	-9.3	0.97	1.6	1.8	-0.24
25-Feb-07	-19.5	0.83	0.0	-8.4	0.96	3.8	-14.2	0.90	1.3	0.2	-1.44
26-Feb-07	-17.4	0.85	2.3	-8.9	0.95	3.4	-12.7	0.90	2.9	0.0	-0.20
27-Feb-07	-12.9	0.71	0.8	-6.8	0.96	3.1	-10.2	0.87	2.2	0.0	-0.57
28-Feb-07	-11.7	0.84	0.8	-4.8	0.97	3.4	-8.4	0.93	1.9	0.2	-0.61
1-Mar-07	-8.9	0.87	1.9	-5.3	0.97	3.8	-7.2	0.94	2.8	0.0	-0.47
2-Mar-07	-13.5	0.62	1.5	-5.3	0.97	4.6	-8.4	0.84	3.1	0.0	-1.16
3-Mar-07	-23.4	0.78	0.0	-5.8	0.97	6.5	-11.5	0.88	2.9	0.0	-0.62

	Minium Daily Values			Maximum Daily Values			Daily Averages and Totals				
Date	Min Daily Temp (^oC)	Min Daily RH (dec)	Min Wind Spd (m/s)	Max Daily Temp (^oC)	Max Daily RH (dec)	Max Wind Speed (m/s)	Avg Daily Temp (^oC)	Avg Daily RH (dec)	Avg Daily Wind Spd (m/s)	Total Daily Precip. (mm)	Total Net Radiaiton (MJ/m2)
4-Mar-07	-29.1	0.49	0.4	-7.3	0.90	9.5	-21.9	0.68	4.8	0.0	-1.09
5-Mar-07	-36.5	0.45	0.0	-18.1	0.80	2.3	-25.2	0.62	0.7	0.0	-0.87
6-Mar-07	-21.8	0.82	0.0	-10.6	0.90	1.5	-17.6	0.87	0.6	1.0	-0.57
7-Mar-07	-16.0	0.74	1.5	-7.9	0.93	4.6	-12.3	0.87	3.2	0.0	-0.10
8-Mar-07	-13.5	0.92	0.4	-6.8	1.00	2.7	-9.6	0.96	1.6	0.0	-0.39
9-Mar-07	-9.5	0.89	0.4	-4.3	1.00	5.0	-6.4	0.95	2.4	0.0	-1.40
10-Mar-07	-7.3	0.47	0.4	2.9	1.04	4.6	-3.1	0.79	2.6	3.0	-0.59
11-Mar-07	-14.1	0.63	3.1	-7.3	0.84	5.0	-11.8	0.72	3.8	0.0	0.36
12-Mar-07	-13.5	0.72	0.8	-6.3	0.99	6.9	-10.0	0.88	3.9	0.0	-0.45
13-Mar-07	-21.8	0.55	1.9	-1.5	0.87	10.3	-10.3	0.71	6.5	0.2	-1.97
14-Mar-07	-28.1	0.39	0.0	-11.1	0.74	5.3	-20.6	0.59	1.5	0.0	-1.62
15-Mar-07	-30.2	0.35	0.0	-6.8	0.79	4.6	-16.7	0.59	1.8	0.0	-0.47
16-Mar-07	-17.4	0.50	0.0	-5.3	0.89	2.3	-11.6	0.70	1.1	0.0	0.19
17-Mar-07	-11.7	0.65	0.0	-3.9	0.99	4.6	-7.8	0.76	2.3	0.0	1.11
18-Mar-07	-21.8	0.74	0.4	-2.4	1.02	9.5	-8.6	0.91	5.5	0.0	-0.75
19-Mar-07	-27.1	0.53	0.0	-14.1	0.80	5.0	-20.5	0.68	2.3	0.0	-0.41
20-Mar-07	-18.1	0.65	2.3	-8.4	0.90	5.0	-13.1	0.82	4.0	0.0	1.66
21-Mar-07	-14.1	0.74	0.4	-10.6	0.95	6.1	-11.8	0.84	3.9	0.0	0.42
22-Mar-07	-14.7	0.71	0.4	1.6	0.89	4.6	-5.7	0.81	2.0	1.2	0.21
23-Mar-07	-6.3	0.35	0.0	9.4	0.97	4.6	2.2	0.65	2.1	0.0	2.19
24-Mar-07	-0.2	0.47	0.0	11.0	0.85	5.0	5.1	0.63	3.0	0.0	4.85
25-Mar-07	1.2	0.57	0.4	11.8	0.94	5.3	5.5	0.78	3.5	0.0	8.25
26-Mar-07	0.7	0.49	0.0	7.0	0.97	4.6	3.3	0.78	2.3	0.0	6.34
27-Mar-07	-3.4	0.49	0.0	8.6	1.01	4.2	2.7	0.79	2.0	0.4	5.99
28-Mar-07	-3.9	0.68	0.4	2.9	1.04	8.8	0.8	0.90	3.7	6.4	-1.26
29-Mar-07	-9.5	0.34	0.0	1.2	0.84	7.2	-4.1	0.60	3.0	0.0	-0.14
30-Mar-07	-7.3	0.21	1.5	7.4	0.75	5.0	-0.1	0.50	3.5	0.0	5.42
31-Mar-07	-5.3	0.61	0.4	0.3	1.10	3.8	-2.0	0.95	2.1	0.4	0.30
1-Apr-07	-10.0	0.82	0.4	-0.2	1.10	5.3	-4.9	0.96	4.0	0.2	1.03
2-Apr-07	-15.4	0.62	3.4	-7.9	0.92	5.3	-11.8	0.78	4.3	0.0	5.45
3-Apr-07	-18.1	0.38	1.9	-8.4	0.80	3.8	-13.0	0.59	3.1	0.0	6.84
4-Apr-07	-18.1	0.31	0.4	-6.8	0.64	2.7	-11.8	0.45	1.7	0.0	6.80
5-Apr-07	-18.8	0.43	0.8	-6.3	0.69	5.3	-11.8	0.53	3.0	0.0	6.93
6-Apr-07	-17.4	0.26	0.8	-3.9	0.63	3.8	-10.0	0.43	2.9	0.0	6.98
7-Apr-07	-17.4	0.22	0.0	-0.2	0.78	1.1	-7.5	0.43	0.6	0.0	6.96
8-Apr-07	-12.3	0.33	0.0	1.2	0.68	3.8	-4.9	0.46	1.9	0.0	8.13
9-Apr-07	-10.0	0.38	1.5	0.3	0.65	5.0	-4.5	0.53	3.3	0.0	7.99
10-Apr-07	-8.9	0.30	0.0	2.9	0.64	4.2	-2.9	0.47	2.2	0.0	7.86
11-Apr-07	-7.3	0.26	0.0	4.2	0.68	3.1	-1.6	0.45	1.1	0.0	7.93
12-Apr-07	-7.9	0.54	0.0	4.2	0.86	2.7	-0.6	0.66	1.0	0.0	3.69
13-Apr-07	-4.3	0.40	0.0	9.8	1.01	3.4	3.3	0.69	1.6	0.0	9.24
14-Apr-07	-2.0	0.31	0.4	15.6	0.97	4.2	6.6	0.61	2.5	0.0	9.18
15-Apr-07	2.0	0.36	0.4	11.8	0.89	4.2	6.5	0.68	2.3	0.0	4.19
16-Apr-07	0.7	0.26	1.9	12.6	0.74	4.2	6.3	0.50	3.0	0.0	8.72
17-Apr-07	2.5	0.34	0.8	15.2	0.71	8.0	8.2	0.51	4.3	0.0	8.09
18-Apr-07	1.2	0.34	0.0	10.6	0.93	3.1	5.3	0.44	1.7	0.0	4.19

	Minium Daily Values			Maximum Daily Values			Daily Averages and Totals				
Date	Min Daily Temp (^oC)	Min Daily RH (dec)	Min Wind Spd (m/s)	Max Daily Temp (^oC)	Max Daily RH (dec)	Max Wind Speed (m/s)	Avg Daily Temp (^oC)	Avg Daily RH (dec)	Avg Daily Wind Spd (m/s)	Total Daily Precip. (mm)	Total Net Radiaiton (MJ/m2)
19-Apr-07	5.0	0.24	1.5	17.1	0.65	6.5	10.5	0.44	4.1	0.0	6.89
20-Apr-07	2.0	0.57	0.8	10.2	0.97	5.7	6.3	0.73	3.5	0.4	2.02
21-Apr-07	2.9	0.95	0.8	5.4	1.10	5.3	4.3	1.04	2.8	1.4	2.30
22-Apr-07	-0.6	0.36	0.0	8.2	1.01	4.6	3.5	0.70	3.0	0.0	10.88
23-Apr-07	-2.0	0.36	0.0	7.4	0.94	5.0	2.4	0.58	2.3	0.0	9.08
24-Apr-07	-2.4	0.20	0.0	12.6	0.99	3.8	5.3	0.49	1.9	0.0	9.68
25-Apr-07	2.9	0.31	1.9	17.9	0.71	8.8	10.7	0.47	4.4	0.0	10.01
26-Apr-07	2.9	0.24	1.1	16.4	0.62	3.8	10.8	0.42	2.5	0.0	7.90
27-Apr-07	4.6	0.31	0.4	17.5	0.94	4.2	11.2	0.60	2.9	0.0	6.11
28-Apr-07	3.3	0.26	0.4	13.7	0.78	3.4	9.1	0.50	2.1	0.0	3.23
29-Apr-07	4.2	0.35	0.8	13.3	0.76	6.1	9.0	0.57	3.8	0.0	8.74
30-Apr-07	4.6	0.30	0.0	14.1	0.87	3.4	8.5	0.62	1.5	0.0	5.67
1-May-07	1.2	0.16	0.0	17.9	1.03	3.8	11.1	0.48	1.8	0.0	8.92
2-May-07	7.0	0.34	0.8	15.6	0.60	6.9	11.3	0.48	3.2	0.0	4.03
3-May-07	8.2	0.45	4.2	12.9	0.73	7.2	10.9	0.58	5.7	0.0	2.26
4-May-07	9.4	0.50	4.6	18.3	1.10	8.4	12.2	0.73	6.1	4.6	4.56
5-May-07	7.0	0.97	1.5	12.9	1.10	4.6	9.7	1.09	3.0	0.0	4.30
6-May-07	6.6	0.51	0.0	16.8	1.10	3.8	10.5	0.92	1.6	0.0	7.64
7-May-07	6.2	0.37	0.8	16.4	1.10	11.8	11.4	0.72	5.4	0.2	8.10
8-May-07	5.4	0.29	0.4	19.8	0.88	5.0	13.2	0.57	2.5	0.0	7.76
9-May-07	2.5	0.49	2.3	18.7	1.04	9.1	10.2	0.74	5.3	0.4	8.13
10-May-07	2.5	0.47	1.5	9.8	1.03	6.1	5.7	0.76	3.5	0.0	7.86
11-May-07	1.2	0.27	1.9	16.8	1.03	5.3	9.6	0.63	3.8	0.0	10.32
12-May-07	5.0	0.45	1.9	18.7	0.91	7.6	12.7	0.64	4.4	0.0	8.45
13-May-07	9.4	0.25	0.8	18.3	1.03	5.0	13.7	0.53	3.3	0.0	10.50
14-May-07	3.3	0.21	0.0	16.4	0.84	8.8	10.4	0.49	4.5	0.0	7.90

O'Kane, M. 1996. Instrumentation and monitoring of an engineered soil cover system for acid generating mine waste. M.Sc. Thesis, Department of Civil and Geological Engineering, University of Saskatchewan, Saskatoon, Saskatchewan, Canada

O'Kane, M., Wilson, G.W., Barbour, S.L., 1998. Instrumentation and monitoring of an engineered soil cover system for mine waste rock. Canadian Geotechnical Journal, Vol. 35, pp. 828–846.

Onset Computer Corporation. 2003. HOBO® Micro Station User Guide

Park, K., 2005, Evaluation of a geosynthetic capillary break. M.Sc. Thesis, Department of Civil and Geological Engineering, University of Saskatchewan, Saskatoon, Saskatchewan, Canada

Park, K.D.,I.R. Fleming, 2005. One-dimensional column testing for evaluation of a geosynthetic capillary break. 58th Canadian Geotechnical Conference, Saskatoon. CD. Session 9. Paper 621.

Park, K. D., Fleming, I. R., 2006, Evaluation of a geosynthetic capillary barrier, Geotextiles and Geomembrane*s*, Vol. 24, pp 64-71.

Penman, H.L. 1948. Natural evaporation from open water, bare soil and grass. Proceedings of the Royal Society of London, 193: 120–146.

Reynolds, W.D., Elrick, D.E., Topp, G.C., 1983, A reexamination of the constant well head permeameter method for measuring saturated hydraukic conductivity above the water table, Soil Science, Issue 136, Volume 4

Reynolds, W.D., Elrick, D.E., 1985, In-situ measurements of field-saturated hydraulic conductivity, sorptivity and α parameter using the Guelph permeameter, Soil Science, Issue 140, Volume 4

Rooney, D. J., Brown, K. W., Thomas J. C. 1997, The effectiveness of capillary barriers to hydraulically isolate salt contaminated soil, Water, Air, and Soil Pollution 104: 403–411

Sentek. 2003. TriSCAN® Agronomic User Manual Version 1.2.

Sentek. 2004. Diviner 2000® Portable Soil Moisture Monitoring Solution, User Guide Version 1.21.

Soilmoisture Equipment Corp., 1991, Guelph Permeameter Operating Instructions.

Stormont, J.C., Morris, C.E., 1998. Method to estimate water storage capacity of capillary barriers. Journal of Geotechnical and Geoenvironmental Engineering 124 (4), 297–302.

Stormont, J.C., Morris, C.E., 2000. Characterization of unsaturated nonwoven geotextiles. In: Shackelford, C.D., Houston, S.L., Chang, N.Y. (Eds.), Advances in Unsaturated Geotechnics. ASCE, Reston, VA, USA, pp. 153–164.

Strunk, R. 2007. Evaluation of soil cover alternatives on a municipal landfill. M.Sc. Thesis in progress, Department of Civil and Geological Engineering, University of Saskatchewan, Saskatoon, Saskatchewan, Canada

Terrafix Geosynthetics Inc. Internet source. http://www.terrafixgeo.com, accessed: March, 2006.

Yanful, E.K., 1991. Engineered soil covers for reactive tailings management: Theoretical concepts and laboratory development. Second International Conference on the Abandonment of Acidic Drainage, Montreal, Vol. 1, pp. 461-485

Yanful, E.K. 1993, Oxygen diffusion through soil covers on sulphidic mine tailings. Journal of Geotechnical Engineering, Vol. 119, pp. 1207-1228.

Yanful, E.K., Simms, P.H., Payant, S.C. 1997. Soil covers for controlling acid generation in mine tailings: A laboratory evaluation of the physic and geochemistry. Water, Air, and Soil Pollution 114: 347-375

Yanful, E.K., Simms, P.H., Rowe, R.K., Stratford, G. 1999, Monitoring an experimental soil waste cover near London, Ontario, Canada, Geotechnical and Geological Engineering 17: 65–84,